NEUROPROTECTION STRATEGIES AGAINST CHEMOTHERAPY INDUCED PERIPHERAL NEUROPATHY

by

Bayne Albin

A thesis submitted to the faculty of
The University of North Carolina at Charlotte
in partial fulfillment of the requirements
for the degree of Master of Science in
Mechanical Engineering

Charlotte

2024

Approved by:

_____
Dr. In Hong Yang

_____
Dr. Ahmed El-Ghannam

_____
Dr. Harish Cherukuri

_____
Dr. Stuart Smith

ABSTRACT

BAYNE ALBIN. Neuroprotective Strategies Against Chemotherapy Induced Peripheral Neuropathy
(Under the direction of DR. IN HONG YANG)

Neural engineering is the application of engineering processes and principles to the nervous system for treatment against diseases and disorders such as Neurodegeneration, Mental Health, Peripheral Neuropathy, Etc. Through the application of novel technologies such as additive manufacturing, microfluidics, and advanced imaging techniques, mechanistic insights of neuromodulation can be determined to help develop key therapeutics. Neuromodulation is an aspect of Neural Engineering which focuses on development of modulatory techniques to alter neuronal functions through stimulation methods such as, chemical, mechanical, electrical etc. Stimulation techniques such as Electrical Stimulation (ESTIM) and Magnetic Stimulation (MSTIM) focus on external electric field induction in pulsed patterns which mimic action potential firing rates. Through modification in frequency patterning, neurons can be excited or depressed, changing characteristics such as growth, energy production, synapse formation and plasticity. **This study focuses on the development and application of Electrical Stimulation (ESTIM) and Magnetic Simulation (MSTIM) to enhance mitochondrial trafficking in Dorsal Root Ganglion neurons as a protective mechanism against Chemotherapy Induced Peripheral Neuropathy (CIPN).** CIPN is a dose limiting side effect of chemotherapy treatment which causes discomfort and pain due to induced degeneration of axon fibers translated as a tingling sensation in the patients' extremities such as fingertips and feet. Initially, this study focused on neuroprotective effects of FDA approved drug Fluocinolone Acetonide (FA) against CIPN, where FA was found to enhance axon length and mitochondrial trafficking after anticancer drug treatment. Enhanced mitochondrial trafficking by FA led us to believe mitochondrial play a key role in neuroprotection of axon fibers. Through development of neuromodulation techniques, we studied the effect of ESTIM and MSTIM against CIPN through frequency dependent control of mitochondrial trafficking.

ACKNOWLEDGEMENTS

This research was supported by the College of Engineering (COEN) Seed Grant (101502) and faculty start-up fund Department of Mechanical Engineering and Engineering Science, UNC Charlotte (100041). This Research was also supported by the National Science Foundation (NSF) Career Award (2238723).

Human SKOV-3 Ovarian cancer kindly provided by Dr. Mukherjee from the Biology Department at UNCC.

DEDICATION

I dedicate my dissertation work to my family. A special feeling of Gratitude towards my Parents, Summer and Jereme Albin who pushed me beyond what I ever believed I was capable of.

Additionally, I dedicate this dissertation to my partner, Nicola Brown, who always supported my journey and never left my side. Your words of encouragement and love will always stay with me.

TABLE OF CONTENTS

LIST OF FIGURES

LIST OF ABREVIATIONS

CIPN	Chemotherapy Induced Peripheral Neuropathy
PN	Peripheral neuropathy
PTX	Paclitaxel
CDDP	Cisplatin
L-OHP	Oxaliplatin
VCR	Vincristine
MMAE	Monomethyl Auristatin E
BDNF	Brain Derived Neurotrophic Factor

CHAPTER 1: MITOHICNDRIAL TRAFFICKING AS A NEUROPROTECTIVE MECHANISM AGAISNT CHEMOTHERAPY INDUCED PERIPHERAL NEUROPATHY: IDENTIFYING KEY SITE OF ACTION

Analysis of Mitochondrial trafficking as a Neuroprotective mechanism

This study proposes mitochondrial trafficking as a key mechanism associated with neuroprotection against Chemotherapy Induced Peripheral Neuropathy (CIPN). FDA approved corticosteroid drug Fluocinolone Acetonide was determined to have neuroprotective activity based on a high throughput drug screening of ____. This study observed site specific vulnerability of four common chemotherapy drugs, each with different targeting mechanisms of target cancer cell therapeutics. Each of the four chemotherapeutic drugs used, Paclitaxel (PTX), Cisplatin (CDDP), Monomethyl auristatin E (MMAE), and Vincristine (VCR), were administered on primary sensory neurons either on the cell body or axon through microfluidic isolation and compartmentalization. Axon length and mitochondrial trafficking changes were observed over a 24-hour timestamp. Optimal concentrations of chemotherapy drugs were determined through a varying concentration analysis, where axonal degradation was characterized over a range of chemotherapy drug concentrations, combined with FA concentrations. Ranges of drug concentrations were determined from previous in vitro studies. It was important to determine optimal concentrations of chemotherapy drugs to induce peripheral neuropathy without sudden cell death. CIPN is a dose limiting factor for patients who undergo Chemotherapy treatment which can cause major discomfort, and debilitating pain. Axon length and mitochondrial trafficking were examined using fluorescent microscopy to understand how varying concentrations of chemotherapy drugs were affected by FA. Secondly, this study used compartmentalized microfluidic cell culture chambers to isolate axons and cell bodies to determine the site of action for chemotherapy drugs, and whether FA was effective on axons only. Results from this study found that Microtubule targeting drugs, PTX, VCR and MMAE, had higher degradation rates when exposed to the axonal chamber, whereas CDDP, a DNA targeting drug had higher toxicity when treated with cell bodies. FA was then treated globally, or focally on the cell body or axonal compartment to understand the mechanism of protection. FA treatment was found to have the ability to enhance mitochondrial trafficking

and reduce axonal degeneration by all CIPN drugs. Although microtubule and platinum based anti-cancer drugs have different cancer killing mechanisms, FA was able to enhance mitochondrial trafficking and axon length regardless of mechanism. Observation of enhanced mitochondrial dynamics by FA treatment led to development of electrical and magnetic stimulation devices to modulate axonal length and mitochondrial trafficking of DRGs.

Mitochondrial Trafficking as a Protective Mechanism against Chemotherapy Drug-Induced Peripheral Neuropathy: Identifying the Key Site of Action

Bayne Albin[1,2], Khayzaran Qubbaj[1,2], Arjun Prasad Tiwari[1], Prashant Adhikari[1], In Hong Yang[1]*

[1]Center for Biomedical Engineering and Science, Department of Mechanical Engineering and Engineering Science, University of North Carolina at Charlotte, Charlotte, North Carolina 28223, United States

[2]Equal Contributing Authors

* Corresponding author: In Hong Yang; E-mail: iyang3@charlotte.edu

Abstract:

Aims

Chemotherapy induced peripheral neuropathy (CIPN) is a common side effect seen in patients who have undergone most chemotherapy treatments to which there are currently no treatment methods. CIPN has been shown to cause axonal degeneration leading to Peripheral Neuropathy (PN), which can lead to major dosage reduction and may prevent further chemotherapy treatment due to oftentimes debilitating pain. Previously, we have determined the site-specific action of Paclitaxel (PTX), a microtubule targeting agent, as well as the neuroprotective effect of Fluocinolone Acetonide (FA) against Paclitaxel Induced Peripheral Neuropathy (PIPN).

Main Methods

Mitochondrial trafficking analysis was determined for all sample sets, wherein FA showed enhanced anterograde (axonal) mitochondrial trafficking leading to neuroprotective effects for all samples.

Key Findings

Using this system, we demonstrate that PTX, Monomethyl auristatin E (MMAE), and Vincristine (VCR), are toxic at clinically prescribed levels when treated focally to axons. However, Cisplatin (CDDP) was determined to have a higher toxicity when treated to cell bodies. Although having different targeting mechanisms, the administration of FA was determined to have a significant neuroprotective effect for against all chemotherapy drugs tested.

Significance

This study identifies key insights regarding site of action and neuroprotective strategies to further development as potential therapeutics against CIPN. FA was treated alongside each chemotherapy drug to identify the neuroprotective effect against CIPN, where FA was found to be neuroprotective for all drugs tested. This study found that treatment with FA led to an enhancement in the anterograde movement of mitochondria based on fluorescent imaging.

Key Words:

Chemotherapy induced peripheral neuropathy; axonal degeneration; paclitaxel, monomethyl auristatin E; cisplatin; vincristine; fluocinolone acetonide.

1. Introduction:

Chemotherapy Induced Peripheral Neuropathy (CIPN) is a debilitating disorder that affects more than 30-40% of individuals treated with chemotherapy drugs.[1] CIPN negatively affects the peripheral nervous system, degrading sensory, motor, and autonomic neurons, causing patients to feel major discomfort and pain starting at the end of extremities.[2] Patients diagnosed with Peripheral Neuropathy (PN) experience

tingling, sensory loss, and burning at the site of injury.[3] PN causes pathological changes coined as “Dying Back Neuropathies” where the distal axons are targeted and degrade towards the proximal cell bodies.[4] CIPN is a common side effect of anti-cancer drug treatments which can lead to inflammation, pain, and dosage reductions for patients undergoing chemotherapy treatment, to which there are currently no effective treatments for PN, other than symptomatic pain management[5].

Commonly used drugs for pain management and treatment of PN have a direct effect on the global neuronal environment in the nervous system.[6] PN pain management drugs such as duloxetine and gabapentin have an unfortunate side effect of being a Serotonin and norepinephrine reuptake inhibitors (SSNRI), which are primarily used to treat disorders such as depression and anxiety.[7, 8] Such drugs primarily effect the inhibition of neurotransmitters, serotonin, and norepinephrine with a secondary effect on pain management for PN.[9] Side-effects and complications of using these types of drugs have significant repercussions on patients’ quality of life and have the potential to cause discomfort, nausea, cyclothymia, and withdrawals among other common side effects.[10] Current drugs used for neuropathic pain management are not best suited to aid patients in treatment. Therefore, focal neuroprotection would be a better approach to determine specific treatment methods while avoiding side effects of conventional pain-relieving agents against CIPN.

In this study, we examined axonal susceptibility to degradation induced by four commonly used anti-cancer drugs: Cisplatin (CDDP), Monomethyl auristatin E (MMAE), Vincristine (VCR), Paclitaxel (PTX). The site of action for PTX has previously been determined and has been used as a reference model for the remaining drugs[4]. VCR and MMAE are common anti-cancer drugs which are known to target microtubule structure, similar to PTX.[11] For this reason, a comparison of the site of action for PTX, VCR and MMAE is necessary to further understand the fundamental mechanism of action for these drugs. CDDP likewise, is a common anti-cancer drug, however, it targets DNA replication, preventing tumor growth. CDDP was initially chosen due to its prevalence in chemotherapy treatment, as well as to use as a comparison drug with a different targeting mechanism. The site-specific mechanism of action for each of these drugs was determined in order to understand the focal susceptibility in vitro.

PTX is a well-known chemotherapy drug for breast, lung, and ovarian cancer.[12] It directly targets the mitotic spindle during mitosis, which leads to disruption of cell division and can help stop tumor development and cancer cell growth.[12] PTX is also a known drug that induces CIPN in patients, leading to heavy dosage reductions and treatment alterations.[13] PTX has been shown to induce dying back neuropathy, where distal axons are more susceptible to degradation by PTX.[4] Recently, Fluocinolone Acetonide (FA), has been shown to be neuroprotective against Paclitaxel induced peripheral neuropathy (PIPN).[14] The use of FA can protect sensory neurons from PIPN, without reducing the anticancer effects of PTX, making it a valued, potential neuroprotective agent against CIPN. Additionally, MMAE is a well-known and commonly used Chemotherapy drug similar to PTX used to treat relapsed Hodgkin's lymphoma and anaplastic large cell lymphoma.[15] MMAE in itself is not approved directly for cancer treatment, however in conjunction with an antibody-drug conjugate (ADC), MMAE is linked to a monoclonal antibody which allows MMAE to specifically target a cancer cell.[16] Antibody drug conjugates (ADC) are used to focally target the cancerous cells through administration of the drugs directly at the cancerous tumor.[17] By using ADC, extremely toxic drugs such as MMAE are able to be administered without having as significant of an effect on the global cellular environment.[18] Similar to PTX, MMAE is a microtubule-impacting agent which in clinical settings, leads to CIPN complications in patients.[18] The neurotoxicity of MMAE is not fully known, however MMAE tends to cause peripheral sensory, and motor neuropathy leading to impactful dosage reductions, and occasionally treatment discontinuation. Similarly, VCR is a known Vinca Alkaloid drug used for cancer treatment. VCR targets microtubule polymerization to prevent mitosis associated with cancer cells similar to PTX and MMAE.[19] VCR is an FDA approved anti-cancer drug used for patients who suffer from Ewing sarcoma, gestational trophoblastic tumors, multiple myeloma, ovarian cancer, primary CNS lymphoma, small cell lung cancer, and advanced thymoma.[19, 20] VCR is known to cause peripheral sensory and motor neuropathy, which leads to dosage modification and loss of effectiveness during treatments.[21, 22] VCR is a dose dependent drug where PN was shown in patients when administered 4-10mg.[21] Due to the widespread use of VCR as a treatment method, it is imperative to understand the neurotoxicity mechanisms and identify treatment methods to

prevent CIPN onset. Due to the similarities between MMAE, VCR and PTX, it is assumed that distal axons would be more susceptible to degradation as seen with PTX and herein we tested this hypothesis to study the site of action. On the other hand, CDDP is a platinum based antineoplastic drug used for chemotherapy treatment against testicular, ovarian, bladder, head and neck, lung, and cervical cancer.[23] CDDP targets DNA replication by binding to DNA, directly affecting replication and transcription.[23] CDDP is referenced in the world health organization's list of essential medicines, targeting many types of tumors.[24] CDDP has been seen to cause axonal degeneration, which is the primary dose limiting factor for CIPN.[25] Specific mechanisms of toxicity from CDDP are not yet known, however it is speculated that, peripheral sensory neurons, changes in cell signaling cascades, changes to calcium homeostasis and signaling, oxidative stress, mitochondrial dysfunction and induction of apoptosis as a result of DNA platination, are all potential mechanisms behind cisplatin-induced peripheral neuropathies[26].

A dosage response for each drug was identified to choose proper concentration levels for CIPN analysis. To better understand the specific site of action of each drug, a differentiation of cell bodies to axons was created via a PDMS based microfluidic chamber system.[4] Previous studies have not yet determined if the cell bodies or axons are the site-specific targets for the drugs.[27] Using the compartmentalized microfluidic cell culture platform, we demonstrate that axons are more susceptible to the toxicity induced by the chemotherapy drugs which target micro-tubules (PTX, MMAE, VCR), whereas cell bodies are more susceptible for DNA targeting samples (CDDP) in vitro. Using this information, more effective treatment methods can be developed to specifically target the most vulnerable region in CIPN patients.

Previously, it has been shown that the FDA approved drug, FA, is neuroprotective against PTX.[14] In a similar manner, we have identified the neuroprotective effect of FA on the FDA approved chemotherapy drugs. The findings of this study are important for identification of site of action for degradation susceptibility and FA-induced neuroprotection. In this study, we determine the role of Fluocinolone Acetonide (FA) in mitochondrial enhancement as a neuroprotective mechanism against common CIPN. The observation of focal susceptibility is an important factor in creating effective treatment methods for

patients experiencing CIPN. Treatments may vary depending on the susceptibility whether at the site of injury (axon) or at the cell body imbedded in the spinal cord. This distinction helps understand the fundamental mechanism behind CIPN and how to develop effective strategies to combat axonal degeneration in patients who suffer from CIPN.

Independent to site of susceptibility, we determine mitochondrial trafficking response to treatment with chemotherapy drugs.[28] It is speculated that CIPN mechanism is induced through mitochondrial dysfunction caused by drug administration.[29] In this study, we determine the effect of each stated drug on mitochondrial trafficking and determine its correlation with CIPN. As mitochondrial motility is an essential subcellular mechanism for axon growth and general health, it is essential to understand how CIPN drugs effect mitochondrial trafficking.[30, 31] Using this information, new therapeutic strategies can be developed to enhance mitochondrial trafficking in CIPN patients.

2. Materials and Methods:

Preparation of compartmentalized chamber.

The master mold used to create the microchannels for the compartmentalized device was produced using a photolithographic method. Standard silicon wafers were coated with SU-8 2002 and spun and soft baked according to the manufacturer's specifications, to result in a thickness of 2.5-3 micrometers of the resist. The microchannels with the following dimensions: width of 10 micrometers, length of 500 micrometers, and depth of 3 micrometers, were cured by UV light exposure using high resolution DPI transparency. The same process was repeated using SU-8 3050 to help outline the chambers with a width of 3mm, and length of 13mm. Sylgard 184 polydimethylsiloxane (PDMS) (Dow chemical company USA) was used to conduct standard soft lithography, where it was poured onto the master micro-mold developed in house followed by the removal of bubbles by a desiccator (SP Scienceware, USA) and was allowed to cure overnight at 80°C. PDMS was removed from the master mold where two adjacent holes were punched using a 6 mm

diameter biopsy punch (Robbins Instruments). The dual compartmentalized chambers were then bonded to a thin glass slide (Fisher Scientific) using the Plasma Etch PE-75 Plasma Asher oxygen plasma device. After oxygen plasma bonding, the chamber devices were sterilized by autoclave before cell seating. Once sterilized, microchannels were cleaned using 98% ethanol (Carolina Biological) and further diluted out using Distilled water. Chambers were coated with Poly-D-Lysine (PDL) (Sigma-Aldrich) and Laminin (Corning) and left overnight at -4°C. Chambers were then washed thoroughly using media to prepare for cell seating. Chambers were then placed into a sterilized primary cell incubator, Binder C-150 UL Incubator.

Dorsal root ganglion culture.

All experiments related to animals were conducted in accordance with protocols approved by the Institutional Animal Care and Use Committee (IACUC). Dorsal Root Ganglion (DRG) neurons were isolated from an E-15 Sprague Dawley Rat. The DRG explants were then enzymatically dissociated with 0.25% Trypsin in L15 medium (Sigma Aldrich) and suspended in media. DRGs were maintained in Neurobasal medium containing 1 % fetal bovine serum (FBS), 20 % glucose, 1% penicillin/streptomycin, B-27 supplement, 2 M $_{L}$-glutamine, and 10 mg/ml glial derived nerve growth factor (GDNF) (Sigma Aldrich). Neurobasal media that contains 10 μM of Cytosine arabi-noside was added to the cultures, two days after seeding the cells, to help decrease the number of glial cells and other cell type contamination. To further limit evaporation, a small cotton ball soaked in sterile distilled water and 1.0% Penicillin/Streptomycin was placed in the same petri dish as the chambers. DRG neurons were seated into the marked somal chamber of the devices and left to grow for 5-7 days to allow for axons to grow through the channels into the axonal side at an adequate length.

Evaluation of FA Interference on Chemotherapeutic Activity

Human SKOV-3 Ovarian cancer cells were seated in a 96 well culture chamber using $1x10^4$ cells in 100 μL of media. SKOV-3 cells were incubated 24 hours prior to drug treatment. Cancer cells were then treated

using CDDP 10µM; MMAE 1µM; VCR 5µM; PTX 5µM respectively with varying concentrations of FA 10nM – 100nM. Cells were stained with Hoechst 33342 stain (Invitrogen) 48 hours after drug treatment in order to measure cell viability. Fluorescent images were captured using a Leica DMI8 thunder Microscope. Cell count was determined using Fiji-ImageJ, where fluorescent images were processed by, first, making the image 16 bit, then changing the threshold so that only the cells were identified. After threshold alteration, the image was converted to binary and made into a mask, where accurate cell count was measured using the analyze tool.

Preparation of cancer drugs.

Stock solutions for each anti-cancer drug were prepared using the necessary concentration needed for each experimental application and data concentration. A stock solution of 1 mM was prepared, where MMAE (Selleck chemicals) and VCR (Selleck chemicals) were dissolved in DMSO while CDDP (Sigma Aldrich) was dissolved in NaCl, and PTX (Selleck chemicals) was dissolved in ethanol, where they were then stored at -20 °C. The concentrations used were based off the Clinical concentration published [32], which demonstrate neurotoxicity in vitro models to help achieve similar conditions as those in real world application. Different concentrations for each of the drugs was made in culture medium using the stock solution for the dosage response, cell body and axonal treatment and stored in -4°C. The drugs were administered on either the cell body or the axonal side for each experiment by removing approximately 75% of the existing media and readministering with the drug in question. The cells were stained using calcein AM (ThermoFisher) dye for 30 mins- 1 hour and imaged using a Leica DMi8 Thunder Fluorescence Microscope immediately after the drug was administered as well as 24 hours after treatment. Mitoview Orange was obtained from Biotium, USA, and was used to stain the somal chamber containing cell bodies prior to drug treatment for 30 mins-1 hour. Mitochondria were imaged immediately after dilution of the dye using the Leica DMi8 Thunder Fluorescence and then again, 24 hours after initial imaging.

Data Analysis.

Data was collected using Fiji-ImageJ to measure axon lengths in triplicate samples. Microsoft Office Excel 2022 was used to compile all measurement data, where average and standard deviation was calculated. Axon integrity was found by calculating percent difference compared to the average control (0hr) for each sample. Differences in percent change were used to analyze the effect of site-specific treatment. All control samples are characterized by untreated conditions in complete neurobasal media.

Statistical Analysis.

All data sets were presented as a mean ± standard deviation except where noted. Data sets were grouped as triplicate. The probability *(P*-value*)* between groups was analyzed by the two-tailed *t*-test provided in Microsoft Office Excel 2022 unless otherwise stated. *P*-value less than 0.05 was considered statistically significant.

3. Results

Global Response.

Figure 1 illustrates the fundamental experimental design used to perform the site of action analysis. A microfluidic compartmentalized cell culture device was used to selectively isolate the cell bodies and axons for focal administration of anti-cancer drugs. Aside from the microchannels, the chambers were open air and were subjected to 5.0% Carbon Dioxide to maintain a high buffering capacity. The microchannels were able to hold approximately 250 µL of volume. Equal volume of media was placed into the chambers, making sure to keep hydrostatic pressure equal and prevent diffusion of media from one chamber to the next. After drug administration hydrostatic pressure was changed by adding an extra 50 µL of media to the untreated chamber to ensure the drugs would not diffuse to the adjacent (untreated) chamber. Axons traveled through the microchannels within 3-5 days and were monitored continuously until proper axon length could be determined.

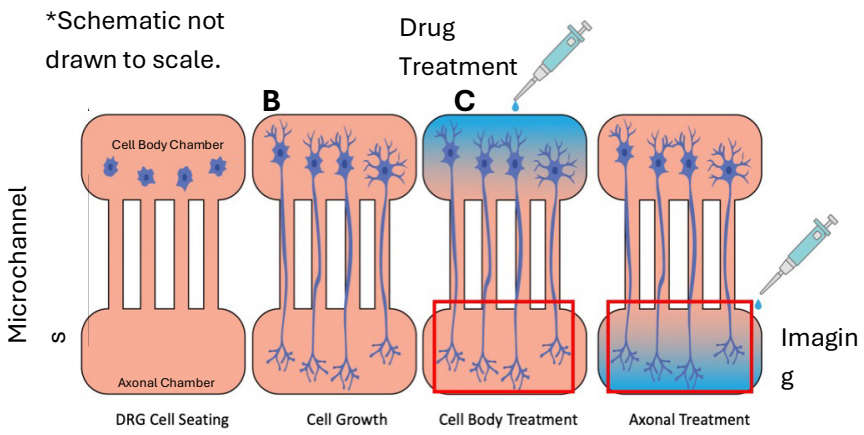

Figure 1.1. 2D-Schematic of experimental methods. Figure 1A illustrates the cell seating of the isolated DRG's. Figure 1B illustrates the illu h che f the isolated DRG's with chemotherapy drugs. The red box represents the region of examination by fluorescent microscopy.

To determine axonal susceptibility to CIPN, the dosage response of each chemotherapy drug was observed to understand the neurotoxicity on sensory DRG neurons. Different concentrations of each drug were analyzed based on previous literature and clinical data.[33-36] Global (cell body and axonal) response was imaged 24 hours after drugs were added. Fiji-ImageJ was used to measure axon lengths for each corresponding drug and concentration where axon length was analyzed. In Figure 2, we show the dosage response for each drug as well as each drug alongside FA and the control samples used were untreated DRG's that were under the same conditions and imaged at the same time as the other cells. Each drug induced a state of peripheral neuropathy on the sensory DRGs shown as a decrease in axon length. All drugs observed show that axon degeneration is dependent on dosage of each drug. Optimal concentrations of each drug were used for further analysis of axon susceptibility to CIPN.

DRG neurons were seated in a glass bottom 96 well cell culture system 24 hours prior to drug administration. After drugs were added in different concentrations, axon lengths were measured using Fiji-ImageJ. Shown in Figure 2 A-D, the axon lengths were measured in comparison to the control group. The neurotoxic effect of the chemotherapy drugs can be seen with in vitro conditions in Figure 2. Using the appropriate toxicity response of each drug observed, FA was added in conjunction to the drugs, and was used to determine the neuroprotective effect on the global cell treatment. Axon length measurements were

measured for each drug and corresponding FA treatment. The dosage response was used to identify the optimal concentration for each of the drugs, which is 10μM (1.67 mg/kg) for CDDP and 10μM/20nM for CDDP/FA, 1μM (0.1-3.2 mg/kg,) for MMAE and 1μM/20nM for MMAE/FA, 5μM (0.013-0.047 mg/kg) for VCR and 5μM/100nM for VCR/FA, 5μM (4.5-5.8 mg/kg) for PTX and 5μM/10nM for PTX/FA.

For CDDP 28.12 ± 37.28 μm was recorded, while FA treatment showed, CDDP/FA 217.66 ± 101.37 μm. For MMAE 20.47± 17.33 μm was recorded, while treatment showed, MMAE/FA 92.11 ± 21.71 μm. For VCR 47.42 ± 18.83 μm was recorded, while FA treatment showed, VCR/FA 39.39 ± 31.32 μm. Additionally, For PTX 102.85 ± 32.33 μm was recorded, while FA treatment showed, PTX/FA 198.82 ± 81.05 μm. Using the microfluidic cell culture platform, DRGs were seated in the cell body chamber where axons were allowed to grow through the microchannels, to the axonal chamber for 3-5 days. Cells were monitored every 24 hours until axons could be seen microscopically in the axonal chamber. Using the compartmentalized model, the site of action of chemotherapy drugs was analyzed to further understand the mechanism of toxicity. Drug concentrations were applied to the cell body *or* the axonal chamber, where axon lengths were recorded as seen in Figure 3&4. Imaging analysis was done at 0 and 24 hours for each drug. Axon lengths were measured using Fiji-ImageJ to understand the axonal susceptibility of each drug. Figure 3 represents drug treatment in the *axonal* chamber, showing 0 and 24 hours after focal treatment. Figure 4 represents drug treatment in the *cell body* chamber, where response was analyzed 0 and 24 hours after focal treatment. In Figure 3, axons are shown to be more susceptible to CIPN compared to cell body application in Figure 4. The chemotherapy drugs used, targeted axons of DRGs, demonstrating axonal susceptibility in CIPN.

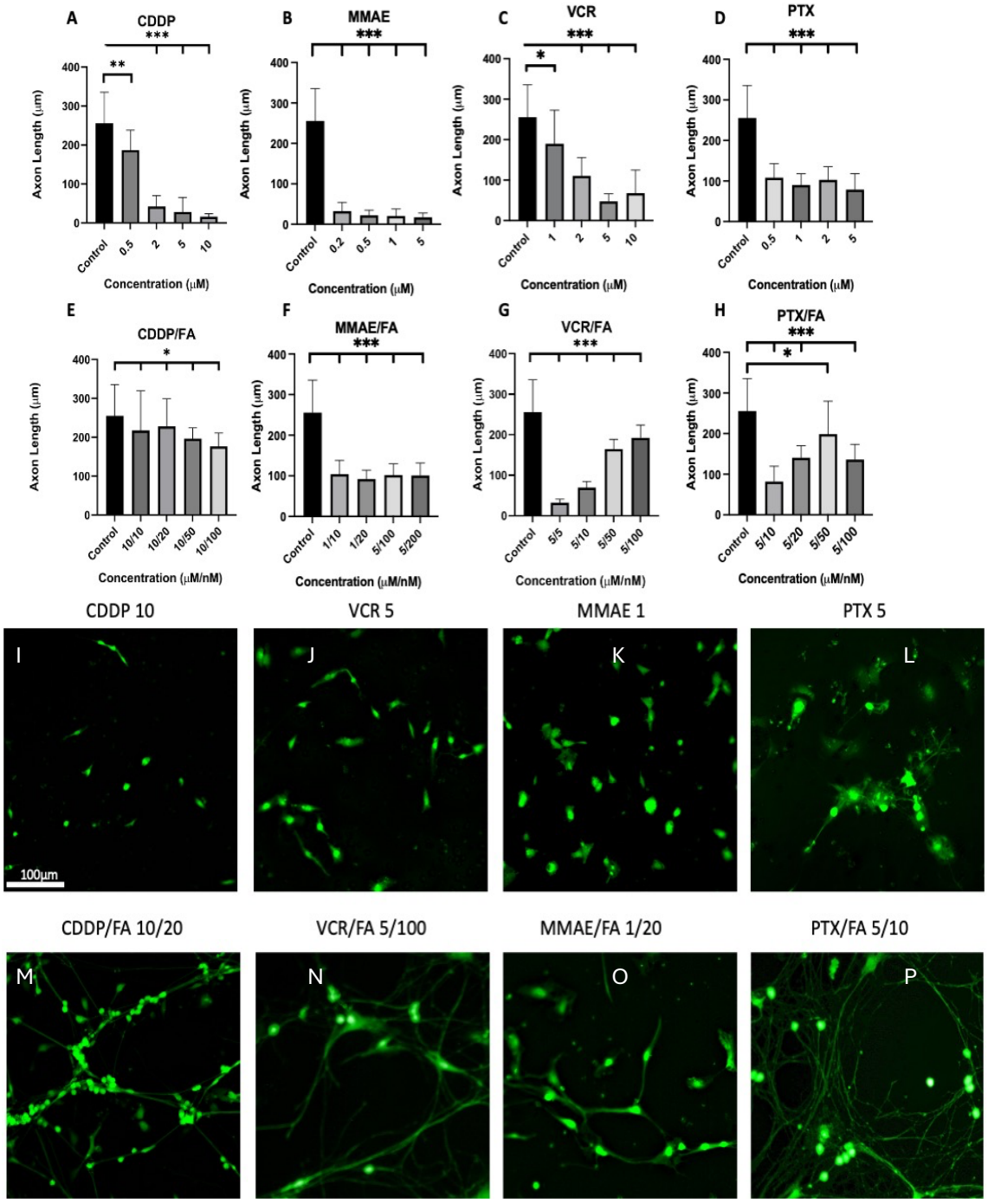

*Figure 1.2. Axonal response to local chemotherapy drug treatment. Axonal length measurement 24 hours after administration of chemotherapy drugs (A-D). Axonal length measurement of drug concentration with increasing FA concentration (E-H). Corresponding global treatment and cellular concentrations determined were, CDDP and CDDP-FA was imaged using 10μM and 10μM/20nM. MMAE and MMAE-FA was imaged using 1μM and 1μM/20nM.VCR and VCR-FA was imaged using 5μM and 5μM/100nM. PTX and PTX-FA was imaged using 5μM and 5μM/10nM. ***p<0.001.*

The dosage response data analyzed in Figure 2 allows for a better understanding of the global cellular response to chemotherapy drugs and their concentrations used in this study: PTX 5µM, MMAE 1µM, CDDP 10µM, and VCR 5µM. Analysis of PN induced by the selected drugs was performed in the same conditions to reduce any external effects. A noticeable decrease in axonal length is a result of peripheral neuropathy and was identifiable by comparison of the axonal length pre and post drug treatment. Based on the graphical data, a toxicity response of each chemotherapy drug was shown. Optimal concentrations based on Figure 2 were used for the remaining study. Clinical concentration of the chemotherapy drugs help highlights the concentrations used in the dosage graph to show each drugs neurotoxicity in comparison to real world application[27]. PTX was found to be administered at a dose of approximately 4.5-5.8 mg/kg,

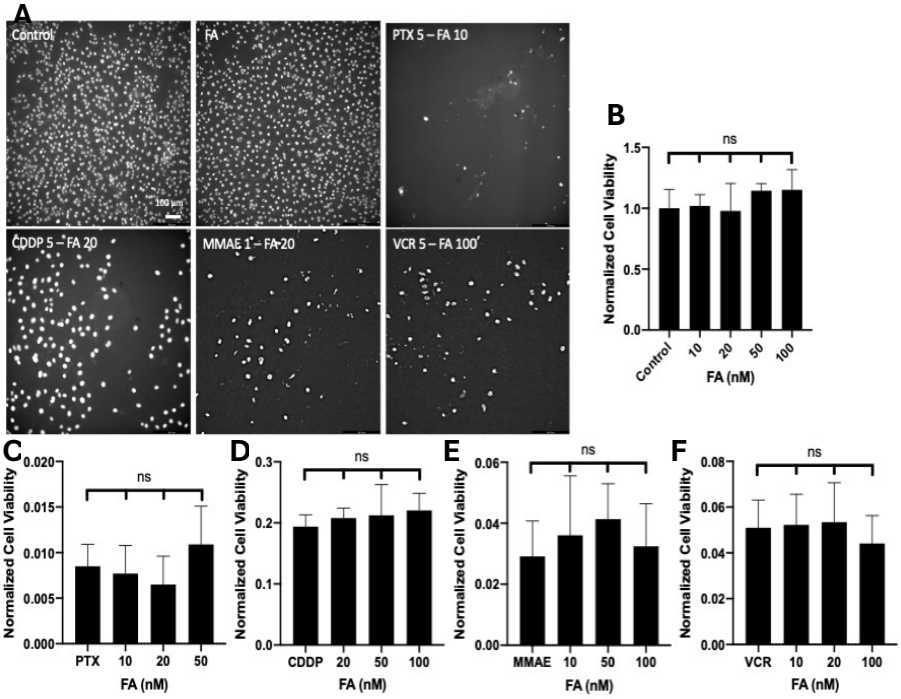

Figure 1.3 Anticancer effect of CDDP, MMAE, VCR, and PTX with varying FA concentrations.

with varying concentrations of FA, 20 nM, 50 nM, and 100 nM (D). MMAE treated samples at

MMAE at a [20] .047

mg/kg. Shown by Figure 2, FA had the ability to protect against degradation induced by CDDP, 55.21%, MMAE, 32.62%, VCR, 43.86%, and PTX, 48.27% compared to drug treatment without FA on average.

These values identify the neuroprotective effect of FA on the four different CIPN drugs outlined. Although there are different mechanisms for the drugs used, FA was found to be neuroprotective in all cases, and even resulting in similar protection levels.

In order to identify FA as a neuroprotective drug against common anticancer drugs, the effect of FA on the anticancer ability of each drug was characterized. SKOV-3 Human Ovarian cancer cell lines were used to determine the effect of FA at different concentrations used for the dosage response in Figure 2. Seen in Figure 3, Hoechst stain was used to identify cell viability count after 48-hour treatment. Based on the results, FA did not have any significant negative effect on the anticancer activity for each drug. Based on these results FA is shown to be an effective drug to test its neuroprotective ability on DRGs against common chemotherapy drugs. For CDDP cell viability of 0.1939% was recorded, while FA treatment showed, CDDP/FA was 0.2080%. For MMAE cell viability of 0.0291% was recorded, while FA treatment showed, MMAE/FA was 0.0360%. For VCR cell viability of 0.0510% was recorded, while FA treatment showed, VCR/FA was 0.0441%. Additionally, For PTX cell viability of 0.0085% was recorded, while FA treatment showed, PTX/FA 0.0077%. The maximum difference in cell viability seen by FA treatment was still seen to be less than 0.02% indicating a non-significant change. These results identify that FA does not inhibit anticancer effect of the drugs used, therefore it does not prevent the activity of the drugs from killing cancer.

Site of Action.

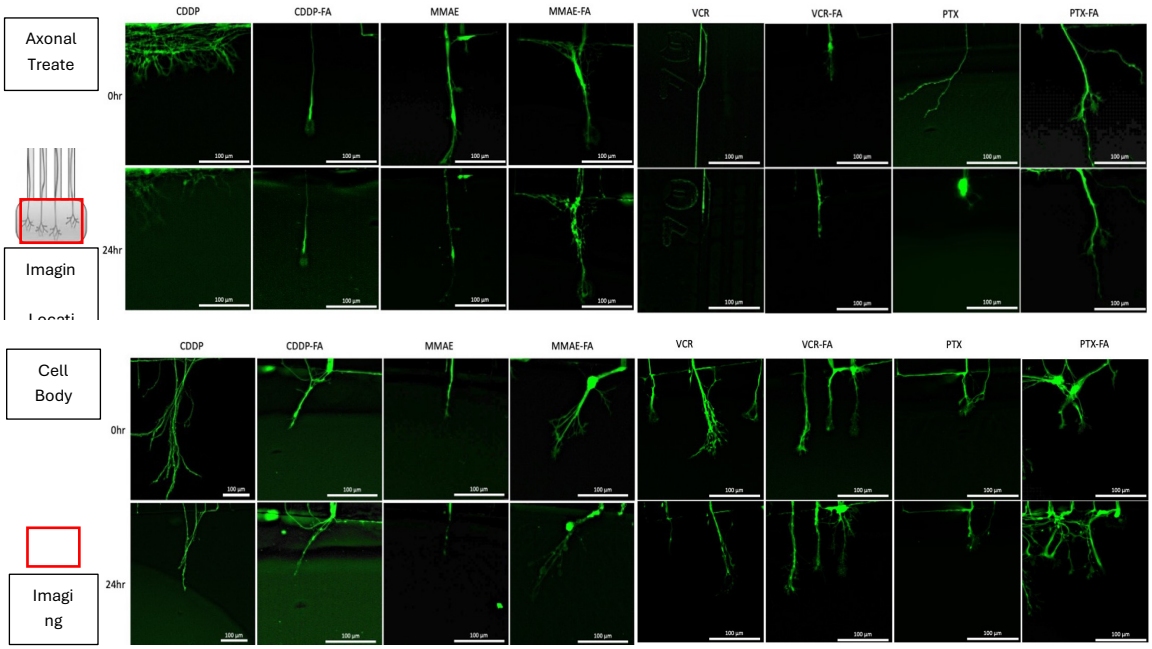

*Figure. 1.4 Axonal response to focal **Cell Body** treatment of chemotherapy drugs. Fluorescent images at 0 hours and 24 hours at the same location for each sample. CDDP (A) and CDDP-FA (B) was imaged using 10µM and 10µM/20nM. MMAE (C) and MMAE-FA (D) was imaged using 1µM and 1µM/20nM.VCR (E) and VCR-FA (F) was imaged using 5µM and 5µM/100nM. PTX (G) and PTX-FA (H) was imaged using 5µM and 5µM/10nM. Axonal response to focal **Axon** treatment of chemotherapy drugs. Fluorescent images at 0 hours (A-H) and 24 hours (I-P) at the same location for each sample. CDDP (I) and CDDP-FA (J) was imaged using 10µM and 10µM/20nM. MMAE (K) and MMAE-FA (L) was imaged using 1µM and 1µM/20nM.VCR (M) and VCR-FA (N) was imaged using 5µM and 5µM/100nM. PTX (O) and PTX-FA (P) was imaged using 5µM and 5µM/10nM.*

Axonal susceptibility was analyzed using the compartmentalized platform where drugs were added to the cell body and axonal chamber with FA treatment and the control samples used were untreated DRG's that were under the same conditions and imaged at the same time as the other cells. Shown in Figure 5 axon integrity was measured by comparison of axon length between 0- and 24-hour timestamps for each sample. Percentage integrity was determined based on the length difference compared to the control. Data collected shows the axonal susceptibility compared to the cell body response. Figure 5. Shows apparent axonal susceptibility with VCR and PTX, however as expected, CDDP is more susceptible on the cell body side

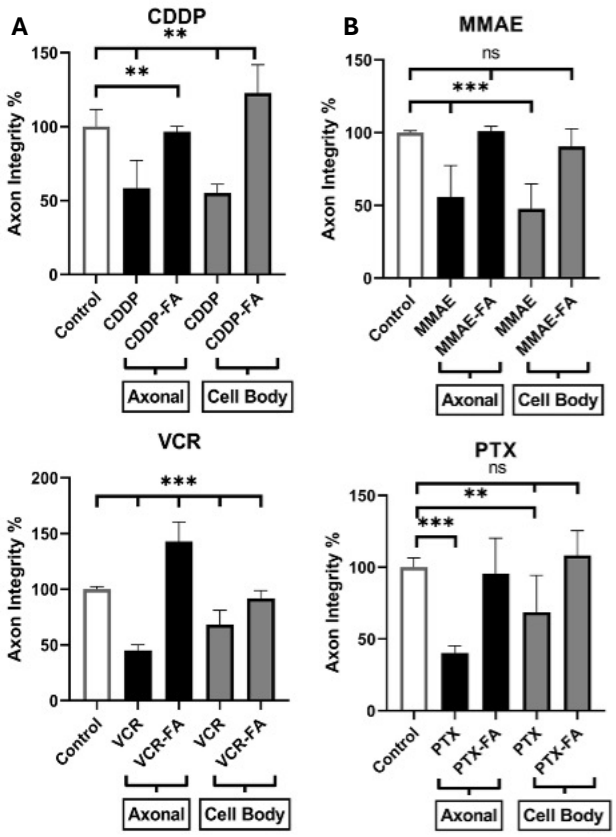

*Figure 1.5. Neuroprotective effect of FA on cell body and axonal administration. Each graph in the figure 5 represents axonal and cell body administration of each drug, and corresponding FA treatment. All samples were normalized and calculated as a percentage of axonal integrity compared to [illegible] control samples. Triplicate samples we[illegible] processed. CDDP (top left), MMAE (to[illegible] (bottom left), PTX (bottom right). ***p<0.001, **p<0.01.*

due to its different targeting mechanism. MMAE is seen to have similar results between the cell body and axonal treatment samples, with FA having a slightly higher neuroprotective effect with axon treatment. We believe that the high toxicity of MMAE could be the reason why there is no specific site of action observed for MMAE. Based on Figure 5. We have identified that FA is neuroprotective against both targeting mechanisms associated with CIPN. FA not only protected against PN for all drugs but even had some regeneration effect for both microtubule and DNA targeting mechanisms. Based on these findings we can assume that neuroprotection by FA can be attributed to enhanced mitochondrial trafficking.

Neuroprotection.

Figure 6. identifies the mitochondrial trafficking effect on axonal treated samples, with and without FA administration and the control samples used were untreated DRG cells were under the same conditions and imaged at the same time as the other cells. Fluorescent images of mitochondria were captured using Mito-Orange at 0hr and 24hr after drug treatment. The open-source Image J software was used to quantify mitochondria numbers along the microchannels. We used a size-based mask to identify the individual mitochondria (5-50 μm in size) typically observed in axons and to

eliminate fluorescent debris along the micro-channel. Figure 6. Shows clear mitochondrial inhibition due to CIPN degradation. Mitochondrial population decreased 73.45±9.57% for CDDP, 92.83±6.25% for MMAE, 45.58±24.67% for VCR, and 69.60±12.85% for PTX. For all drug samples, mitochondrial population was diminished significantly.

The treatment of FA alongside CDDP, MMAE, VCR, and PTX shows an increased mitochondrial number along the axons in comparison to the control sample. It is significantly noticeable in CDDP, where 83.45±9.57% increase is seen. This enhanced anterograde mitochondrial trafficking when treated with FA, resulted in axonal neuroprotection.

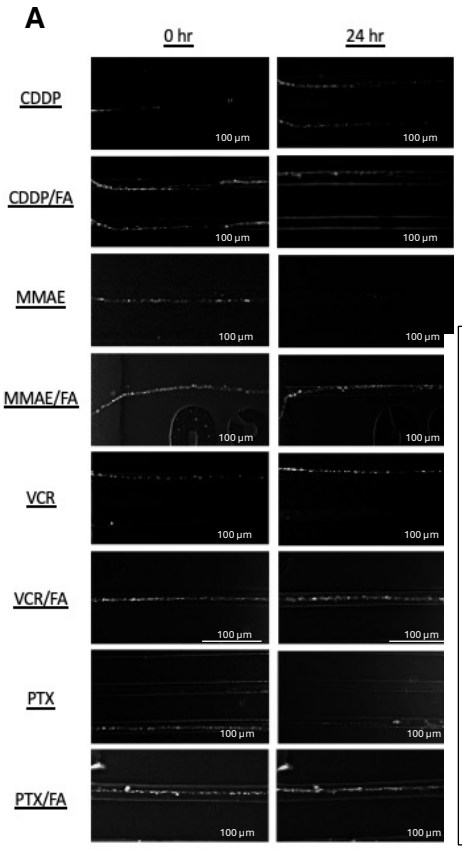

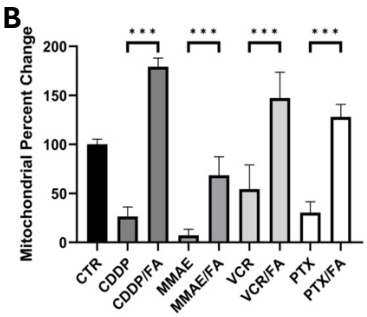

Figure 1.6: Mitochondrial trafficking effect on axonal administration of drug treated DRG's. Figure 6A, Mito-Tracker Orange was used to fluorescently stain mitochondria for axonal treated samples. Mitochondria were imaged at 0hr and 24hr in correspondence with the site of action experiments. All drug concentrations used were the exact same for axonal treated 5µM, PTX-5µM. Likewise with FA treatment 5µM/10nM. Mag. 63X. Fig 6B. Graphical representation of Mitochondrial Count analysis. Normalized percent change was

Using mitochondrial dyes, it is possible to see an increase in mitochondrial movement towards distal axons when focally treated. By comparison, it can be assumed that FA's effect on microtubules and mitochondria is a primary factor for neuroprotection against CIPN onset. Data provided shows that FA was neuroprotective against CDDP 39.5% in axonal focally treated samples as seen by Figure 5A. Initially it

was assumed that CDDP would not have a negative effect on cells when focally treated on axons, however, it was clear to see CIPN induced from CDDP focally treated axons in vitro. Data provided showed that CDDP directly affects the distal axons of DRGs, and FA was found to be neuroprotective in axonal treated samples. This new finding is exciting to develop a better understanding of the mechanism of CIPN induced by CDDP as well as the neuroprotective mechanism of FA on CIPN.

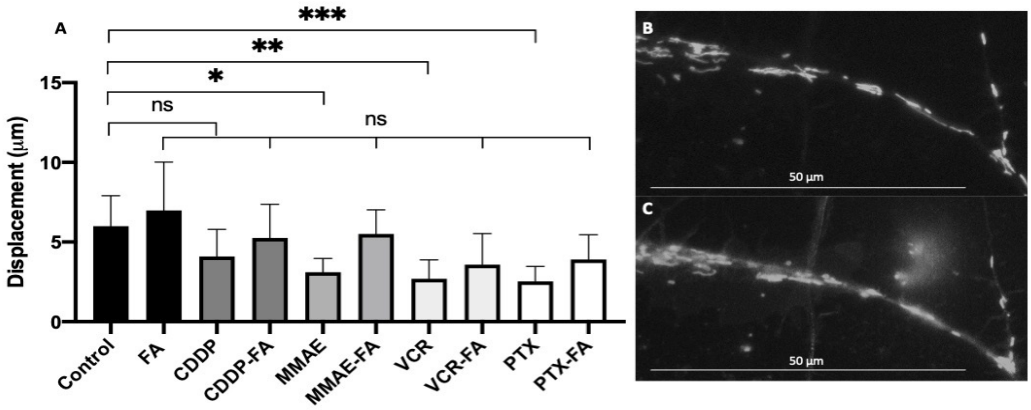

Figure 1.7. Mitochondrial Displacement during a 30-minute timelapse. Measured

Mitochondrial motility was characterized by performing timelapse imaging of fluorescently stained mitochondria over a 30-minute time period with 1-minute intervals. Displacement was measured using Fiji-ImageJ where mitochondria movement can be seen to decrease when treated with chemotherapy drugs. Figure 7A shows FA's ability to increase mitochondrial displacement during the 30-minute period compared to non-FA treated samples.

4. Discussion

Peripheral Neuropathy (PN) is a common and dose-limiting side effect frequently observed in patients undergoing chemotherapy treatment.[37] Previous studies have not identified the site of action or specific

mechanism of the degenerative effect that takes place.[38, 39] The in vitro microfluidic device used in this study allowed for demonstration of axonal and cell body susceptibility to CIPN and FA neuroprotection. This model enabled us to separately treat the cell body and axonal compartment for each drug sample and examine the degenerative result, which helped clarify important mechanisms behind axonal degeneration induced by CIPN.[40]

Although degeneration effects were seen using the global, cell body, and axonal models, based on the graphs in Figure 5, it is clearly seen that axons are more susceptible to degradation in focal axonal treatment on average for MMAE, VCR, and PTX. However, CDDP was seen to cause higher levels of degradation with cell body exposure, as expected from our initial hypothesis as it is a known DNA replication disruptor.[26] CDDP was the only platinum-based drug that primarily targeted the DNA replication while the other chemotherapy drugs targeted microtubule structure. Since the vast majority of DNA is located in the cell body, CDDP was expected to have significantly higher degeneration effect when exposed to the cell body. However, this poses the question, if CDDP primary targets the cell body, why does it cause peripheral neuropathy rather than acute cell death? Likewise, why does CDDP also result in degeneration when cell bodies are not exposed?

Previously, it had been determined that FA was found to be neuroprotective against PTX induced CIPN.[41] Based on these findings, FA was treated alongside MMAE, VCR, and CDDP to determine the neuroprotective mechanism against the drugs using microfluidic chambers. Similar to PTX; MMAE and VCR directly target the microtubules of the cell, leading to inevitable cell death. Herein, we focally administered FA to each drug treated sample to gain a better understanding of its neuroprotective mechanism against CIPN. Optimal concentrations were used based on the global dosage response data provided in Figure 2. Based on the data collected, our results have shown that FA is neuroprotective against CIPN for each drug analyzed, leading us to assume that FA targets a mechanism involved with microtubule formation and organelle transport. FA was also found to be neuroprotective against CDDP which is known to affect DNA replication. Focal administration of FA treatment with CDDP shows neuroprotection against

CIPN in vitro. Recently, we discovered FA's role in mitochondrial transport and its effect on retrograde and anterograde mitochondrial trafficking.[41] Previous studies have identified mitochondrial dysfunction associated with PIPN, however they do not discuss the mitochondrial effect of other common CIPN drugs.[42] Studies have shown that CDDP directly affects the DNA of neuronal cells, however, we have shown neuroprotective effect of FA alongside CDDP when administered focally on distal axons.[43] The neuroprotective effect of FA shows that CDDP may not affect only DNA in the nucleus of the cell, but also the DNA of mitochondria in the axon.[44] Based on this, it is believed that FA enlists mitochondrial movement, and recruitment at the site of injury.[41] FA is likewise known to suppress membrane permeability due to its nature as a corticosteroid.[45] The ability to suppress membrane permeability is a potential reason as to why CDDP is unable to effect mitochondria as compared to without FA treatment. By blocking CDDP from permeating mitochondrial membrane, FA is able to protect axonal mitochondria from damage.

Mitochondrial motility characterized by Figure 7 shows an increase in mitochondrial movement when treated with FA compared to non-FA treated samples. Although figure. 7 shows minor increases in movement, this can be attributed to experimental conditions associated with timelapse imaging. Significant changes in axonal structure, mitochondrial movement, and dye degradation make timelapse imaging difficult to produce accurate results. For this reason, the immediate effect of FA on chemotherapy treated samples was determined by treating cells one hours prior to imaging. Due to the time-dependent nature of the chemotherapy drugs tested, significant axonal degeneration, and mitochondrial dysfunction may not be able to be shown by this result. However, the immediate change in mitochondrial trafficking helps give a better representation of motility associated with drug treatment. Although the results shown do not show drastic differences, Figure 7. Shows an accurate representation of the immediate effect on mitochondrial trafficking by chemotherapy drugs and FA treatment. Further velocity characterization is needed to identify the full effect of chemotherapy drug treatment on mitochondrial trafficking, along with FA treated samples.

As expected PTX, VCR, and MMAE had a greater effect on degradation when focally treated on axons. Due to the neuronal cell structure, microtubule formation is key for nutrient transport.[46] Sensory neuron cells have an average axon length that can reach up to 1.5 meters, requiring more microtubules to ensure proper nutrient support.[47] For this reason, the degeneration effect of PTX, VCR, and MMAE were expected to be higher when treated in regions with more microtubules. MMAE however shows similar results for cell body and axonal treatment. It is believed that MMAE site of action may be difficult to determine due to its high toxicity level.[48] MMAE has a similar mechanism to PTX and VCR and shows great neuroprotection with the treatment of FA, however due to the high toxicity, it is difficult to specifically determine the site of action given the concentrations. Further research regarding the high toxicity response of MMAE is needed to conclude this finding in detail. While for CDDP, the degeneration effect was greater when treated on the cell body side due to the site of action that targets DNA replication, where majority of the DNA is located in the cell body region. Understanding the site of action of the drugs allowed for a better understanding of the delivery mechanism of CIPN. FA was treated alongside each of the drugs to examine its neuroprotective site of action effect. Although FA was neuroprotective in all treatment methods, the higher effect of neuroprotection on axonal treated samples can be seen by Figure 5. These results suggest that the use of FA as a treatment option for CIPN is more effective when focally treated at the site of injury.

To answer these questions, we presume that each of the drugs used, has the ability to negatively affect an aspect of mitochondrial trafficking within the axon and cell body.[41] PTX, VCR and MMAE typically affect microtubule formation, and structure leading to the degradation of these microstructures which in turn negatively affects mitochondrial transport in the axon.[11, 49] Within the axon of a neuronal cell, the microtubules have the vital function of sending organelles to and from the tip of the axon, or growth cone. Without proper nutrient transport, we assume that the cell slowly dies due to the decrease in mitochondrial trafficking and therefore energy availability.[50] The lack of nutrient transport could be a groundbreaking mechanism for understanding why dying back neuropathy occurs in CIPN patients.[28, 51] Although CDDP has a greater effect on the cell body than axons, we believe that CDDP also has the ability to target

mitochondrial DNA within the axon, affecting energy transport, which in turn causes peripheral neuropathy. Based on CDDP's ability to cause degeneration when focally treated to axons, it must have a mechanism that targets within the axonal section of the neuron. Since mitochondria are the only organelle aside from the nucleus to have DNA, we believe CDDP has the ability to disrupt the mitochondrial DNA replication cycle.[52] To prevent against CIPN, it is imperative to develop a deeper understanding of the functional mechanism behind it. From this experiment, treatment methodologies can be created to focally target the site of action of CIPN. Considering that FA is neuroprotective against the 4 different chemotherapeutic drugs tested, we believe that more research needs to be done to be able to identify whether axonal transport is a primary or secondary effect as a result of peripheral neuropathy.

5. Conclusions

Using the in vitro model, axonal susceptibility to chemotherapy drugs along with the neuroprotective mechanism of FA was analyzed using a compartmentalized microfluidic system (Figure 2-5). Key results from this experiment show higher axonal susceptibility to microtubule targeting anti-cancer drugs and FA induced mitochondrial trafficking leading to neuroprotection[41]. The largest difference in axon integrity was shown with VCR, where cell body showed 31.80% decrease in axon integrity while axonal treated sample showed 54.89% decrease in axon integrity. This shows that for VCR, axons were 23.1% more susceptible to axonal compared to cell body treatment. For the other drugs analyzed; axons were 20.21% more susceptible to *axonal treatment* for PTX, and 7.97% more susceptible for MMAE. DRGs were more susceptible to *cell body treatment* 3.27% for CDDP. For the samples analyzed, FA was found to have higher neuroprotection at the site of susceptibility. FA was 51.06% more neuroprotective for axonal treated VCR, 15.24% for PTX, and 10.51% MMAE. On the other hand, FA was 26.66% more neuroprotective for cell body treated CDDP. The results demonstrate important findings regarding the mechanism of CIPN and the neuroprotection by FA. Enhanced mitochondrial trafficking by FA proved increased neuroprotection for all CIPN models. Disregarding the mechanism of action for chemotherapy drugs, FA was found to be an effective neuroprotection strategy in vitro. Through subcellular mitochondrial trafficking analysis, we

found that any form of enhanced trafficking may lead to increased neuroprotection against CIPN. The information gathered from this experiment can potentially lead to coadministration of chemotherapy drugs and further create a lower risk of CIPN. In this study, the site of action for each chemotherapy drug, CDDP, MMAE, VCR, and PTX was determined to help develop a better understanding of CIPN targeting mechanisms. FA was treated alongside each chemotherapy drug to identify the neuroprotective effect against CIPN, where FA was found to be neuroprotective for all drugs tested. This study found that treatment with FA led to an enhancement in the anterograde movement of mitochondria based on fluorescent imaging. Additional studies need to be performed to understand the fundamental mechanism and signaling pathways associated with enhanced mitochondrial trafficking. In vivo characterization of mitochondrial trafficking enhancement is necessary to fully consider FA as a neuroprotective treatment against CIPN.

Author Contributions

Bayne Albin: Conceptualization, Methodology, Validation, Formal analysis, Writing, Visualization. **Khayzaran Qubbaj:** Conceptualization, Methodology, Validation, Formal analysis, Writing. **Arjun Prasad Tiwari:** Methodology, Validation, Visualization, Supervision. **Prashant Adhikari:** Methodology, English correction. **In Hong Yang:** Conceptualization, Validation, Visualization, Supervision, Resources, Project administration, Funding acquisition.

Statement of Declaration of Interest

There are no conflicts of interests among authors.

Acknowledgements

This research was supported by the College of Engineering (COEN) Seed Grant (101502) and faculty start-up fund Department of Mechanical Engineering and Engineering Science, UNC Charlotte (100041). This Research was also supported by the National Science Foundation (NSF) Career Award (2238723).

Human SKOV-3 Ovarian cancer kindly provided by Dr. Mukherjee from the Biology Department at UNCC.

CHAPTER 2: ELECTRICAL STIMULATION ENHANCES MITHOICNDIRAL TRAFIFKCING AS A POTENTIAL NEUROPROTECTIVE MECHANSIM AGAINST CHEMTOHERAPY INDUCED PERIPHERAL NEUROPATHY

Based on the promising results from the first study, this project shifted to develop an electrical stimulation device to examine the correlation between external excitation and enhanced mitochondrial trafficking. Due to the steroid nature of Fluocinolone Acetonide (FA), we believe that FA has the ability to alter metabolic activity within neurons, which leads to mitochondrial trafficking enhancement and neuroprotection. To test this theory, we developed an electrical stimulation device to deliver an external pulse pattern to Dorsal root ganglion neurons in vitro. Due to previously observed neuroprotective roles of ESTIM, along with its ability to modulate neural activity, we believed that ESTIM has the ability to alter mitochondrial trafficking similar to FA. Paclitaxel (PTX) and Oxaliplatin (L-OHP) were studied due to their role in dying back neuropathy. PTX and L-OHP were similarly chosen due to their differences in cancer killing mechanism to understand if ESTIM effected only one or both types of drugs. Furthermore, this study observed how focal stimulation using a microfluidic compartmentalization platform affected modulation of cellular and subcellular dynamics of DRGs. Results from this study found that low frequency (>1kHz) ESTIM enhanced mitochondrial trafficking and reduced axonal degeneration by chemotherapy drugs. Focal stimulation had insignificant differences in enhancement of axon length or mitochondrial trafficking, leading us to believe that neuromodulation is not site specific. These findings are essential to development of neuromodulation techniques for the peripheral and central nervous system. Stimulation of axon fibers, or cell bodies within the CNS had similar effects, which allows for focal stimulation devices able to target specific tissues and injury sites. Results from this study show enhanced mitochondrial trafficking by low frequency (>1 kHz) electrical stimulation for the first time as we know. The impact of this study will help engineers and researchers develop modulation devices to treat neurological disorders without the need for potentially toxic drugs.

Electrical Stimulation Enhances Mitochondrial Trafficking as a Neuroprotective Mechanism Against Chemotherapy Induced Peripheral Neuropathy

Bayne Albin[1], Prashant Adhikari[1], Arjun Prasad Tiwari[1], Khayzaran Qubbaj[1], In Hong Yang[1]*

[1]Center for Biomedical Engineering and Science, Department of Mechanical Engineering and Engineering Science, University of North Carolina at Charlotte, Charlotte, North Carolina 28223, United States

* Corresponding author: In Hong Yang; E-mail: iyang3@charlotte.edu

Abstract:

Electrical stimulation (ESTIM) has shown to be an effective symptomatic treatment to treat pain associated with peripheral nerve damage. However, the neuroprotective mechanism of ESTIM on peripheral neuropathies is still unknown. In this study, we identified that ESTIM has the ability to enhance mitochondrial trafficking as a neuroprotective mechanism against Chemotherapy Induced Peripheral Neuropathies (CIPN). CIPN is a debilitating and painful sequalae of anti-cancer chemotherapy treatment which results in degeneration of peripheral nerves. Mitochondrial dynamics were analyzed within axons in response to two different antineoplastic mechanisms by chemotherapy drug treatments, Paclitaxel (PTX) and Oxaliplatin (L-OHP) in vitro. Mitochondrial trafficking response to chemotherapy drug treatment was observed to decrease in conjunction with degeneration of distal axons. Using low frequency ESTIM, we observed enhanced mitochondrial trafficking to be a neuroprotective mechanism against CIPN. This study confirms ESTIM enhances regeneration of peripheral nerves by increased mitochondrial trafficking.

Key Words:

Chemotherapy induced peripheral neuropathy; axonal degeneration; paclitaxel, oxaliplatin; neuromodulation, electrical stimulation, mitochondrial trafficking.

Introduction

The use of electrical stimulation (ESTIM) on peripheral nerves has been well studied since 1967, when Wall and Sweet reported on the use of ESTIM for pain relief for the first time {Melzack, 1965 #70}. For the past 50 years, neuromodulation has been implemented in many ways to reduce pain, or as a treatment method for neurological diseases and conditions [53]. Although peripheral nerves have significant regenerative capabilities compared to other cell types, functional recovery is proven to be poor. ESTIM is currently available to the public as a treatment strategy to mitigate pain seen in the form of a Transcutaneous Electrical Nerve Stimulator (TENS) {Ragnarsson, 2008 #78}. ESTIM is approved for a variety of clinical situations, including physical therapy, spinal cord injuries, neuro-prosthesis, mental health, and neuropathy among others {Abd-Elsayed, 2021 #79;Zhao, 2022 #80;Hamid, 2008 #81}. Many researchers believe that the use of ESTIM on peripheral nerve injuries may be a key therapy for peripheral nerve regeneration in clinical settings[54]. Pulsed electrical stimulation has shown to be an effective treatment strategy for peripheral injury conditions [55, 56]. Previous studies have shown that using a low frequency (>100 Hz) pulsed biphasic stimulation for 1hr per day is able to increase sensory nerve regeneration and myelination. Low frequency stimulation is also considered to be optimal conditions for nerve growth and protection [54, 57-59], however it is important to identify a larger range of frequencies to fully understand the effect of ESTIM against CIPN by PTX and L-OHP {Geremia, 2007 #73;Willand, 2016 #7;Yang, 2012 #16}. Although ESTIM has been a well-researched phenomenon, the underlying mechanism regarding peripheral nerve regeneration is poorly understood.

Mitochondrial population and trafficking are significant indicators of neuronal health [60]. Low population and trafficking of mitochondria along the axons can be directly related to low energy production, which in turn can lead to peripheral nerve degeneration and cell death [61]. Energy demands within the neuron change dependent on location, circumstance and injury [62]. For example, the growth cone and synapse require significant energy resources in order to deliver signals to target locations [63]. Due to this high, dynamic energy demand, mitochondria are needed in different locations as well as in different densities to supply energy in the form of ATP on demand [64]. Mitochondrial trafficking and dynamic responses help

maintain homeostasis regarding energy demands. Neuronal activity has been found to affect mitochondrial trafficking responses, where increased signaling and neuronal activity increases mitochondrial trafficking in localized regions of the neuron [65]. The dynamic nature of energy distribution by mitochondrial trafficking is an important mechanism to understand, due to increased energy demands in a disease state such as CIPN [66, 67]. The effect of specific drugs and treatment methods on mitochondrial transport can help provide an indication on the targeting mechanism for such treatment strategies. Using this information, better methods can be developed to alter subcellular trafficking for neuroprotection. Using imaging techniques, it is possible to determine the trafficking response and communication between transport mechanisms.

Chemotherapy Induced Peripheral Neuropathy (CIPN) is a debilitating health condition associated with common chemotherapy drugs [27]. CIPN is a painful side effect of chemotherapy treatment which affects 67% of all cancer patients undergoing chemotherapy treatment {Park, 2013 #69}. Chemotherapy is an effective treatment method targeting the cancer cell division process, to eliminate cancer from the body. However, there are many adverse side effects as a result of chemotherapy treatment, including Peripheral Neuropathy (PN). Currently, there are no treatment methods for peripheral neuropathy other than symptom mitigation[68]. CIPN is the most common dose limiting factor during chemotherapy treatment, oftentimes leading to suboptimal conditions to fight cancer, and even termination of treatment in extreme cases. Using this knowledge ESTIM is shown to be an effective treatment option against common Chemotherapy drugs, Oxaliplatin (L-OHP) and Paclitaxel (PTX). L-OHP and PTX were chosen due to their common application in chemotherapy treatment which results in CIPN, as well as to compare against different targeting mechanisms.

PTX is known as an effective agent in disrupting the cell division cycle of cancer cells by targeting the microtubules associated with mitosis [69]. PTX is primarily used against Breast, Lung and ovarian Cancer types [70]. Due to the microtubule targeting effect of PTX, it can be assumed that PTX is directly related to axonal trafficking. The effect of ESTIM on PTX induced peripheral neuropathy (PIPN) was studied

based on our recent study identifying Fluocinolone Acetonide (FA) as a neuroprotective agent, which enhances mitochondrial trafficking leading to neuroprotection against common CIPNs [41]. To fully understand the mechanism of neuroprotection by ESTIM, another drug with different targeting mechanism is needed for comparison. L-OHP is a third-generation platinum based antineoplastic chemotherapy drug primarily used to target colorectal, and stage III colon cancer [71]. L-OHP targets the DNA replication cycle by binding to DNA strands and disrupting the transcription process within cancer cells [72]. DNA damage associated with L-OHP treatment is crucial to anti-cancer treatment as it can disrupt tumor development. CIPN is the leading side effect associated with L-OHP treatment, which can cause major discomfort and pain leading to dosage reductions for patients [73]. The specific mechanisms of toxicity in CIPN for L-OHP are still unknown, however it is speculated that transporter mediated uptake of L-OHP triggers pathophysiological changes seen as disrupt cell signaling cascades, mitochondrial disfunction and oxidative stress in dorsal root ganglion neurons (DRGs), L-OHP also has been noted to have a higher toxicity effect on mitochondria within targeted cells [74, 75]. Using this information, we seek to determine if ESTIM is capable of protecting mitochondrial transport even when directly targeted by L-OHP. Therefore, L-OHP and PTX were chosen to determine if ESTIM was effective at enhancing mitochondrial trafficking and subsequent neuroprotection. The two different mechanisms of action for these drugs are the most commonly used types of chemo drugs, and it is important to understand how ESTIM effects both mechanisms. In order to analyze the effect of ESTIM mediated neuroprotection against PTX and L-OHP induced peripheral neuropathy, axon length responses were measured with varying pulsed electrical stimulation frequencies (10Hz-1MHz). DRG's were similarly stimulated using a compartmentalized cell culture chamber to determine the effect of the frequency range on mitochondrial trafficking. Frequencies which showed positive axon length and mitochondrial responses were used in conjunction with PTX and L-OHP to determine the neuroprotective effect against CIPN. This is the first time that ESTIM is shown to have the ability to enhance mitochondrial trafficking in axons that guarantees neuroprotection against CIPN.

Results

Experimental Set-Up

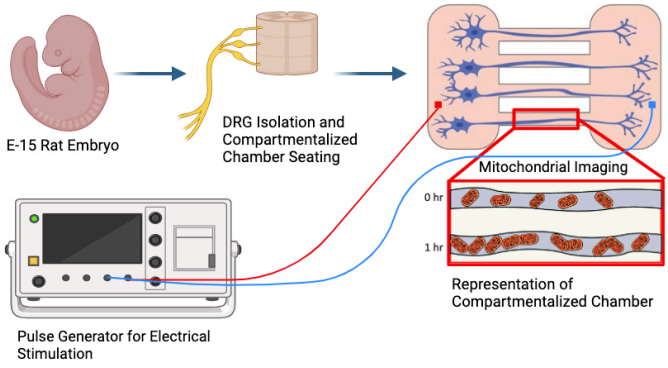

Figure. 2.1 . Experimental Schematic. E-15 Sprague Dawley rat embryonic Dorsal Root Ganglion (DRG) isolation and enzymatic disassociation. Processed DRGs plated into the cell body chamber of the compartmentalized chamber system. Cells are allowed to grow for 3-5 days until they grow through the channels to the axonal compartment, where chemotherapy drugs and dyes are administered. Electrical stimulation was performed for 1 hour per day using a constant 3V power supply to generate a biphasic rectangular pulse lasting 0.5s every 2s with a pulse width of 0.2 ms. Imaging of axons was completed in the axonal compartment, while mitochondrial trafficking imaging was performed within the parallel micro-channels. Created with BioRender.com

Figure. 1 illustrates the experimental ematic for the outlined ESTIM eriments. DRG neurons were lated and processed from E-15 gnant rats and cultured on a custom well compartmentalized culture te seen in Figure. 2.1. emotherapy drugs and fluorescent s were treated in culture chambers l incubated for 1 hour prior to TIM. ESTIM was performed by ding bi-phasic square pulse wave nals from a Siglent waveform generator to platinum electrodes attached to the lid of the culture device. Imaging using a Leica-DMi8 Fluorescent Microscope was performed before and after one hour of stimulation to determine axon length or mitochondria trafficking response.

Global Stimulation Frequency Response

To determine the effect of each frequency on axon length, DRGs were seated in a non-compartmentalized sterile 24 well glass bottom cell culture plate shown in Figure. 2A. DRGs were cultured and allowed to grow for 24 hours prior to stimulation. 1 hour stimulation at 10 Hz, 100 Hz, 1 kHz, 100 kHz, and 1MHz was induced to the cells once per day for 3 days shown in Figure. 2B, C. Cells were treated with Calcien AM and imaged before and after stimulation using a fluorescent microscope. Fluorescent images were

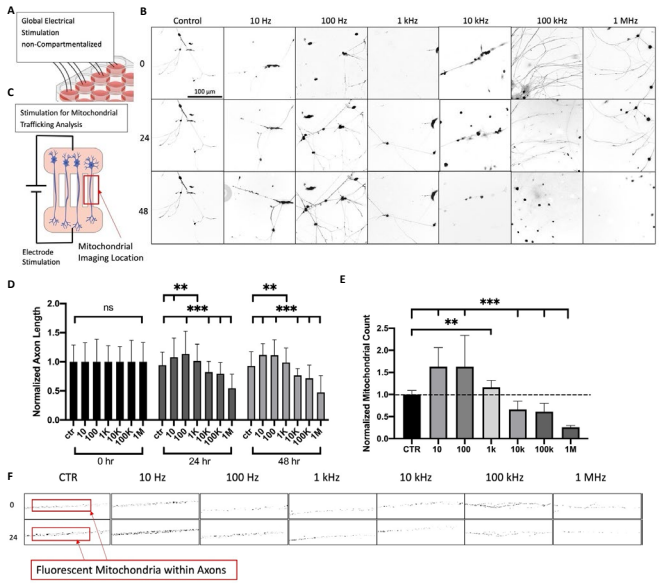

Figure. 2.2. Pulsed Electrical stimulation enhances Axon growth and Mitochondrial Trafficking. Schematic for global DRG stimulation for axon length measurement analysis (A). The axonal response after stimulation for 0, 24 and 48 hours, for 10Hz, 100Hz, 1 kHz, 10 hHz, 100 kHz, and 1 MHz showed that low frequency (10 Hz, 100 Hz and 1 kHz) proved to enhance axon length measurements at each timestamp (B). Mitochondrial imaging was performed in a compartmentalized microfluidic chamber to identify the immediate trafficking response to each frequency (C). Quantification of normalized axon length measurements were used to compare against the initial 0hr length (D). Mitochondria were shown to increase between the 0hr and 1hr stimulation for low frequency stimulation parameters (E). Mitochondria were imaged before and after 1hr stimulation to identify the trafficking enhancement by ESTIM (F). It was proven that 100 Hz stimulation enhanced mitochondrial trafficking the most compared to control samples (E). Data is shown by mean ± SD. ***P<0.001, **P<0.01, *P<0.05 as determined by two-tailed t test (E), Scale bar is 100 µm unless otherwise stated.

processed using Fiji-ImageJ to measure axon length at each corresponding frequency and timestamp. As seen in Figure. 2 B, C, the frequency response was characterized, where low frequencies (>1 kHz) enhanced axon growth, whereas high frequencies (<1 kHz) had a detrimental effect on axon length. Over the three-day stimulation period, 10 Hz accelerated growth 9.71±0.26%, 100 Hz accelerated growth 12.28±0.33%, 1 kHz accelerated growth 0.07±0.27%, whereas 100 kHz inhibited growth 24.43±0.21%, 1 MHz inhibited growth 49.03±0.27%. Based on these values, optimal frequencies were chosen when preforming the experiment alongside chemotherapy drugs to characterize the neuroprotective effect of each frequency. Seen in Figure. 2B, representative figures for 0, 24, and 48 hours when exposed to the 5 different frequencies are shown. Graphical representation of Axon length as a comparison to the control can be seen from Figure. 2C. After 24 and 48 hours, 100 Hz had the highest growth rate. These results are found to be consistent with current research, showing low frequency stimulation to have the largest positive impact on axon growth.

Fluorescent imaging of mitochondria was performed for each frequency to characterize the trafficking response to the full frequency range (10 Hz – 1 MHz). In order to properly measure the frequency response

on mitochondrial trafficking, DRG's were seated into the PDMS-based microchannel device and allowed to grow for 3-5 days in order to ensure proper growth through the microchannels. Mito-View Green dye was then added to the cell body chamber and incubated in correspondence with manufacturers protocol. Fluorescent imaging of mitochondria before and after stimulation at each frequency can be seen by Figure. 2G. The specific timestamps in Figure. 2C were chosen to measure the direct impact of each frequency on mitochondrial count after 1 hr stimulation. Variables, such as dye degradation, media changes, and light exposure had the potential to skew data if recorded over an extended period of time, therefore, mitochondrial images were collected directly before and after 1hr stimulation at each frequency. A microfluidic compartmentalized cell culture system was used to properly stimulate and identify mitochondrial movement within the axons. Using a parallel array of microchannels, DRG's were compartmentalized in order to fully isolate the cell bodies from the axons. By doing this, axons are aligned perfectly within the microchannels, enabling us to image and count mitochondrial population at each timestamp. Mito-View Green dye was placed into the cell body chamber of the compartmentalized system, while neurobasal media was added in higher volume to the axonal chamber, inducing hydrostatic pressure to prevent excess dye diffusion. Cell body dye administration further helped show anterograde movement of mitochondria to focus on the change in energy demand at the site of injury during CIPN. Using this data, we were able to understand how mitochondria were affected by the initial stimulation. After 1 hour stimulation, mitochondria population increased 62.79±0.43% for 10 Hz, 62.59±0.71% for 100 Hz, 15.96±0.16% for 1 kHz, however decreased 38.90±0.19% for 100 kHz, and 74.28±0.04% for 1 MHz. All values were normalized according to the 0-hour control count to provide a proper increase/decrease ratio. Values above '1.0' represent an increase in mitochondrial number, whereas values below '1.0' represent a decrease. The trends seen in the results for mitochondrial population match those with axon length measurements leading us to believe electrical stimulation directly modulates mitochondrial trafficking, and other subcellular axonal trafficking mechanics to increase axonal growth.

Global Electrical Stimulation as a Neuroprotective Method Against CIPN

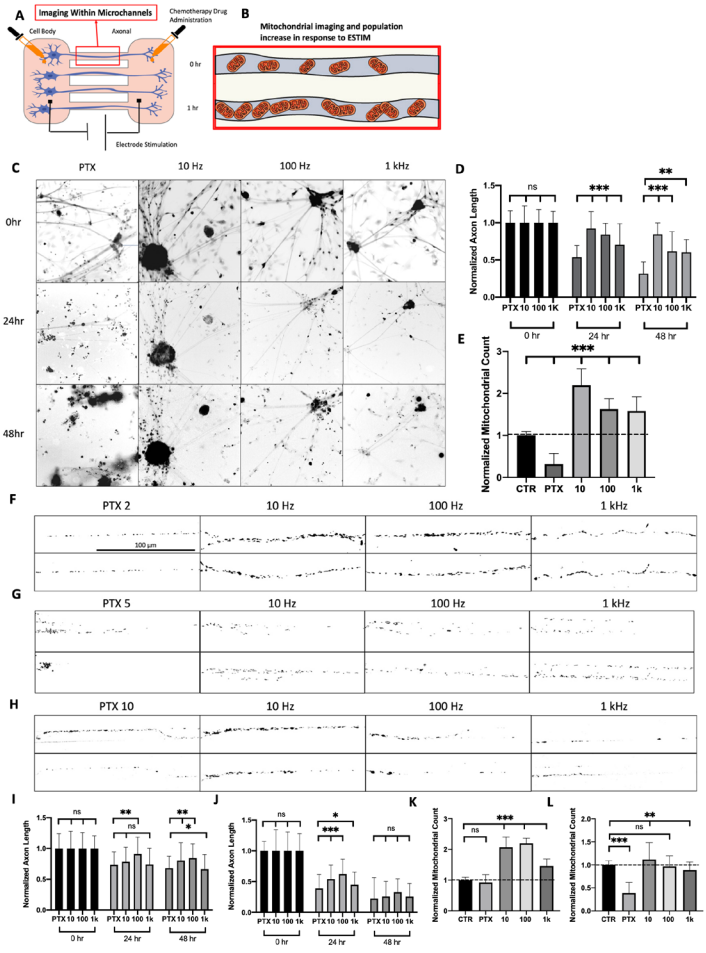

Figure. 2.3. Electrical stimulation enhances mitochondrial trafficking as a neuroprotective mechanism against PTX. Global stimulation set up using 10 Hz, 100 Hz, 1 kHz (A). PTX treated samples were stimulated for 1hr per day using the same parameters as frequency response (C). Quantification of neuroprotection by ESTIM against PTX 5µM induced peripheral degeneration (D). Quanification of neuroprotection by ESTIM against PTX 2µM and 10µM induced degeneration respectively (I, J). Mitochondrial imaging was preformed using the compartmentalized chamber system where imaging was preformed within microchannels after axons grew through (A). Image analysis of mitochondrial trafficking effect of 1-hour ESTIM after PTX treatment using 2µM, 5µM, and 10µM (F-H). Quantification of mitochondrial trafficking effect by ESIM against PTX 2µM and 10µM (K,L). Data is shown by mean ± SD. ***P<0.001, **P<0.01, *P<0.05 as determined by two-tailed t test, Scale bar is 100 µm unless otherwise stated.

The same global stimulation experimental set up was used to identify the neuroprotective effect of ESTIM against CIPN by PTX and L-OHP shown in Figure. 3 & 4 respectively. Optimal concentrations for PTX and L-OHP with in vivo experimentation ranges from 5-20 mg/kg and 5-25 mg/kg respectively [76, 77]. Based on in vivo settings, In vitro concentrations were chosen which highlighted proper dying back neuropathy. PTX and L-OHP were tested using concentrations, 2 µM, 5µM, and 10µM, where axon length and mitochondrial response were characterized. For each concentration, neurons were stimulated using 10Hz, 100Hz, and 1kHz. The optimal concentration of PTX and L-OHP was determined to be 5µM, where PTX and L-OHP showed degradation of axons without inducing sudden cell death[67, 78, 79]. Based on the toxicity response of PTX and L-OHP, concentrations of 5µM are used for additional results. Axon length results showed that PTX and L-

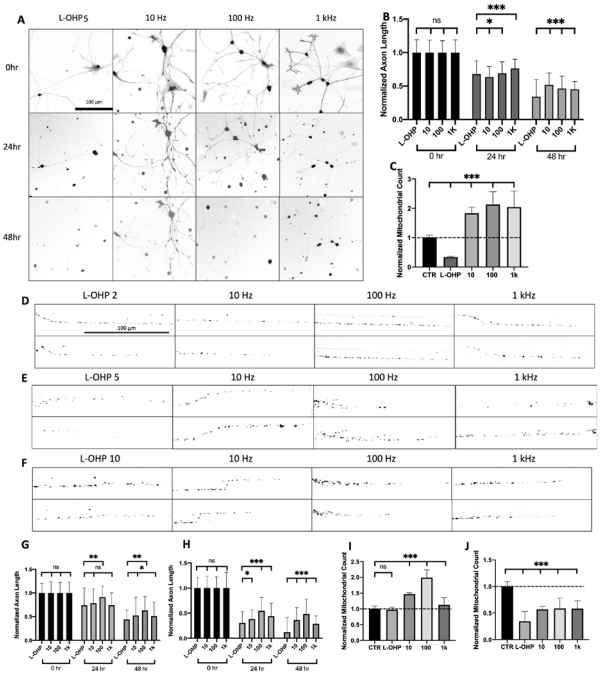

Figure. 2.4. Electrical stimulation enhances mitochondrial trafficking as a neuroprotective mechanism against L-OHP. L-OHP treated samples were stimulated for 1hr per day using the same parameters as frequency response (A). Quantification of neuroprotection by ESTIM against L-OHP 5µM induced peripheral degeneration (B). Quanification of neuroprotection by ESTIM against L-OHP 2µM and 10µM induced degeneration respectively (G, H). Image analysis of mitochondrial trafficking effect of 1-hour ESTIM after L-OHP treatment using 2µM, 5µM, and 10µM (D-F). Quantification of mitochondrial trafficking effect by ESIM against L-OHP 2µM and 10µM (I, J). Data is shown by mean ± SD. ***P<0.001, **P<0.01, *P<0.05 as determined by two-tailed *t* test. Scale bar is 100 µm unless otherwise stated.

OHP at 5µM had an average degradation of 67.85% and 65.97% after 3-day exposure compared to control respectively. For PTX, ESTIM was found to inhibit degradation, where 10 Hz showed 15.55%, 100Hz, 38.57%, and 1kHz, 39.75% degradation, showing a decrease in PTX degradability where 10Hz had the highest protection. Alternatively, ESTIM was found to be neuroprotective against L-OHP treatment where 10 Hz showed 48.12%, 100Hz, 53.74%, and 1kHz, 54.95% degradation. Although PTX and L-OHP had different targeting mechanisms, ESTIM was found to have a neuroprotective effect on both drugs. This result leads us to conclude, the underlying mechanism of neuroprotection by

Focal Stimulation as a Neuroprotective Method Against CIPN

Axonal stimulation was used to identify the neuroprotective effect against PTX and L-OHP induced CIPN. It was important to understand any differences between global and focal stimulation due to treatment application of ESTIM against CIPN. Focal vs. Global ESTIM can provide important data regarding treatment methodologies in a clinical setting. Focal stimulation of DRGs was performed by placing both electrodes in the axonal compartment. In a previous paper, it was determined that the electric field was localized to the axonal compartment when preforming focal stimulation [80]. The same parameters and

experimental set up were used in order to ensure proper electrical field isolation. Chemotherapy drugs were added in both compartments, mimicking global treatment similar to Figure. 2,3&4. ESTIM was performed in the axonal compartment using optimized parameters the same as the global stimulation. Focal ESTIM proved to be just as effective as global stimulation for neuroprotection against CIPN seen by Figure. 5. Axon length results showed that PTX and L-OHP at 5μM had an average degradation of 78.69% and 51.66% compared to control respectively seen in Figure. 5B, C and F, G. For PTX treated samples, ESTIM was found to have a neuroprotective effect, where 10 Hz showed only 39.65%, 100Hz, 27.38%, and 1kHz, 34.78% degradation, showing a decrease in PIPN effect on DRGS, where 10Hz had the highest neuroprotection. Alternatively, ESTIM was also found to be neuroprotective against L-OHP treatment where non stimulated samples showed 51.66%, however, 10 Hz showed 42.58%, 100Hz, 33.25%, and 1kHz, 30.48% degradation. Focal stimulation effect in response to PTX and L-OHP can be seen by Figure. 5.

Mitochondrial Motility

Figure. 6 shows representative imaging from a timelapse captured during a 30-minute stimulation period. Using a mitochondrial staining approach, displacement of motile mitochondria using timelapse imaging was determined [41]. Using Mito-View Green dye, mitochondrial displacement was characterized in response to optimal stimulation parameters. DRG's were cultured in a non-compartmentalized glass bottom culture dish. A non-compartmentalized device was used due to the ease of use, and mitochondrial clarity when stained. Using 100 Hz Global ESTIM, displacement of mitochondrial movement was determined in

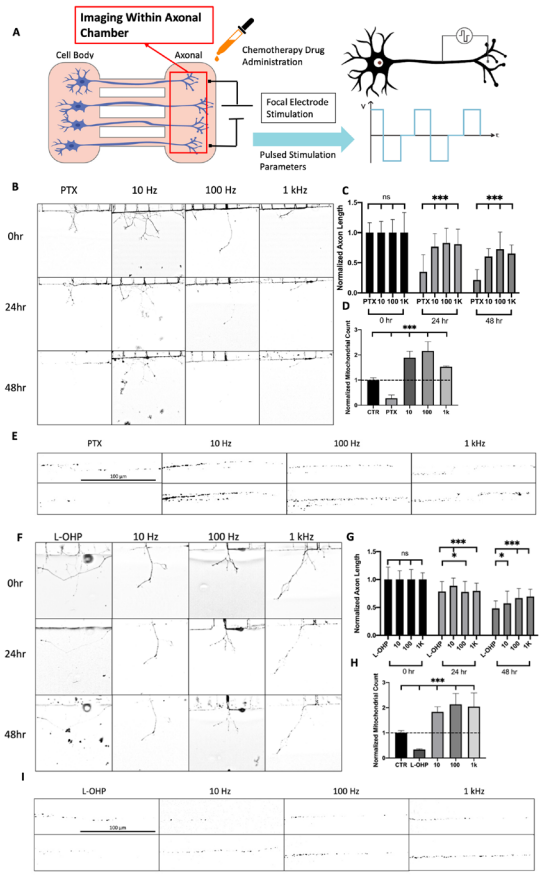

Figure. 2.5. Focal pulsed stimulation on DRGs using the microfluidic compartmentalized cell culture chamber. Global drug treatment was administered using PTX and L-OHP with optimal concentrations (A). Axon length measurements were collected and quantified in response to PTX treatment and ESTIM (B, C). Mitochondrial imaging was performed before and after stimulation at each frequency (D, E). Axon length measurements were collected and quantified in response to L-OHP treatment and ESTIM (F, G). Mitochondrial imaging was performed before and after stimulation at each frequency (H, I). Data is shown by mean ± SD. ***P<0.001, **P<0.01, *P<0.05 as determined by two-tailed t test, Scale bar is 100 µm unless otherwise stated

response to PTX, and L-OHP treatment. Displacement over the 30-minute timelapse was determined to be 3.76±1.55 µm on average for untreated samples and increased to 5.96±1.38 µm during 100 Hz stimulation. PTX treatment measured displacement to be reduced to 2.53±0.94 µm, however increased to 4.43±1.48 µm when stimulated at 100Hz. Similarly, L-OHP treatment showed an average displacement of 2.31±0.78 µm, however increased to 4.95±1.63 µm when stimulated at 100 Hz. All samples were dyed and treated for 1hr prior to timelapse imaging. Samples were stimulated using the same parameters as all other experiments. Based on velocity determination, 100 Hz stimulation was able to accelerate mitochondrial trafficking 58.36% for untreated, 42.90% for PTX, and 53.36% for L-OHP. Changes in velocity represent significant movement of motile mitochondria in response to the different conditions outlined. Motile mitochondria were analyzed due to their ability to regulate energy demands along the axon[81]. Based on the results from Figure. 6, neuroprotection by ESTIM enhanced mitochondrial transport can further be assumed.

Discussion

Electrical Stimulation (ESTIM) has a great potential as a symptomatic pain management option for chronic pain conditions [82]. In this study, we determined the neuroprotective effect of ESTIM against CIPN. Prior to determination, optimal frequencies for stimulation were determined. Optimal parameters were used to analyze the axonal response to ESTIM mediated neuroprotection. ESTIM was found to increase axon length when stimulated at low frequencies, however, was inhibited at higher frequencies (>1 kHz). Mitochondrial trafficking response was then characterized using the full range of frequencies, where only low frequencies (< 1 kHz) showed enhanced trafficking effect. Using the optimal frequencies, PTX and L-OHP treated samples were stimulated to determine ESTIM enhanced neuroprotection and mitochondrial trafficking against CIPN.

This study focused on axonal regeneration and trafficking response to global ESTIM using a frequency range of 10 Hz, 100 Hz, 1 kHz, 10 kHz, 100 kHz, and 1MHz. Results from the frequency response showed that, over the three-day stimulation period, 10 Hz accelerated axonal growth 9.71±0.26%, 100 Hz accelerated growth 12.28±0.33%, 1 kHz accelerated growth 0.07±0.27%, whereas 10 kHz inhibited growth 24.43±0.21%, 100 kHz inhibited growth 24.43±0.21%, 1 MHz inhibited growth 49.03±0.27%. As expected, low frequency (<1 kHz) stimulation increased growth rates of DRGs. Historically, ESTIM has been reported to increase neural activity within neuron cells when exposed to low frequency stimulation [83]. The increased neural activity induced by low frequency stimulation within embryonic DRGs showed increases in axonal growth rates significantly [84]. Subsequently, mitochondria trafficking was analyzed due to its significance in energy production and overall health of the neuron, as well as its association with neurodegenerative disorders [85, 86]. Mitochondrial trafficking response to the frequency range was analyzed using fluorescent dyes to live image the effect of ESTIM. ESTIM enhanced mitochondrial trafficking 62.79±0.43% for 10 Hz, 62.59±0.71% for 100 Hz, 15.96±0.16% for 1 kHz, however decreased 33.78±0.18% for 10 kHz, 38.90±0.19% for 100 kHz, and 74.28±0.04% for 1 MHz. Control samples showed mitochondrial population increase of 0.05±0.09% which can be attributed to mitochondrial motility under normal conditions. Although no external stimulation was provided, motile mitochondria are still seen to

traffic in an anterograde manner shown in Figure. 2. due to changing energy demands[81]. Due to the increased neural activity induced by ESTIM, we believe total axonal transport was enhanced as shown by the mitochondrial trafficking data. Increased axonal transport is a key component in plasticity development which can be correlated to the increased neural activity by ESTIM [87-89]. Enhanced mitochondrial trafficking is likewise heavily associated with increased Adenosine Triphosphate (ATP) levels[90]. Increased ATP by enhanced mitochondrial trafficking is directly correlated with neuroprotection in peripheral nerve injuries[41, 91]. The findings for axon length and mitochondrial trafficking correlate significantly, as the most effective increase in trafficking and axon length seemed to be 100 Hz. High frequency stimulation (>1 kHz) showed a decrease in axon length and mitochondrial trafficking respectively. These findings were expected as high frequency stimulation is a known phenomenon to induce excitotoxicity in neurons [92]. Due to the negative effect of high frequency stimulation, further experimentation opted to not use these frequencies. The global stimulation results show significant findings regarding mitochondrial trafficking enhancement, where proper application could result in neuroprotection against CIPN.

In this study we show increased mitochondrial trafficking because of low frequency ESTIM, however the underlying mechanism behind this observation is still unclear. Future studies are necessary to determine signaling pathways associated with ESTIM enhanced mitochondrial trafficking. Herein, we believe one potential mechanism that could be attributed to enhanced trafficking observed in this study is increased Brain Derived Neurotrophic Factor (BDNF) expression[93]. BDNF, is thought to have a direct association with peripheral nerve regeneration, due to its increased expression in injured conditions. BDNF is shown to have rapid upregulation which can be sustained for weeks, strongly suggesting its role in regeneration[94, 95]. One study suggests that during ESTIM, intracellular Ca^{2+} is increased, leading to overexpression of BDNF[96, 97]. Recently, BDNF is believed to modulate mitochondrial trafficking through downstream activation of Protein Kinase A[98]. Further research is needed to correlate enhanced BDNF expression by ESTIM and enhanced mitochondrial trafficking.

Previously we determined that Paclitaxel (PTX) has the ability to inhibit mitochondrial transport when treated on sensory neurons [41, 67]. Based on this finding, we sought to determine the effect of ESTIM as a neuroprotective mechanism against two different antineoplastic drugs, PTX, as well as Oxaliplatin (L-OHP). Global stimulation with chemotherapy drug treatment was initially performed to analyze the effect of ESTIM on axon length and mitochondrial trafficking, similar to the frequency response experiment. PTX is a common microtubule targeting anti-cancer drug, which in turn affects the axonal transport mechanisms leading to peripheral degeneration. From our results, 10 Hz stimulation provided the highest degree of neuroprotection against PIPN, significantly reducing the degeneration effects of PTX compared to control sample. Likewise, mitochondrial trafficking was enhanced, where 100 Hz provided the largest change in trafficking after stimulation. Based on ESTIM's ability to enhance mitochondrial trafficking, it was speculated that if we could enhance the axonal trafficking within the cell in response to PTX treatment, it would provide neuroprotection against PIPN. Similarly, L-OHP was treated globally at a concentration of 5μM based on in vitro toxicity response [78, 79]. Due to the DNA targeting mechanism of L-OHP treatment, the effects of enhanced axonal transport were expected to be less than that of PTX. L-OHP treatment targets DNA replication cycle within the nucleus and it is assumed to likewise effect the DNA within mitochondria [99, 100]. Mitochondrial observation is key in response to L-OHP treatment as mitochondria has recently been associated with signaling responses associated with cell death [101]. Although L-OHP targets DNA replication, ESTIM is still shown to have a neuroprotective effect on L-OHP treated samples. Mitochondrial trafficking was also analyzed for L-OHP treated samples to further understand how enhanced axonal transport can be used as a neuroprotective mechanism against CIPN. Although L-OHP has a different targeting mechanism than PTX, based on the results it can be seen that low frequency stimulation still enhanced anterograde mitochondrial trafficking, where 100 Hz showed the highest increase over the stimulation period. It is important to note that mitochondrial trafficking enhancement was surprisingly similar when comparing PTX and L-OHP. Although axon length analysis showed a difference in results for each drug, mitochondrial enhancement was similar between the two, potentially indicating a similar enhancement mechanism by ESTIM. Based on our results, the axonal

transport enhancement by ESTIM proved an effective neuroprotection mechanism against CIPN. Further research is needed to determine if ESTIM directly affects mitochondria trafficking as a primary, or secondary mechanism. Based on this study, we speculate that the increased neural activity by low frequency stimulation enhances axonal transport, however the specific signaling mechanisms are still unknown at this time. Further research is needed to fully understand the signaling pathways behind neuromodulation enhanced regeneration. Based on the results found, ESTIM has the ability to be an effective method to help patients who are experiencing painful CIPN.

In order to determine the most effective treatment method for ESTIM, axonal stimulation was performed on PTX and L-OHP treated samples. It was necessary to understand if there were any major differences between global and axonal stimulation since axonal stimulation is a preferred treatment method in clinical settings. Axonal stimulation allows for isolated electric fields at the region of injury, which in turn can be a safer and more effective treatment option for patients. Axonal stimulation effect against PTX and L-OHP induced degeneration was significant due to CIPN being a focal injury model in patients. For PTX treated samples, 100 Hz stimulation had the highest neuroprotective effect, while for L-OHP treated samples, 100 Hz and 1 kHz stimulation had equally the highest protection. Based on the results, axonal and global stimulation had similar effectiveness, justifying the ability to use focal stimulation as an effective method for neuroprotection against CIPN. The similarities between global and focal stimulation could be attributed to the electric field distribution within the cell. Previous studies have confirmed that single cell stimulation can illicit increased neural activity throughout the entire cell in vitro and in vivo [80, 102]. Axonal stimulation does not have any lesser effect on neuroprotection than global and can be determined as an effective treatment method in clinical settings.

Although mitochondrial trafficking was the governing subcellular organelle that was studied, it may not be the only organelle that is affected by neuromodulation. Further research is needed to determine how other mobile organelles are affected by ESTIM. To help answer the question of enhanced axonal transport as a neuroprotective mechanism, a supplementary lysosome trafficking study was performed as a supplementary study. The effect of lysosome trafficking mirrored mitochondrial data, showing that ESTIM enhanced

trafficking of lysosomes within DRG's. This supplementary data helps back up the claim that ESTIM may enhance axonal trafficking as a neuroprotective mechanism against CIPN.

Based on the results of this study, mitochondrial enhancement by ESTIM is a proposed mechanism behind ESTIM mediated neuroprotection against CIPN. Mitochondrial trafficking enhancement shows to be a key aspect of neuroprotection, which has the potential to help many patients suffering from CIPN. Based on this study, non-invasive techniques can be developed to generate electric fields, enhancing mitochondrial trafficking in clinical settings to treat CIPN or other neurodegenerative disorders or diseases.

Limitations of the Study

There were several limitations of this study. First, mitochondrial trafficking dye has an inherent diffusion rate, which may influence the trafficking analysis. Hydrostatic pressure and flow induction was performed to reduce this aspect; however, we have no way to ensure total blockage of dye diffusion at this time. Displacement over time data was manually recorded, where timelapse images showed frame shifting, and axonal degradation in response to chemotherapy drugs, making it difficult to collect accurate velocity data from mitochondrial trafficking. At this time, we are unable to determine the signaling pathways and direct mechanism associated with ESTIM enhanced mitochondrial transport. We hope to address all these challenges in future studies.

Acknowledgments

This Research was supported by the National Science Foundation (NSF) Career Award (2238723).

Author contributions:

Bayne Albin: Conceptualization, Methodology, Validation, Formal Analysis, Investigation, Data Curation, Writing, Visualization. **Prashant Adhikari:** Methodology, Software, Validation, Formal Analysis, Data curation, Review & Editing. **Arjun Tiwari:** Conceptualization, Validation, Resources, Review & Editing, Supervision, Project Administration. **Khayzaran Qubbaj:** Validation, Formal Analysis, Data Curation,

Editing & Review, Visualization. **In Hong Yang:** Conceptualization, Validation, Recourses, Review & Editing, Supervision, Project Administration, Funding Acquisition.

Declaration of interests:

All other authors declare they have no competing interests.

Data and materials availability:

All data are available in the main text or the supplementary materials.

Main Figure Titles and Legends

Figure. 1. Experimental Schematic. E-15 Sprague Dawley rat embryonic Dorsal Root Ganglion (DRG) isolation and enzymatic disassociation. Processed DRGs plated into the cell body chamber of the compartmentalized chamber system. Cells are allowed to grow for 3-5 days until they grow through the channels to the axonal compartment, where chemotherapy drugs and dyes are administered. Electrical stimulation was performed for 1 hour per day using a constant 3V power supply to generate a biphasic rectangular pulse lasting 0.5s every 2s with a pulse width of 0.2 ms. Imaging of axons was completed in the axonal compartment, while mitochondrial trafficking imaging was performed within the parallel micro-channels. Created with BioRender.com

Figure. 2. Pulsed Electrical stimulation enhances Axon growth and Mitochondrial Trafficking. Schematic for global DRG stimulation for axon length measurement analysis (A). The axonal response after stimulation for 0, 24 and 48 hours, for 10Hz, 100Hz, 1 kHz, 10 hHz, 100 kHz, and 1 MHz showed that low frequency (10 Hz, 100 Hz and 1 kHz) proved to enhance axon length measurements at each timestamp (B). Mitochondrial imaging was performed in a compartmentalized microfluidic chamber to identify the immediate trafficking response to each frequency (C). Quantification of normalized axon length measurements were used to compare against the initial 0hr length (D). Mitochondria were shown to increase between the 0hr and 1hr stimulation for low frequency stimulation parameters (E). Mitochondria were

imaged before and after 1hr stimulation to identify the trafficking enhancement by ESTIM (F). It was proven that 100 Hz stimulation enhanced mitochondrial trafficking the most compared to control samples (E). Data is shown by mean ± SD. ***P<0.001, **P<0.01, *P<0.05 as determined by two-tailed t test (E), Scale bar is 100 μm unless otherwise stated.

Figure. 3. Electrical stimulation enhances mitochondrial trafficking as a neuroprotective mechanism against PTX. Global stimulation set up using 10 Hz, 100 Hz, 1 kHz (A). PTX treated samples were stimulated for 1hr per day using the same parameters as frequency response (C). Quantification of neuroprotection by ESTIM against PTX 5μM induced peripheral degeneration (D). Quanification of neuroprotection by ESTIM against PTX 2μM and 10μM induced degeneration respectively (I, J). Mitochondrial imaging was preformed using the compartmentalized chamber system where imaging was preformed within microchannels after axons grew through (A). Image analysis of mitochondrial trafficking effect of 1-hour ESTIM after PTX treatment using 2μM, 5μM, and 10μM (F-H). Quantification of mitochondrial trafficking effect by ESIM against PTX 2μM and 10μM (K,L). Data is shown by mean ± SD. ***P<0.001, **P<0.01, *P<0.05 as determined by two-tailed t test, Scale bar is 100 μm unless otherwise stated.

Figure. 4. Electrical stimulation enhances mitochondrial trafficking as a neuroprotective mechanism against L-OHP. L-OHP treated samples were stimulated for 1hr per day using the same parameters as frequency response (A). Quantification of neuroprotection by ESTIM against L-OHP 5μM induced peripheral degeneration (B). Quanification of neuroprotection by ESTIM against L-OHP 2μM and 10μM induced degeneration respectively (G, H). Image analysis of mitochondrial trafficking effect of 1-hour ESTIM after L-OHP treatment using 2μM, 5μM, and 10μM (D-F). Quantification of mitochondrial trafficking effect by ESIM against L-OHP 2μM and 10μM (I, J). Data is shown by mean ± SD. ***P<0.001, **P<0.01, *P<0.05 as determined by two-tailed t test, Scale bar is 100 μm unless otherwise stated.

Figure. 5. Focal pulsed stimulation on DRGs using the microfluidic compartmentalized cell culture chamber. Global drug treatment was administered using PTX and L-OHP with optimal concentrations (A). Axon length measurements were collected and quantified in response to PTX treatment and ESTIM (B, C). Mitochondrial imaging was performed before and after stimulation at each frequency (D, E). Axon length measurements were collected and quantified in response to L-OHP treatment and ESTIM (F, G). Mitochondrial imaging was performed before and after stimulation at each frequency (H, I). Data is shown by mean ± SD. ***P<0.001, **P<0.01, *P<0.05 as determined by two-tailed t test, Scale bar is 100 μm unless otherwise stated.

Figure.6. Mitochondrial motility analysis. Mitochondrial Staining using Mito-View Green within axonal section of DRG (A). Mitochondrial velocity with drug treated samples and 100 Hz ESTIM (B). Data is shown by mean ± SD. **P<0.01, *P<0.05 as determined by two-tailed t test.

Materials and Methods

Compartmentalized chambers

Photolithography was used to develop a master mold which contained the microchannels for the compartmentalized chamber system. Sylgard 184 polydimethylsiloxane (PDMS) (Dow chemical company USA) was used to conduct standard soft lithography, where it was poured onto the master micro-mold followed by the removal of air bubbles by a desiccator (SP Scienceware, USA) and was allowed to cure overnight at 80°C. PDMS was removed from the master mold where two adjacent holes were punched on either side of the channels using a 6 mm diameter biopsy punch (Robbins Instruments). The dual compartmentalized chambers were then bonded to a thin glass slide (Fisher Scientific) using the Plasma Etch PE-75 Plasma Asher oxygen plasma device. After, the chamber devices were sterilized by autoclave before cell seating. Once sterilized, chambers were coated with 100μg/mL Poly-D-Lysine (PDL) (Sigma-Aldrich) and 10.0 μg/mL Laminin (Corning) and left overnight at 2-8°C refrigerator. Chambers were then

washed thoroughly using media to prepare for cell seating. Chambers were then placed into a sterilized primary cell incubator supplying 5% CO_2 (Binder C-150 UL) to accustom for the cell culture environment.

Cell culture

All animal experiments were conducted in accordance with protocols approved by the Institutional Animal Care and Use Committee (IACUC). Dorsal Root Ganglion (DRG) neurons were isolated from E-15 embryos collected from a Sprague Dawley Rat. DRG explants were carefully collected and enzymatically dissociated using 0.25% Trypsin in L-15 medium (Sigma Aldrich). DRGs were suspended in a modified Neurobasal medium containing 1.0% Fetal Bovine Serum (FBS), 20.0% Glucose, 1.0% Penicillin/Streptomycin, B-27 supplement, 2 M $_{L}$-glutamine, and 10 ng/ml Glial Derived Nerve Growth Factor (GDNF) (Sigma Aldrich). DRG neurons were seated into the marked somal chamber of the compartmentalized devices and left to grow for 3-5 days to allow for axons to grow through the channels into the axonal side at an adequate length.

To limit evaporation, a small cotton ball soaked in sterile distilled water and 1.0% Penicillin/Streptomycin was placed in the same petri dish as the chambers.

Drug treatment and mitochondria staining

PTX and L-OHP were prepared as 1mM stock solutions prior to making the working solution and stored at -20°C freezer. PTX (Selleck Chemicals) was dissolved in ethanol, and L-OHP (Sigma) was dissolved in 0.9% sodium chloride. Stock solutions were further diluted using Neurobasal media. 5μM was used for both drugs as they show proper dying back neuropathy and similar neurotoxicity as in in vivo situations. Drugs were administered to the compartments by removing 75% of existing media and readministered with the drug containing media at 37°C for one hour prior to fluorescent staining. Cells were stained using Calcien AM (ThermoFisher) and allowed to incubate for 30 mins to 1 hour after initial drug treatment. DRG's were imaged using a Leica DMi8 Thunder Fluorescent Microscope immediately after drug treatment, and likewise 24, and 48 hours after imaging. In order to image mitochondria, MitoView Green

was obtained from Biotium, USA and was added to the cells for 30 mins to 1 hour after drug treatment, similar to the previous protocol. Media was replaced twice to reduce any background fluorescence, and immediately imaged. The compartmentalized system was covered in aluminum foil to prevent any light degradation.

Axon length measurements were performed using a glass bottom non-compartmentalized cell culture array, where embryonic DRGs were cultured for 24 hours prior to CIPN drug treatment. PTX was treated at a concentration of 5 μM and administered globally one hour prior to stimulation for all experiments. Due to the Mitochondrial trafficking effects, we previously studied with FA, it was decided to use a similar toxicity concentration for each drug to understand the neuroprotective mechanism of ESTIM against CIPN.

ESTIM Setup

Pulse wave signal generators (Siglent) were used to create the proper square wave signal needed for proper stimulation. A constant 3 Volt power source was used to create a biphasic rectangular pulse lasting 0.5s every 2s with a pulse width of 0.2 ms. Platinum wires were attached to the cell culture system's lid, where wires were attached to the signal generators shown in the schematic. The platinum wires were placed into the wells, where one electrode was placed in each well pair for global stimulation, and both electrodes were placed into the axonal chamber for focal stimulation. Control wells were not connected to the stimulation device.

Data Analysis

Data was collected using Fiji-ImageJ to measure axon lengths in triplicate samples. Microsoft Office Excel 2022 was used to compile all measurement data, where average and standard deviation was calculated. Axon integrity was found by calculating percent difference compared to the average control (0hr) for each sample. Differences in percent change were used to analyze the effect of site-specific treatment. Mitochondrial analysis used a similar approach, where mitochondrial number was compared against the

control (0hr), normalizing the data set. Data was presented as a percentage of the control value, showing a positive or negative change in comparison.

To quantify the mitochondrial displacement, images were analyzed with the aid of 'MTrackJ' plugin for manual tracking of individual mitochondria across the frames until the mitochondria disappears from view, stops moving, or moves out of frame. 30-minute timelapse imaging was preformed using the built-in Leica software. Images were taken at one-minute intervals for 30 mins. Manual displacement was calculated by measuring the distance traveled of a singular mitochondrion along the thirty frames.

Statistical Analysis

All data sets were presented as a mean ± standard deviation except where noted. Data sets were grouped as triplicate N=3. The probability *(P*-value*)* between groups was analyzed by the two-tailed *t*-test provided in Microsoft Office Excel 2022 unless otherwise stated. *P*-value less than 0.05 was considered statistically significant.

Supplemental Figures

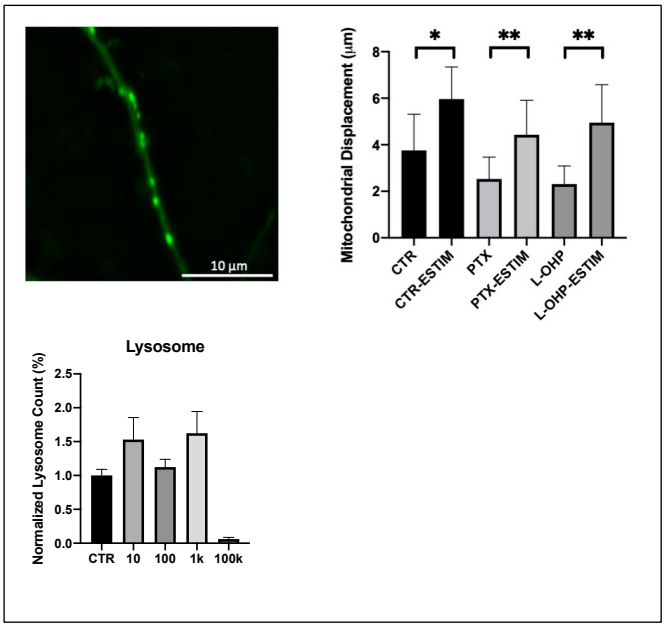

Figure. S1. Lysosomal trafficking response to electrical stimulation frequency range. Lysosome trafficking was determined using the same experimental methodologies as ESTIM. Using a lysosomal staining kit, trafficking response was determined using the compartmentalized chamber. Stimulation was performed at 10 Hz, 100 Hz, 1 kHz, and 100 kHz to analyze the trafficking response. Results found that low frequency stimulation enhanced lysosomal trafficking similar to mitochondria.

CHAPTER 3: MAGNETIC STIMULATION ENHANCES MITHOICNDIRAL TRAFIFKCING AS A POTENTIAL NEUROPROTECTIVE MECHANSIM AGAINST CHEMTOHERAPY INDUCED PERIPHERAL NEUROPATHY

Based on the results from the first and second studies, the ESTIM device inspired the development of a non-invasive approach that aids with the understanding of and application of an external excitation resulting in enhanced mitochondrial trafficking similar to electrical stimulation. Although ESTIM was shown to have the ability to enhance mitochondrial trafficking and reduce axonal degeneration by CIPN drugs, there are issues with ESTIM in a clinical setting, which makes development difficult. The largely invasive nature of ESTIM, makes development of implantable devices difficult due to power delivery, material properties, heat generation, and surgical implantation. Issues such as glial scarring, immune response, inflammation, and device translation within the body cause significant challenges for engineers and surgeons. Therefore, the development of a magnetic stimulation device is important to study the effect of Magnetic stimulation (MSTIM) on DRGs against Chemotherapy Induced Peripheral Neuropathy. This study focused primarily on the design and development of the magnetic stimulation device, as there are challenges to develop a magnetic field generator to induce a similar external excitation on neurons as ESTIM. In order to properly stimulate DRGs, a pulsed monophasic square wave was sent through a copper coil in order to induce 11-13 mT on the cells *in vitro*. The coils chosen were decided based on Lenz Law, which states how magnetic field is induced in a flat coil. Coils were chosen to have a ferrite core in order to reduce interference and enhance magnetic field generation. Litz wire was used in the design of the coils in order to reduce the "Skin effect" and reduce heat generation. However, sending a signal from a pulse generator to the coils was not efficient for delivering ideal magnetic field intensities. Therefore, this study worked with Dr. Stuart Smith to modify an amplification circuit he designed for this application. The amplification circuit was paired with the signal generator to increase the output amperage to approximately 0.5 Amps. Using this amplifier design, optimal MSTIM parameters were achieved for stimulation of DRGs. Due to previously observed neuroprotective roles of ESTIM, along with its ability to modulate neural activity, we believed that MSTIM also has the ability to have an effect on the trafficking of mitochondria and axon length. Paclitaxel (PTX) and Cisplatin (CDDP) were studied due to their role in dying back neuropathy. PTX and CDDP were

similarly chosen due to their differences in cancer killing mechanism to understand if MSTIM affected only one or both types of drugs. Likewise, CDDP was used rather than L-OHP due to its commonality and wider range of target cancers. Furthermore, this study observed how frequency dependent MSTIM using a microfluidic compartmentalization platform affected modulation of cellular and subcellular dynamics of DRGs. Results from this study found that low frequency (>1kHz) MSTIM enhanced mitochondrial trafficking and reduced axonal degeneration by chemotherapy drugs. However, there were slight differences in frequency response of ESTIM and MSTIM. MSTIM stimulation at 1 kHz was similar to control samples, where this frequency did not have much effect on DRGs unlike ESTIM which showed enhancement of mitochondrial trafficking and axon lengths. Herein, we believe the differences observed may be due to the mechanism of electric field induction. ESTIM may have more efficient delivery of electrical field modulation due to its invasive nature, allowing for direct contact with cells, however MSTIM electric field generation is not quite as precise, and varies dependent on distance from the source. Similarly, magnetic fields disperse in a non-linear fashion which may have affected how the cells responded to MSTIM. However, results from this study found enhanced mitochondrial trafficking and axon length for frequencies under 1 kHz and showed that MSTIM still resulted in neuroprotective effects against CIPN. Such findings are essential to development of neuromodulation techniques for the peripheral and central nervous system. Results from this study show enhanced mitochondrial trafficking by low frequency (>1 kHz) electrical stimulation for the first time as we know. Due to the clinical relevance of MSTIM and its use in Transcranial Magnetic Stimulation (TMS), wearable MSTIM devices have the ability to modulate energy dynamics in patients suffering from pain or neurological disorders in a non-invasive manner.

Magnetic Stimulation enhances Mitochondrial Trafficking as a Protective Mechanism Against Chemotherapy Induced Peripheral Neuropathy

Bayne Albin[1,2], , Khayzaran Qubbaj[1,2] , Prashant Adhikari[1] , Alexandria Traynham[1], Rahul Guha[1], In Hong Yang[1]*

[1]Center for Biomedical Engineering and Science, Department of Mechanical Engineering and Engineering Science, University of North Carolina at Charlotte, Charlotte, North Carolina 28223, United States

[2]Equal Contributing Authors

* Corresponding Author: In Hong Yang; E-mail: iyang3@charlotte.edu

Key Terms: chemotherapy induced peripheral neuropathy, axonal degeneration, paclitaxel, cisplatin, astrocyte, microfluidics

Abstract

Magnetic Stimulation (MSTIM) is a non-invasive technique to modulate neuronal activity through induced electric fields of the nervous system. MSTIM is used to excite or inhibit neurons to induce a particular response such as release of neurotransmitters or enhanced growth and plasticity. However, underlying mechanisms behind MSTIM are still unknown. In this study, we characterize the neuroprotective effect of MSTIM against Chemotherapy Induced Peripheral Neuropathy (CIPN) through enhanced mitochondrial and lysosomal trafficking. Mechanistic insights were observed to further understand how MSTIM affects regulation of energy dynamics in a frequency dependent manner. CIPN is a painful and debilitating side effect of chemotherapy treatment which results in degradation of the peripheral nervous system. Currently, there are no treatment options for patients suffering from CIPN, other than symptomatic management. Recently, studies have found evidence to support bioelectronic modulation ability to regulate subcellular trafficking in neurons. This study observes MSTIM enhanced mitochondrial trafficking as a neuroprotective mechanism against Chemotherapy Induced Peripheral Neuropathy (CIPN). Results from this study similarly demonstrate MSTIM ability to reduce Paclitaxel- and Cisplatin- Induced degeneration under low-frequency pulsed stimulation *in vitro*. This study investigates potential mechanisms involved in MSTIM as a neuroprotective therapy against CIPN.

Introduction

The effects of magnetic stimulation were first discovered in 1896, when scientist Arsène d'Arsonval started implementing magnetic fields upon living tissues.{Geddes, 1991 #171} d'Arsonval was also the first scientist to discover the effects of MSTIM specifically on brain tissue, and regions of the nervous system.{Vidal-Dourado, 2014 #169} However, it wasn't until 1985, that scientists, Barker, Jalinous, and Freeston presented results involving Transcranial Magnetic Stimulation (TMS) as a non-invasive, therapeutic technique for neurological and psychiatric conditions.{Lisanby, 2024 #170} During the 89 years between the discovery of MSTIM ability to induce effects on tissue, to the first clinically relevant TMS device, parameters for MSTIM were highly researched.{Pascual-Leone, 2007 #172} Magnetic field intensity, power input, pulse width, frequency, treatment duration, and coil designs were looked at in many different types of neurological models to understand the effect of the various MSTIM parameters on muscle activation, and cell proliferation/ death. Extensive research on MSTIM's ability to change neuronal functions has been studied for over a century, however underlying mechanisms for MSTIM mediated neuroprotection is still unknown. Building off of previous results, this study focuses on the investigation of mechanisms associated with MSTIM on neurons *in vitro.*

Magnetic Stimulation (MSTIM) is an emerging non-invasive therapy for neurological conditions, specifically, Transcranial Magnetic Stimulation (TMS) is currently being used to help treat depression and anxiety [1]. However, the cellular mechanisms behind MSTIM enhanced axon growth and regeneration are still unknown. TMS and other MSTIM therapies utilize non-invasive pulsed magnetic field generation, to stimulate electrical activity in the brain and spinal cord[2]. MSTIM has the ability to externally induce neuronal activity in order to modulate excitability in neurons and physiological conditions[3]. MSTIM efficacy has been shown to have a direct correlation with frequency output, where low frequency (10 – 1000 Hz) pulsed stimulation shows increased growth rates, plasticity and excitability in neurons *in vitro*. MSTIM is seen to be an effective neuromodulation method for nerve regeneration and protection. MSTIM devices are non-implantable and can deliver optimal pulsed magnetic fields to selective regions of the body. The non-invasive manner of MSTIM technology makes it a highly desirable treatment strategy due to the

ease of use and effectiveness. Likewise, an electromagnetic coil can be designed for focused magnetic field delivery, allowing for focal treatment at the site of injury, rather than exposing a large area of tissue to the induced electrical field. As opposed to electrical stimulation, there is more control over the directionality of the generated magnetic field using magnetic stimulation based on the orientation of the magnetic coils utilized. Although MSTIM has proven to be an effective strategy for neuromodulation, underlying mechanisms are still unknown. Through in-depth analysis of pathophysiological and metabolic changes in the form of axonal integrity and mitochondrial trafficking, key mechanistic insights can be determined to develop effective neuromodulation strategies to prevent and treat CIPN conditions.

Magnetic stimulation, in a time-varying manner, induces an electric field on neurons which generates transmembrane currents in cytoplasmic as well as internal organelle membranes.{Ye, 2010 #148;Pashut, 2011 #149} The induced electric field superimposes the resting membrane potential, triggering action potential propagation and increased neural activity.{Pashut, 2011 #149;Stern, 2017 #150} Despite clinical applications of magnetic stimulation in the form of TMS, specific mechanisms involving neuronal excitation are still unknown. Through numerical modeling, researchers have tried to understand how MSTIM affects neurons.

Neural activity is known to have a direct effect on metabolic regulation for neurons, where mitochondrial dynamics are enhanced dependent on activity.{Obashi, 2013 #151} However, specific mechanisms regarding how neural activity changes mitochondrial dynamics is still unknown.[103] Recent studies have found correlation between neural activity dependent release of BDNF and $Ca2^{+}$ concentrations which may contribute to enhanced mitochondrial trafficking.[104] Due to neuron cells high energy consumption compared to other cell types, energy management and transfer is vital for homeostasis and neuroprotection.[105] Through enhanced mitochondrial trafficking, large energy demands due to axonal injury can be met and allow the cell to utilize protective mechanisms more efficiently. Using magnetic stimulation, induced neural activity may result in protective mechanisms within the cell and increase

neuroprotection against CIPN. Herein, we determine frequency dependent MSTIM parameters to induce neural activity for dynamic mitochondrial enhancement as a protective mechanism against CIPN.

Mitochondrial trafficking

Mitochondrial dynamics such as directionality, motility and velocity are significant indicators of neuronal health and survivability.[106] Mitochondrial population and trafficking within the neuron are dynamic and change due to energy demands, metabolic activity, and environmental conditions.[107] Due to the high energy demands of neuronal cell types, mitochondrial dynamics are essential for neuronal survival and function. Energy demands of neuronal cells also change significantly dependent on location, circumstance and injury.[107] For example, locations such as the growth cone require more energy during axon growth due to the high protein synthesis and axonal pathfinding.[108] High energy demands require effective mitochondrial transport in order to deliver sufficient energy in the form of Adenosine Triphosphate (ATP). Mitochondrial trafficking within the neuron helps maintain intracellular homeostasis through motor proteins such as Kinesin and Dynein.[109] Recently, changes in neuronal activity based on environmental conditions have been found to alter mitochondrial dynamics where an increase in action potential propagation has shown an increase in mitochondrial trafficking within the axon.[110] Although this phenomenon seems straightforward, the underlying mechanism connecting neural activity and mitochondrial trafficking is still unknown. It is well known that environmental changes can elicit intracellular signaling responses, which activate neuronal activity for a variety of reasons. Whether neurons increase neural activity as a primary response to an external stimulus, or as a secondary response, is still unknown.[111] Injury conditions such as peripheral neuropathy (PN) have been shown to cause disruptions in neural activity and decrease mitochondrial trafficking.[110] Due to the increased energy demands facilitated by chemotherapy-induced peripheral neuropathy (CIPN) and other neuronal injuries, mitochondrial trafficking is an essential mechanism for understanding subcellular responses to neuropathic conditions. Thorough analysis of mitochondrial trafficking, treatment strategies can be determined to help

combat specific disease conditions. Using this information, better treatment strategies can be developed to prevent PN.

Peripheral neuropathy

Chemotherapy Induced Peripheral Neuropathy (CIPN) is a severe, debilitating side effect of chemotherapy treatment. Approximately 60% of patients who undergo chemotherapy treatment experience CIPN conditions which can lead to dosage reductions or even termination of treatment in extreme cases.[110, 112] Patients who are diagnosed with CIPN experience numbness, tingling, pain and loss of feeling starting in extremities.[113] In extreme cases, CIPN may lead to amputation or complete motor dysfunction.[114] Due to advancements in chemotherapy and other anti-cancer treatments, survival rates have increased significantly. However, given an increase in survival, this phenomenon leaves many patients suffering from CIPN.[115] At this time there are no effective treatment strategies for CIPN other than symptomatic management. However, recent advancements in neuromodulation technology have shown to be effective strategies to protect against, and even recover peripheral nerves during CIPN.[116] In this study, low frequency magnetic stimulation was used to protect peripheral sensory neurons against CIPN. Subcellular organelle trafficking and dynamics were analyzed as a potential mechanism for neuroprotection.[117] Although chemotherapy is a lifesaving treatment strategy for cancer patients, many who undergo this procedure deal with painful side effects such as CIPN.[118] Chemotherapy drugs utilize different targeting mechanisms in order to disrupt the cell division process of cancer cells. However, due to the non-site-specific treatment of chemotherapy drugs, non-cancerous cell types such as peripheral neurons are also affected.[27] Currently, there are no effective treatments methods for peripheral neuropathy other than symptomatic management. Due to the severity of PN in cancer patients, CIPN is a major dose limiting factor, and can even lead to termination of treatment all together. The dose limiting factor of CIPN can often lead to suboptimal cancer killing conditions, allowing cancerous cells to mutate and enter new areas of a patient's body.[119] CIPN can lead to painful and debilitating conditions whether it be directly related

to PN or indirectly associated with dose limitation. Due to the severity of CIPN onset in cancer patients it is essential to develop treatment strategies to prevent or even reverse the effects of CIPN.

Common drugs like Gabapentin or Duloxetine are used to mitigate symptoms for patients suffering from CIPN tend to have adverse effects on the entire nervous system.[120, 121] Due to the lack of treatment options for CIPN, many patients take medication for symptomatic relief.[122] PN pain management drugs, however, are not well suited for treatment against CIPN, and tend to be serotonin and norepinephrine reuptake inhibitors (SNRI), which are primarily used to treat anxiety and depression.[123] Most commonly, Duloxetine is widely used to reduce symptoms associated with CIPN, however only to a moderate degree.[124] Additionally, Duloxetine is widely used as an antidepressant and antianxiety medication which has many side effects such as withdrawal symptoms, loss of appetite, increased blood pressure and heart rate, among others.[125] The primary effect of these drugs are to help patients suffering from anxiety and depression, with a secondary effect on pain management of PN. Side effects from taking these drugs can include nausea, discomfort, cyclothymia, and withdrawals among others.[126] Current drugs utilized to help patients suffering from PN are not well suited for treatment against CIPN.[66, 127] Alternative methodologies are necessary to develop suitable treatment strategies against CIPN. Neuromodulation techniques, such as magnetic stimulation (MSTIM) have been shown to have a positive effect on neuroprotection and neuronal physiological conditions.[128] Herein, we identify MSTIM as a non-invasive neuroprotection strategy against CIPN.

Drugs

In this study, we examined the neuroprotective effect of MSTIM on axonal integrity and mitochondrial trafficking of Dorsal Root Ganglion (DRG) neurons affected by two distinct cancer killing mechanisms. Most commonly, chemotherapy drugs can be characterized into two major groups based on the killing mechanism. Microtubule-targeting chemotherapy drugs, for example, target cell mitosis through the disruption of mitotic spindle formation. Microtubules are filament-like structures which occur throughout the cell to offer structural stability, and subcellular transport. Through the degradation of microtubule

structures; transport mechanisms, structural support and cell proliferation are negatively affected.[129] This method for killing cancer cells is especially effective due to the rapid proliferation of cancer cells. Drugs such as Paclitaxel (PTX), disrupt the microtubule structures, blocking cell proliferation, inevitably killing the cell as all transport and structural mechanisms are disrupted.[69] PTX is one of the most common anti-cancer drugs that is used to target many types of cancer, such as ovarian, lung and breast cancers.[130] Due to the microtubule targeting effect of PTX, it can be interpreted that PTX has a direct correlation with axonal trafficking within DRG's.[131] Recently, PTX was shown to inhibit mitochondrial trafficking within the axons of DRGs, where Fluocinolone Acetonide (FA) was used as a neuroprotective agent to enhance mitochondrial trafficking in PTX treated samples.[132] These findings help suggest the role of organelle trafficking as a neuroprotective mechanism against CIPN.

In order to develop an understanding of the role of MSTIM as a neuroprotective agent against CIPN, it is important to understand how MSTIM affects axon growth and mitochondrial trafficking against drugs with different targeting mechanisms. DNA-replication targeting drugs such as Cisplatin (CDDP), are the second most common type of chemotherapy drug.[133] CDDP, is a platinum-based antineoplastic which disrupts the DNA replication cycle and inhibits cancer cell proliferation.[134] CDDP targets the DNA replication cycle by binding to DNA strands and disrupting the transcription process.[135] The DNA damage associated with CDDP is crucial to the drugs cancer killing ability, as it prevents the replication of cancer cells and inhibits tumor development. Although CDDP targets cancer cells, it also causes CIPN, a leading side effect for many patients.[136] CIPN onset due to CDDP can have major complications for patients which can lead to discomfort, numbness, pain, and treatment discontinuation. Specific mechanisms of toxicity by CDDP are still unknown however researchers assume changes in cell signaling cascades, calcium homeostasis and signaling, oxidative stress, mitochondrial dysfunction and induction of apoptosis as a result of DNA platination are all potential mechanisms behind CDDP-induced peripheral neuropathies.[137] Recently, platinum-based antineoplastics have been likely associated with mitochondrial DNA disruptions, specifically in axons.[138, 139] Based on these findings, it is important to

understand if MSTIM is able to have a neuroprotective effect against CDDP-induced PN. Through the analysis of mitochondrial and lysosome trafficking, as well as axon growth, key mechanistic insights can be identified regarding how each chemotherapy drug induces CIPN. Likewise, the effect of MSTIM on the two different mechanisms of action of these drugs is very important to help draw conclusions regarding treatment strategies against CIPN. Axon length, and mitochondrial trafficking were analyzed under varying MSTIM frequencies in order to understand the effect of MSTIM induced neuroprotection against PTX and CDDP. DRG samples were stimulated at varying frequencies to help understand how MSTIM effects pathophysiological changes in control and drug treated conditions. Through in depth analysis of cellular responses, this will be the first time that MSTIM is shown to have the ability to increase subcellular trafficking in axons as a neuroprotective strategy against CIPN.

Materials and Methods

Cell Culture

All animal experiments were conducted in accordance with protocols approved by the Institutional Animal Care and Use Committee (IACUC). Dorsal Root Ganglion (DRG) neurons were isolated from E−15 embryos collected from a Sprague-Dawley Rat. DRG explants were carefully collected and enzymatically dissociated using 0.25% Trypsin in L-15 medium (Sigma Aldrich). DRGs were suspended in a modified Neurobasal medium containing 1.0% Fetal Bovine Serum (FBS), 20.0% Glucose, 1.0% Penicillin/Streptomycin, B-27 supplement, 2 M $_{L}$-glutamine, and 10 ng/mL Glial Derived Nerve Growth Factor (GDNF) (Sigma Aldrich). DRG neurons were seated into the marked somal chamber of the compartmentalized devices and left to grow for 3-5 days to allow for axons to grow through the channels into the axonal side at an adequate length.

To limit evaporation, a small cotton ball soaked in sterile distilled water and 1.0% Penicillin/Streptomycin was placed in the same Petri dish as the chambers.

PDMS

In order to create the microfluidic device to help isolate and align axons, a master mold of the channel features was made using photolithography. Sylgard 184 polydimethylsiloxane (PDMS) (Dow chemical company USA) was used to create the chambers where the polymer was mixed with the proper curing agent and poured into the mold with the microchannel pattern. All air bubbles were removed via desiccator (SP Scienceware, USA) and was cured overnight at 70°C. The PDMS was then removed from the mold where excess was cut away from the device. Using a 6mm biopsy punch (Robbins Instruments), two adjacent holes were punched on either side of the microchannel array. Sets of chambers were then cut out and bonded to 1.5H glass slides (Fisher Scientific) using a Plasma Etch PE-75 Plasma Asher oxygen plasma device. Samples were then sterilized and coated with 100µg/mL Poly-D-Lysine (PDL) (Sigma Aldrich) and 10.0 µg/mL Laminin (Corning) where it was left overnight in 2°C-8°C refrigerator. Chambers were washed thoroughly using PBS1X and Neurobasal Media (Gibco) and placed into a sterilized primary cell incubator supplying 5.0% CO_2 (Binder C-150 UL).

Drug Treatment and Staining

PTX and CDDP were prepared as 1mM stock solutions prior to making the working solution and stored at −20°C freezer. PTX (Selleck Chemicals) was dissolved in ethanol, and L-OHP (Sigma) was dissolved in 0.9% sodium chloride. Stock solutions were then diluted using Neurobasal media (Gibco). 5µM was used for PTX, whereas 10 µM was optimal for CDDP. These concentrations were determined based on previous studies where we show proper dying back neuropathy and similar neurotoxicity as in *in vivo* situations. Drugs were administered to the compartments by removing 75% of existing media and readministered with the drug containing media at 37°C for 1 h prior to fluorescent staining. For axon integrity studies, DRGs were stained using Calcien AM (ThermoFisher) and allowed to incubate for 30 min to 1 h after initial drug administration. DRG's were imaged using a Leica DMi8 Thunder Fluorescent Microscope immediately after drug treatment, and likewise 24h after imaging. In order to image mitochondrial dynamics, MitoView Green was obtained from Biotium, USA and was added to the cells for 30 min to 1 h after drug treatment, similar to the previous protocol. Media was replaced twice to reduce any background fluorescence, and

immediately imaged. The compartmentalized system was covered in aluminum foil to prevent any light exposure.

Axon length measurements were performed using a glass bottom non-compartmentalized cell culture array (24 or 96 well format), where embryonic DRGs were cultured for 24 h prior to CIPN drug treatment. PTX and CDDP were treated at a concentration of 5 μM and 10 μM respectively and administered globally 1 h prior to stimulation for all experiments. Due to the Mitochondrial trafficking effects, we previously studied with FA, it was decided to use a similar toxicity concentration for each drug to understand the neuroprotective mechanism of MSTIM against CIPN.

MSTIM Setup

A custom built 12 well and 24 well pulsed magnetic stimulator was developed to generate 11mT, 2mm above the surface of the coils. Pulsed waveforms were generated using a Siglent1032x pulse generator. A custom pulse was implemented into the pulse generators using EasywaveX, where monophasic rectangular pulses lasting 0.5s every 2s with a pulse width of 0.2ms were stimulated for 1 hour per day. Input values of 10V from the signal generator were amplified using an amplification circuit, built curtesy of Dr. Stuart Smith. The amplification circuits were powered by a 15V power supply and generated an output current of 0.5A. Magnetic field strength was measured using a PASCO scientific PASSPORT 2-Axis Magnetic Field Sensor connected to a 550 universal Interface. The sensors were used to verify magnetic field strength 2mm away from the coil surface.

Results

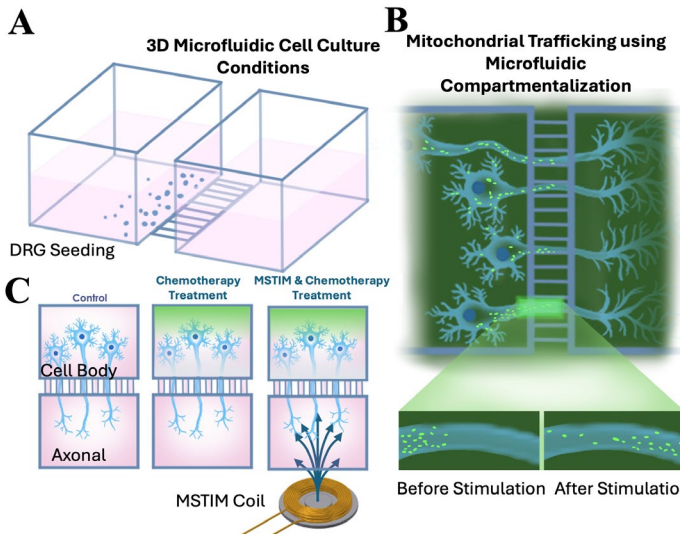

Figure 3.1: Graphical Abstract illustrating experimental set-up using Microfluidic cell culture system. 3D illustration of compartmentalized culture chambers for DRG seeding. (A) 2D illustration of mitochondrial trafficking within compartmentalized chambers. (B). 2D illustration of drug treatment and Magnetic stimulation on DRGs. (C)

ılts from this experiment found ınced mitochondrial trafficking reduction in axon degradation by frequency MSTIM. Figure 1 ines the cell culture set-up and ess for stimulation, and partmentalization of Dorsal Root glion (DRG) neurons. Figure 1A vs an illustration of the PDMS ofluidic device used to culture and ıte axons and cell bodies of DRGs. of the compartmentalized cell culture platform was essential for proper analysis of anterograde mitochondrial trafficking. Due to the alignment and isolation of axons, observation of mitochondrial dynamics can be easily observed. Compartmentalization likewise allows for induction of hydrostatic pressure against the channels. Through volume differences between the two chambers, hydrostatic pressure can be induced to limit diffusion of dye across the channels. This allows for proper analysis of mitochondrial trafficking, where mitochondrial within the channels. Figure 1B outlines the imaging process for mitochondrial trafficking, where mitochondria are stained only within the cell body chamber of the microfluidic device. The staining technique allows for anterograde trafficking analysis. We chose to observe anterograde trafficking in this study due to the dying back neuropathic conditions induced through chemotherapy treatment. This study aimed to observe how mitochondria migrated towards the site of injury and if MSTIM had the ability to enhance the recruitment of mitochondria. Based on the results of this study, a deeper understand of how MSTIM can affect energy dynamics through mitochondrial recruitment would be observed.

Figure 2. illustrates the experimental set-up and design of the magnetic stimulation device. Shown in Figure 1A and B, the magnetic stimulation set up is represented using real images of the coils and pulse wave generator (Siglent). Figure 1C and E show the magnetic field distribution modeled in COMSOL Multiphysics. Simulation shows peak magnetic field intensity of 14mT of a singular coil from our set up. Real time measurements using a PASCO scientific magnetic field sensor showed an intensity of 12mT 2mm above the surface of the coils. These results can be seen in Figure1D where custom waveform is shown which generates a magnetic field intensity of 11-13mT using a monophasic pulse waveform at 10V, with a pulse width of 0.2ms. The custom waveform was developed using the EasyWaveX, recommended by Siglent, the manufacturer of the Pulse generators. Each waveform was then uploaded to the signal generator channel and set to a specific frequency ranging from 10 Hz to 10 kHz. PDMS cell culture chambers were custom made to perfectly align with the coil set-up. Figure 1B shows an image of the stimulation device being used to test axon length and mitochondrial trafficking The coils were wired into the incubator, where cells could be stimulated under primary cell culture conditions, 5.0% CO_2 at 37°C. Figure 1F shows heat generated by the coils for one hour under experimental conditions, using an Omega HH520 Datalogger Thermometer. Heat analysis showed that cells did not experience temperatures above 40°C and did not experience denaturation from stimulation set-up.

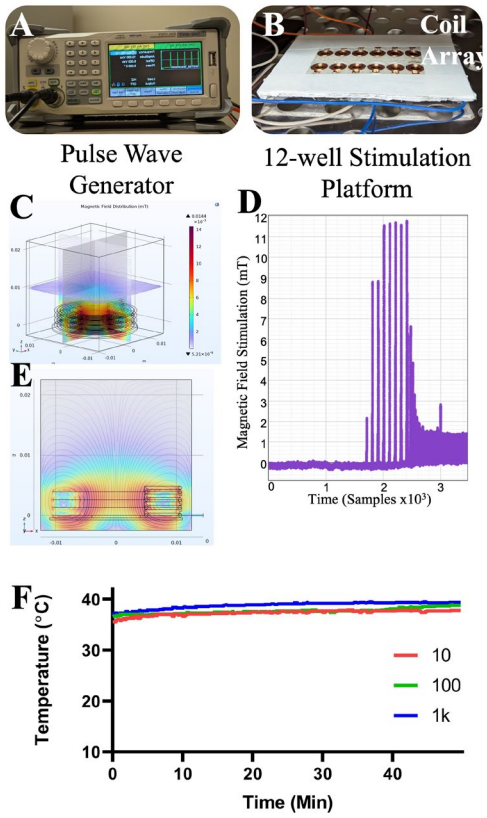

Figure 3.1: Experimental set-up and simulation data for Magnetic Stimulation device. Signal generator programmed to supply ideal pulse wave at varying frequencies at 10V. (A) 12-well coil array for mitochondrial trafficking analysis. (B) Amplification circuit design developed through UNC Charlotte. (C) COMSOL simulation data showing magnetic field distribution of current set-up. (D) PASCO scientific magentif field sensory data showing 12 mT peak 2mm above coil surface. (E) Heat generation during stimulation period using Omega HH520 thermocouple. (F)

Coil design was chosen based on Lenz law show in Equation 1. Ideal magnetic field strength was determined based on previous publications and was used to determine necessary coil parameters. 20mm and 40mm ferrite core flat coils were purchased from Digikey. WT202080-28F2-G coils were used due to the size, coil density and ferrite core. The flat coil was designed with a diameter of 20 mm which allowed for optimal stimulation of each well while small enough to not induce any interference with the adjacent coils. Each coil had a ferrite core with 28 turns with four layers to optimize inductance and efficiency. Coils were tested to have an inductance of 20.9 μH and a DC resistance of 300 mΩ. Ferrite core coils were chosen due to ferrite ability to minimize eddy current losses. Ferrite coils are highly favored for MSTIM devices due to their unique material properties, which enhance the efficiency and effectiveness of neuromodulation therapies. Ferrite's high magnetic permeability significantly boosts the strength and focus of the induced magnetic field, allowing for precise targeting and limited dispersion. Additionally, ferrite cores within coils are highly efficient, minimizing power losses by reducing eddy currents, which results in lower power consumption and less heat generation. This reduction in heating is essential for MSTIM, improving culture conditions overall. Using a ferrite core can help suppress electromagnetic interference (EMI), ensuring cleaner and more accurate stimulation signals.

MSTIM Coils were placed next to each other, 5 mm apart in order to stimulate a triplicate set of compartmentalized channels. Coils were far enough apart to not induce interference upon each other, shown by the simulation in Figure 2E and the numerical analysis in the following equations. A 3D printed enclosure was designed to separate the coils accurately, as well as give a 2mm gap between the coils and 1.5H glass bottom well. Designs for stimulation were custom developed for a single well glass bottom plate, where a PDMS microfluidic culture array was oxygen plasma bonded prior to cell seeding. Cells were placed 2mm above the coils to reduce heat induced on the cells, and to allow for optimal magnetic field strength. Heat generated by coils is shown by Figure 2F where coils, under all frequencies did not surpass 40°C, and did not denature cells within the culture device. Heat analysis was performed using thermocouples at each frequency to observe any changes in heat generated. Results found that heat

generation had minor effect for the varying frequencies, where 1 kHz stimulation had the highest heat generation. The MSTIM device was placed into a primary cell incubator where heat generation studies were performed. Therefore, the MSTIM device is capable of delivering proper magnetic fields without killing cells through denaturation. Through careful design and development of the MSTIM device, primary neurons could be stimulated for repeatable studies.

Governing Equations

Magnetic stimulation of DRG neurons operates through electromagnetic induction, where a time-varying magnetic field generates electric fields in the neurons. When a square wave with a pulse width of 0.2 milliseconds is applied to the DRG neurons, the rapid change in magnetic field (dB/dt) induces electric fields according to Faraday's law. These induced electric fields can depolarize neural membranes and trigger action potentials when they reach sufficient intensity.

The effectiveness of a 0.2 ms square pulse can be understood through the strength-duration relationship, which describes how the threshold for activation varies with pulse duration. This pulse width is particularly relevant as it falls within the optimal range for neural activation, typically close to the chronaxie time of cultured neurons (0.1-0.3 ms). The induced electric field interacts with neural membranes according to the cable equation modified for electromagnetic stimulation. The spatial distribution of this activation follows the activating function, which depends on the spatial derivative of the induced electric field along the neural processes.

The variations in field frequency significantly influence the membrane potential (ψcell) and organelle potential (ψorg). Low-frequency magnetic field (<1 kHz) is generally inadequate to produce noticeable ψorg and ψcell. Both ψorg and ψcell, however, increase proportionally with field frequency as described by Faraday’s law. Due to this frequency dependence, high-frequency magnetic fields are unlikely to selectively target internal organelles, unlike AC electric stimulation with nanosecond pulses, which has been utilized for organelle-specific applications, such as mitochondrial electroporation and the induction of

mitochondria-dependent apoptosis.[140]

Induced Electric Field

The primary equation governing the induced electric field (E) from a time-varying magnetic field (B) is given by Faraday's law:

$$\nabla \times \mathrm{E} = -\frac{\partial \mathrm{B}}{\partial \mathrm{t}} \quad (1)$$

For a square pulse of width $\tau = 0.2$ ms, the magnetic field change can be expressed as:

$$B(t) = B_0[H(t) - H(t-\tau)] \quad (2)$$

where H(t) is the Heaviside step function

Cable Equation for Neurons

The modified cable equation describes the dynamics of the transmembrane potential (V) along a neuron, incorporating the effects of an induced electric field (E). The equation describes how electric signals in neurons are affected by internal properties like resistance and capacitance, as well as external forces like electric field. This equation is:

$$\mathrm{Cm}\left(\frac{\partial \mathrm{V}}{\partial \mathrm{t}}\right) = \left(\frac{1}{Ra}\right)\left(\frac{\partial^2 \mathrm{V}}{\partial \mathrm{x}^2}\right) - \frac{V}{Rm} + \left(\frac{\lambda^2}{Ra}\right)\left(\frac{\partial \mathrm{E}}{\partial \mathrm{x}}\right) \quad (3)$$

Here, C_m represents the membrane capacitance per unit length, which describes the ability of the membrane to store charge. R_a is the axial resistance per unit length, indicating how difficult it is for current to flow longitudinally through the cytoplasm. R_m is the membrane resistance per unit area,

showing the extent to which the membrane allows electrical current to pass through it.[141] The term $\lambda = (R_m/R_a)^{1/2}$ is the space constant, a measure of how far electrical signals can travel along the neuron before they weaken significantly.[142]

Activation Function

The activation function (f) for neural stimulation:

$$f = \lambda^2\left(\frac{\partial E}{\partial x}\right) \tag{4}$$

Threshold condition:

$|f| \geq f_{th}$, where f_{th} is the threshold activation function value

Strength-Duration Relationship

The strength-duration relationship for a square pulse describes the dependency of the threshold magnetic field (B_{th}) on the pulse width (τ).

For a square pulse:

$$Bth = Brh\left(1 + \frac{\tau ch}{\tau}\right) \tag{5}$$

τ_{ch} or the chronaxie time, represents a characteristic time constant of the nerve or tissue being stimulated, indicating its sensitivity to pulse duration. B_{rh}, known as the rheobase, is the threshold field for a stimulus of infinite duration. The parameter (τ) denotes the width of the stimulus pulse, which in this case is set to 0.2 ms. This equation highlights that as the pulse width decreases, the required threshold magnetic field increases, demonstrating the balance between stimulus strength and duration in achieving excitation.

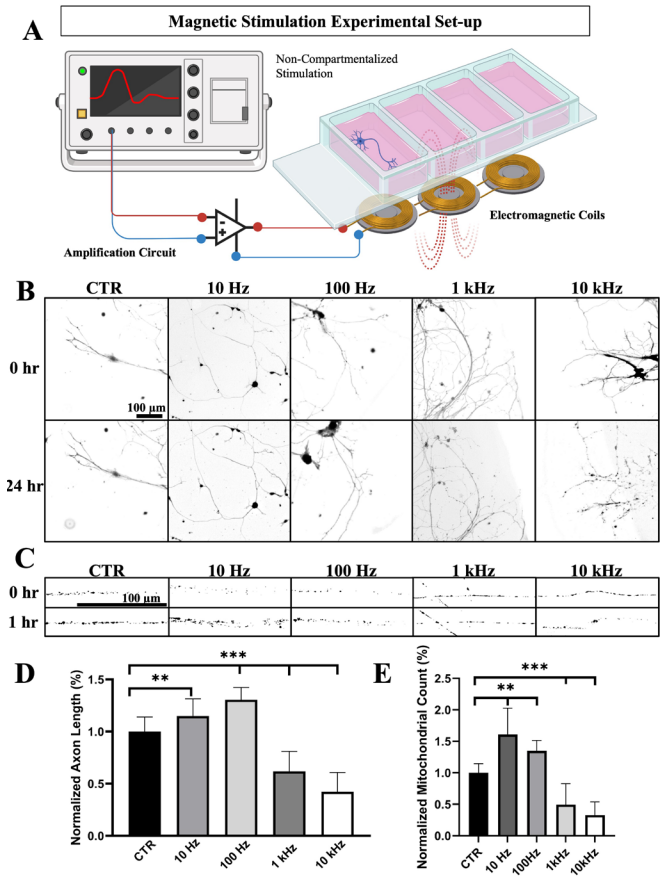

Figure 3.3: Axon length and mitochondrial trafficking response to frequency dependent Magnetic Stimulation. Experimental set-up of frequency response characterization. (A) Representative images showing 24-hour characterization of axon length after stimulation of varying frequencies (B). Representative images of mitochondrial trafficking after 1 hr stimulation at varying MSTIM frequencies. (C) Quantitative analysis of axon length in response to MSTIM frequencies (10 Hz, 100 Hz, 1 kHz, 10 kHz). (D) Quantitative analysis of Mitochondrial trafficking in response to MSTIM frequencies (10 Hz, 100 Hz, 1 kHz, 10 kHz). (E) Data are shown by mean ± SD. ***$p < 0.001$, **$p < 0.01$, *$p < 0.05$ as determined by two-tailed t test (E), Scale bar is 100 µm unless otherwise stated.

Figure 3. Outlines a frequency response using the MSTIM device to observe axonal integrity and mitochondrial trafficking. Samples were allowed to grow for 24 hours prior to stimulation and imaging was performed over 2 days of stimulation cycles. Axon length and mitochondrial trafficking changes were observed and quantified using FIJI ImageJ. The frequency response experimental was designed to identify a frequency range which had positive axon growth and mitochondrial trafficking capabilities. Shown in Figure. 3B, Low frequency stimulation (10 Hz, and 100 Hz) had a positive effect on axon growth where 10Hz showed 14.80±0.16% increase, 100Hz showed 30.51±0.12% increase, 1 kHz showed 50.77±0.19% decrease and 10 kHz showed 57.55±0.19% decrease in axon length compared to initial conditions. Likewise mitochondrial trafficking rates were increased during low frequency stimulation where, 10Hz showed 61±0.16% increase, 100Hz showed34.85±0.15% increase, 1 kHz showed 50.4±0.33% decrease and 10kHz showed 67.27±0.21% decrease in mitochondrial trafficking over the stimulation period. Based on the frequency response experimentation, positive frequencies can be used for regenerative purposes to

regrow axons and increase energy dynamics within neurons. However, it is important to note the negative effect of MSTIM at this higher frequency, which may be attributed to induced excitotoxicity by high frequency stimulation.

Figure 3 shows how low frequency stimulation (>1 kHz) has the ability to enhance axon growth and mitochondrial trafficking during the one-hour stimulation. Samples were stimulated over a two-day period in order to accurately measure axon length and mitochondrial dynamics. Due to the extensive network that DRG neurons create in *in vitro* settings, experimental procedures were started 24 hours after cell seeding. When cells were allowed to grow for more than 24 hours, axonal networks were too vast and dense to accurately measure axon length. For this reason, studies were similarly performed over 24 hours in order to properly measure any changes in axon length. Images were performed in the exact same location in order to show change in axon length, where results were then normalized and compared. Similarly, mitochondrial trafficking was performed over a 1-hour stimulation period due to the size and motility of mitochondrial within DRGs. However, for the mitochondrial experiments, axons needed to grow sufficiently through microchannels, which took 3-5 days. Axonal growth was monitored each day after seeding until sufficient axon growth through the channels was observed. Samples were then imaged, stimulated for one hour, and images again in the same location using numbered markers within the microfluidic device. This method allowed for tracking of mitochondria and allowed us to count mitochondrial population at each timestamp. Using this method, we observed the percent change between the samples at different frequencies and drug treatments.

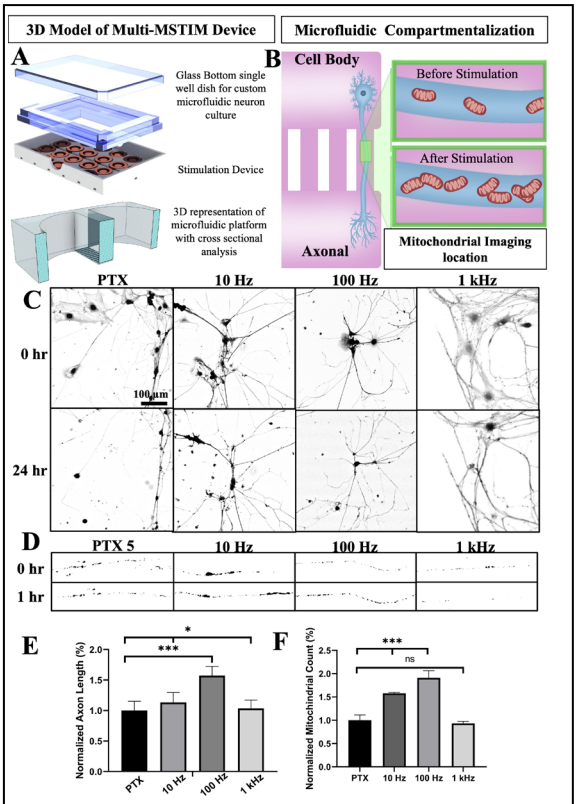

Figure 3.4 Low Frequency Magnetic Stimulation Enhances Mitochondrial Trafficking against PTX and CDDP Induced Degeneration. Experimental set-up illustrating custom microfluidic compartmentalized cell culture system and coil placement **(A)**. Illustration of axon growth through channels and mitochondrial trafficking image analysis **(B)**. Representative images of mitochondria trafficking before and after stimulation at 10Hz, 100Hz, and 1 kHz based on frequency response **(C)**. Graphical analysis of mitochondrial trafficking for each frequency under control, PTX and CDDP induced samples **(D)**. Data are shown by mean ± SD. ***p < 0.001, **p < 0.01, *p < 0.05 as determined by two-tailed t test (E), Scale bar is 100 µm unless otherwise stated.

Figure 4 shows results from MSTIM treated samples in PTX induced peripheral neuropathy DRGs. PTX concentrations were chosen from previously performed experiments, where 5 µM PTX showed optimal dying back neuropathy without inducing sudden cell death. Figure 4A illustrates the custom 24 well stimulation device used for drug treated samples. Using a glass bottom 24 well plate DRGs were cultured for 24 hours prior to PTX administration. PTX was then gestated for one hour in order to allow proper drug response. Samples were stimulated at low frequency MSTIM based on the frequency response from Figure 3. Figure 4B likewise illustrated how mitochondrial trafficking analysis was performed, where hydrostatic pressure was induced against the cell body chamber to limit diffusion of dye and drugs across the channels. Figure 4B similarly shows how cell bodies and axons were compartmentalized for alignment of axons. The specified alignment is critical for this analysis as it allows ideal anterograde tracking of mitochondria. Figure 4B illustrated how imaging before and after stimulation shows an influx of mitochondria into the axon, moving towards the distal end. Results from this study found that low frequency (>1 kHz) MSTIM had the ability to reduce degeneration effects of PTX induced peripheral neuropathy. Figure 4C&E shows representative images of how PTX degenerated axon fibers in DRGs, where 10 Hz, and 100 Hz, increased axonal integrity by 13.45±1.3% and 57.23±0.71%

respectively. However, 1 kHz MSTIM had little to effect on axonal degeneration showing only 3.62±0.15%. Likewise, Figure 4D&F show how low frequency MSTIM can enhance mitochondrial trafficking in PTX treated samples. MSTIM samples showed enhancement where 10 and 100 Hz stimulation was able to enhance mitochondrial trafficking by 57.72±21.5% and 91.17±15.2% respectively. Results from this experiment show how low frequency MSTIM can enhance mitochondrial trafficking in an anterograde manner, sending mitochondria, and energy to the sites of injury. However, it is unclear whether MSTIM is able to rescue mitochondrial trafficking due to a common signaling mechanisms with PTX cancer killing mechanism or if it is unrelated. Due to PTX ability to directly affect transport within neurons, degrading microtubule structures within axons, we were unsure if MSTIM was blocking this ability, or directly interacting with mitochondria. To answer this question, we studied MSTIM neuroprotective ability against CDDP, a DNA replication targeting chemotherapy drug.

Figure 5 discusses the neuroprotective effect of low frequency MSTIM against CDDP treated samples. Optimal concentration of CDDP treatment were determined based on previous studies where 10 μM induced proper dying back neuropathy without induction of sudden cell death. Figure 5A&C show how CDDP induced axonal degeneration and how low frequency MSTIM can reduce degeneration. Results discovered that 10Hz and 100Hz stimulation frequencies had similar results to PTX treated samples. CDDP only samples degenerated axon by 81.13±12.7% after 24 hours of treatment. 10Hz MSTIM was able to

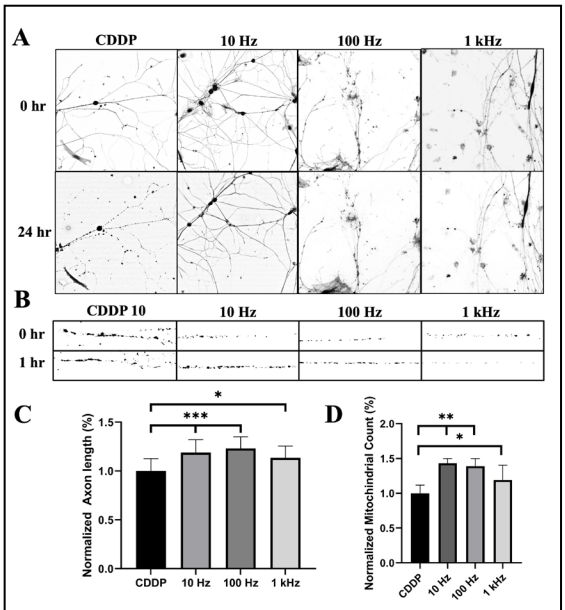

Figure 3.5 Low Frequency Magnetic Stimulation Enhances Mitochondrial Trafficking against CDDP Induced Degeneration. Experimental set-up illustrating custom microfluidic compartmentalized cell culture system and coil placement **(A)**. Illustration of axon growth through channels and mitochondrial trafficking image analysis **(B)**. Representative images of mitochondria trafficking before and after stimulation at 10Hz, 100Hz, and 1 kHz based on frequency response **(C)**. Graphical analysis of mitochondrial trafficking for each frequency under control, PTRX and CDDP induced samples **(D)**. Data are shown by mean ± SD. ***p < 0.001, **p < 0.01, ∗p < 0.05 as determined by two-tailed t test (E), Scale bar is 100 μm unless otherwise stated.

reduce degeneration by CDDP 18.79±1.33% while)Hz stimulation was also shown to decrease generation by CDDP by 23.01±1.20%. However, ike PTX treatment samples, 1kHz was found to ıance axonal integrity by13.42±1.21%. Similarly, v frequency MSTIM was found to enhance ochondrial trafficking by 43.30±6.06% for 10Hz, 02±10.76% for 100Hz, and 19.17±12.04% for 1 z. Results from this experiment showed that STIM mediated neuroprotection is not specific to articular cancer killing mechanism. Results from s study help to understand how MSTIM dulated neurons, and how induction of neural citability can reduce degeneration effects by motherapy drugs, and potentially other generating disorders. Although CDDP targets NA replication, there is a distinct correlation ween CDDP treatment and mitochondrial dysfunction. Based on this analysis, MSTIM ability to modulate mitochondrial trafficking may offset any dysfunction by CDDP. Researchers believe that CDDP may not only affect DNA within the nucleus of the target cell but also the mitochondrial DNA leading to dysfunctions observed. Through modulation of neural activity using MSTIM, we show for the first time, MSTIM ability to enhance anterograde mitochondrial trafficking as a neuroprotective mechanism against CDDP induced peripheral neuropathy. Based on these findings, we can develop a deeper understanding of the mechanisms involved with CDDP induced peripheral neuropathy, and likewise, neuroprotective mechanisms through MSTIM.

Discussion

Dorsal root ganglion neurons were used due to their involvement in peripheral neuropathy and characteristics.[143] DRGs are sensory neurons which transmit pain and other sensations from external stimuli. DRGs are directly involved in PN are traditionally looked at as targets for therapeutics related to pain mechanics, and sensory disorders.[144] Due to the dying back effect of CIPN, DRGs send pain signals to the patient which causes extreme discomfort and pain, oftentimes leading to dosage reductions or termination.[145] Additionally, DRGs were used since they do not exhibit spontaneous neuronal activity, which allowed for optimal conditions for external stimulus such as MSTIM.[146] Unlike other cell types, DRGs only send and receive signals when an external stimulus is induced, therefore MSTIM can effectively induce neural activity on DRGs without interference. Isolation of DRGs allows for culturing of pure sensory neurons due to their location outside the spinal cord. Percentage of glial cell contamination within cell cultures is significantly reduced due to the limited interaction with the CNS. Although, variation in glial cell co culture is highly dependent on the isolation conditions and skills of the individual performing isolation. Additionally, DRGs retain their functional characteristics after culturing, allowing them to perform the same in vitro and in vivo.[147] DRGs express a variety of ion channels, receptors, and neurotransmitter systems, including voltage-gated sodium channels, potassium channels, and transient receptor potential (TRP) channels.[148] Such channels are critical for generating action potentials and are often targets for neuromodulation. DRGs are highly sensitive to neuromodulation, such as, electrical fields, pharmacological agents, and neurotransmitters. Their sensitivity makes them a great model for studying how neuromodulation can influence neuronal activity and signal transmission.[149] Neuromodulation techniques in clinical settings such as, spinal cord stimulation (SCS) and peripheral nerve stimulation (PNS) target DRG neurons to treat chronic pain conditions. DRGs are a relevant and versatile model for studying neuromodulation due to their role in sensory processing, accessibility, electrophysiological properties, and clinical relevance to pain and neuropathy. This makes them ideal for exploring how MSTIM can alter neuronal activity, which is crucial for developing therapies for chronic pain and sensory dysfunction. The

use of MSTIM could provide a significant alternative to chronic pain management for conditions such as CIPN. Not only can MSTIM provide potential pain management, but the regenerative properties can provide the next step – non-invasive restoration of damaged axonal pathways with neuroprotective ability. MSTIM is extremely significant due to its non-invasive ability, which can prevent multiple complications which often come with invasive procedures including infections, scarring, etc.

Prior to the introduction of MSTIM, electrical stimulation (ESTIM) was introduced as an excellent form of pain management with neuroprotective ability and continues to be one of the most common approaches for neuromodulation.[150] ESTIM flourishes under specific frequencies in order to output mitochondrial enhancement for pain management and neuroprotection, where frequencies above 1 kHz (100 kHz and 1 MHz) were found to be particularly inhibitive of growth in terms of axons.[151] Although it has been found that MSTIM and ESTIM are both promising and effective potentials for chronic pain management, MSTIM provides a greater capability when considering many different factors. A significant difference between MSTIM and ESTIM is the non-invasive attribute which MSTIM harnesses.[152] Electrical waves cannot penetrate the skin nearly as far as magnetic waves without the use of external electrodes. This means that, not only can MSTIM provide altogether comfort which ESTIM lacks, but it can penetrate the skin to a much further degree without the use of additional, external technology. The mitigation of external technology is powerful, because it reduces the many complications which can come with invasive treatment. ESTIM techniques must consider factors like biocompatibility, given that electrodes must be implanted to conduct functional and deep stimulation. However, with MSTIM, the completely external technique does not need to consider biocompatible aspects. The actual procedure of implanting electrodes can cause many surgical complications, where the electrodes can be either difficult to place precisely to connect the electrical activity to corresponding tissue or altogether rejected by the system.[153] Even placing the electrodes correctly, tuning them for stimulation can easily cause overexcitation – thereby creating forms of neuronal damage. Long-term, MSTIM can provide a better alternative to ESTIM altogether due to the electrode performance degrading overtime. MSTIM can be applied externally without

attenuation overtime, due to the ability for repeated, non-invasive use. Additionally, MSTIM offers a better degree of focal precision over ESTIM, which can allow for treatment of small, more sectioned areas without the globalized damage or inflammation of surrounding tissue or muscle fibers. Overall, MSTIM offers a promising, stronger argument for pain management and neuroprotection. ESTIM and MSTIM share the same abilities, however the method of application for MSTIM is nonabrasive and better for long-term applications.

Challenges, and Alternative Approaches

Unlike Electrical stimulation, Magnetic stimulation has field directionality and does not induce equal levels of magnetic field intensity on neurons. Due to this challenge, it is difficult to design a device to induce all cells within the culture chamber equally. In order to overcome this challenge, we implemented a ferrite core to attempt to distribute the magnetic fields evenly. However, in order to achieve ideal results, coils should be designed and implemented directly into the cell culture chamber where they have the ability to directly apply magnetic fields on neurons. Similarly, control of heat generation is essential to ensure proper stimulation at the ideal culture environment. However, it is difficult to fully understand how heat generation could play a role in analysis and cellular changes. Although heat generated by our device did not exceed the denaturation temperature, cells were exposed to an environment outside of ideal culture conditions for the stimulation period which may have contributed to differences in experimental results.

Limitations of this study

Limitations of this study derive from a lack of understanding involving specific signaling mechanisms involved with MSTIM. Although we have a general understanding of how MSTIM modulated membrane potential to induce neural activity, it is still not understood how MSTIM alters specific signaling mechanisms to enhance mitochondrial trafficking. Questions such as changes in mitochondrial motility, directionality, fusion and fission are lacking and are needed to develop a full understanding of how MSTIM alters mitochondrial trafficking. It is thought that neuromodulation techniques such as ESTIM and MSTIM have the ability to overexpress Brain Derived Neurotrophic Factor (BDNF) which is directly correlated

with enhanced organelle trafficking. Understanding how MSTIM changes protein and trophic factor expression would be essential for clinical use of MSTIM.

Data analysis

Data was collected using Fiji-ImageJ to measure axon lengths in triplicate samples. Microsoft Office Excel 2022 was used to compile all measurement data, where average and standard deviation was analyzed. Axonal integrity was found through calculation of percent difference compared to the average control (0h) for each sample. Optimal drug concentrations were determined in prior publications as well as additional literature showing CIPN in vitro. Differences in percent change were used to observe the effect of chemotherapy treatment and the neuroprotective effect of varying MSTIM frequencies. Mitochondrial analysis used a similar approach, where mitochondrial count was measured and compared against the control (0h), normalizing the dataset. Data was presented as a percentage of the control value, showing a positive or negative change in comparison. To quantify the mitochondrial displacement, images were analyzed with the aid of 'MTrackJ' plugin for manual tracking of individual mitochondria across the timestamped images. Images were taken before and after 1 hour stimulation.

Quantification and statistical analysis

All datasets were presented as a mean ± standard deviation except where noted. Datasets were grouped as triplicate N = 3. The probability (p-value) between groups was analyzed by the two-tailed *t*-test provided in Microsoft Office Excel 2022 unless otherwise stated. p-value less than 0.05 was considered statistically significant.

Acknowledgments

This research was supported by the National Science Foundation (NSF) Career Award (2238723).

Author contributions

B.A.: conceptualization, methodology, validation, formal analysis, investigation, data curation, writing, visualization. K.Q.: conceptualization, methodology, validation, formal analysis, investigation, data

curation, writing, visualization. P.A.: methodology, software, validation, formal analysis, data curation, review & editing. R.G.: review & editing, visualization. I.H.Y.: conceptualization, validation, recourses, review & editing, supervision, project administration, funding acquisition.

Declaration of interests

The authors declare no competing interests.

Overall Discussion:

Neuromodulation is a rapidly advancing field that focuses on altering neural activity through targeted delivery of electrical or chemical stimuli to specific areas of the nervous system. By utilizing different techniques such as deep brain stimulation, spinal cord stimulation, and transcranial magnetic stimulation, neuromodulation has the potential to treat a wide range of neurological and psychiatric conditions, including chronic pain, epilepsy, Parkinson's disease, and peripheral neuropathy. Unlike traditional pharmaceutical approaches, which can affect the entire body, neuromodulation offers a more targeted, localized intervention which can optimize therapeutic efficacy while minimizing side effects. As our understanding of the nervous system deepens, neuromodulation is emerging as a transformative approach in both clinical and research settings, with the potential to advance technologies for restoring function, alleviating symptoms, and improving patients' quality of life. Stimulation techniques such as Electrical Stimulation (ESTIM) and Magnetic Stimulation (MSTIM) focus on external electric field induction in pulsed patterns which mimic action potential firing rates. Through modification in frequency stimulation, neurons can be excited or depressed, changing characteristics such as growth, energy production, synapse formation and plasticity.

This dissertation focuses on the novelty of modulating mitochondrial trafficking as a potential mechanism against chemotherapy induced peripheral neuropathy. Through drug treatment, electrical and magnetic stimulation, we were able to show neuroprotective effects against common chemotherapy induced peripheral neuropathies. Mechanistic insights into how these three methods modulate mitochondrial

trafficking were observed. Analysis of this dissertation shows that through alteration in mitochondrial trafficking, we have the ability to meet energy demands within sensory neurons as a potential neuroprotective mechanism against CIPN. However, further studies are needed to understand the specific mechanism associated with FA, ESTIM, or MSTIM enhanced mitochondrial trafficking and whether mitochondrial trafficking is a primary or secondary response.

Using advanced imaging techniques such as computationally advanced fluorescent microscopy, combined with microfluidics; physical changes in cellular and subcellular dynamics of DRGs were observed and quantified under different conditions. Using a Leica DMI8 thunder microscope and microfluidic devices, fluorescent imaging of mitochondrial trafficking was characterized and quantified under CIPN conditions. Analysis of mitochondrial dynamics can help to be a physical marker of injury conditions.

Paclitaxel (PTX), Oxaliplatin (L-OHP) and Cisplatin (CDDP) are well-established chemotherapy drugs used to treat a range of cancers, including breast, ovarian, bladder, prostate, skin, esophageal, and non-small cell lung cancers. These drugs are frequently used in combination therapies, where platinum and microtubule-based drugs are used for higher therapeutic efficacy. However, treatment with such drugs induced degeneration of the peripheral nervous system, typically starting at the extremities. This side effect coined Chemotherapy Induced Peripheral Neuropathy (CIPN) is a debilitating and painful aspect of chemotherapy treatment and oftentimes leads to dosage reduction and even termination of treatment. Currently, there are no targeted treatments available for CIPN, other than symptomatic relief. Additionally, conventional drugs, including opioids, do not promote axon regeneration, which is critical for the long-term recovery from CIPN.

Based on the results of this study, we found that modulation of mitochondrial trafficking has the potential to have neuroprotective effects on DRGs against CIPN. Although further details involving how FA, ESTIM and MSTIM enhance mitochondrial trafficking are still unknown, we show a distinct correlation between reduction in degeneration of axons and enhanced mitochondrial trafficking by the three methods shown.

Mitochondria in particular is analyzed due to their significance in cellular homeostasis, regeneration and specific needs in neurons. Neurons consume a significantly high amount of energy within the body, where studies have found that the brain uses 10% of resting energy on a daily basis. Due to the physiology of neurons, mitochondria are extremely important for neuronal functions such as cell survivability, as well as signal collection and transfer. Previous studies have found that when cells are exposed to chemotherapy drugs, it has a direct effect on mitochondrial function, which can result in depolarization of mitochondrial and limited mitochondrial trafficking. Depolarized mitochondria not only produce less ATP but also release toxic reactive oxygen species, leading to significant axonal degeneration. In this study we believed that replacing the damaged mitochondria may have the ability to protect axons from degeneration and support the high energy demands of axonal regeneration. We hypothesized that impaired mitochondrial transport in neurons reduces efficient delivery of healthy mitochondria to distal axons and the removal of damaged mitochondria from injured axons. Previous studies have shown that mitochondrial impairment causes the rapid progression of chemotherapeutic-induced neurodegeneration. PTX treatment for cancer patients results in a decline of the mitochondrial population, health, and interaction of axonal mitochondria in neurons. In order to combat this effect, we initially treated DRG neurons with corticosteroid drug Fluocinolone Acetonide (FA) which was found to be able to enhance mitochondrial trafficking even beyond control samples. FA was chosen based on a drug screening performed by our lab, Regenerative Neural Engineering, at UNCC which discovered FA as a candidate for neuroprotective effects. Although FA was found to have neuroprotective effects, its nature as a glucocorticoid drug makes its effectiveness in a clinical setting skeptical. Unfortunately, glucocorticoids in general have been found to induce side effects such as, inflammation, suppression of the immune system, as well as psychological disturbances.[154] Due to this, we developed neuromodulatory devices which have been shown to alter cellular and subcellular dynamics. Primarily, we developed an electrical stimulation (ESTIM) device to induce an electric field on neurons in vitro.

Electrical Stimulation (ESTIM) has shown to be an effective symptomatic treatment to treat pain associated with peripheral nerve damage. However, the neuroprotective mechanism of ESTIM on peripheral neuropathies is still unknown. In this study, we identified that ESTIM has the ability to enhance mitochondrial trafficking as a neuroprotective mechanism against chemotherapy-induced peripheral neuropathies (CIPNs). CIPN is a debilitating and painful sequalae of anti-cancer chemotherapy treatment which results in degeneration of peripheral nerves. Mitochondrial dynamics were analyzed within axons into two different antineoplastic mechanisms by chemotherapy drug treatments paclitaxel and oxaliplatin in vitro. Mitochondrial trafficking response to chemotherapy drug treatment was observed to decrease in conjunction with degeneration of distal axons. Using low-frequency ESTIM, we observed enhanced mitochondrial trafficking to be a neuroprotective mechanism against CIPN. This study confirms ESTIM enhances regeneration of peripheral nerves by increased mitochondrial trafficking.

ESTIM was shown to have great potential for treatment against CIPN, however due to the invasive nature of ESTIM, there are many complications in developing devices for clinical settings. Therefore, we decided to design and develop a Magnetic stimulation device which induced similar electric fields on neurons, however, in a non-invasive manner. Magnetic Stimulation (MSTIM) is an emerging non-invasive therapy for neurological conditions, specifically, Transcranial Magnetic Stimulation (TMS) is currently being used to help treat depression and anxiety. However, the cellular mechanisms behind MSTIM enhanced axon growth and regeneration is still unknown. MSTIM can induce neuronal activity to modulate excitability in neurons and physiological conditions. MSTIM efficacy has been shown to have a direct correlation with frequency output, where low frequency (10 – 1000 Hz) pulsed stimulation shows increased growth rates, plasticity and excitability in neurons *in vitro*. The non-invasive manner of MSTIM technology makes it a highly desirable treatment strategy due to the ease of use and effectiveness. As opposed to electrical stimulation, there is more control over the directionality of the generated magnetic field using magnetic stimulation based on the orientation of the magnetic coils utilized. Although MSTIM has proven to be an effective strategy for neuromodulation, underlying mechanisms are still unknown. Through analysis of

pathophysiological and metabolic changes in the form of axonal integrity and mitochondrial trafficking, key mechanistic insights can be determined to develop effective neuromodulation strategies to prevent and treat CIPN conditions.

Limitations of this study:

Electrical stimulation and magnetic stimulation are becoming promising tools for peripheral nerve regeneration. However, ESTIM has a significant hindrance to succeeding therapy where, low biocompatibility and problems at the electrode–tissue interfaces during long-period implantation can cause challenges for providers and patients alike. Implanted materials for electrical stimulation placed under the cover of insulated biocompatible materials, such as miniature coils, offer several advantages in biocompatibility and feasibility. Further noninvasive approaches are also considered potential therapies such as magnetic stimulation (MSTIM). MSTIM has been widely studied for the non-invasive treatment of neuronal disfunctions. However, a detailed mechanistic and molecular approach regarding how neurons are benefitted from MSTIM is not fully understood. The challenge of using magnetic field stimulation currently stems from the miniaturization of the device and optimizing the pulse pattern. Source-generating, low-frequency pulses in miniaturized coils can only be generated through the use of large amplifiers which require high power needs. An additional obstacle is the duration of the stimulation pulses. However, lowering power needs to induce a low-frequency pulse may be achieved through design and engineering. Moreover, magnetic stimulation of three-dimensional cellular constructs (such as organoids) would be a promising choice for neural stimulation, and to characterize how MSTIM affects organoid development or regeneration. Studies involving organoids may help lead to a deeper understanding of mechanisms involved in neuromodulation, as well as any differences between in vitro and in vivo stimulation. Electrical and magnetic stimulation approaches can be debatable regarding the effector cells or subcellular organelles upon therapy. However, based on this study, we show a direct correlation between stimulation parameters and subcellular dynamics. Using this knowledge, we can develop a deeper understanding of the nervous system and hopefully engineer devices that can help individuals suffering from neurological disorders

without worry of debilitating side effects. Moreover, through the application of neuromodulation alongside chemotherapy treatment, we show that stimulation can reduce side effects of chemotherapy treatment. This finding is significant as it may allow patients to undergo more optimal chemotherapy treatment without the fear of dose limiting factors such as CIPN.

References

[1] N. P. Staff, A. Grisold, W. Grisold, and A. J. Windebank, "Chemotherapy-induced peripheral neuropathy: a current review," *Annals of neurology,* vol. 81, no. 6, pp. 772-781, 2017.

[2] C. E. Argoff, B. E. Cole, D. A. Fishbain, and G. A. Irving, "Diabetic peripheral neuropathic pain: clinical and quality-of-life issues," in *Mayo Clinic Proceedings*, 2006, vol. 81, no. 4: Elsevier, pp. S3-S11.

[3] J. McLeod, "Investigation of peripheral neuropathy," *Journal of neurology, neurosurgery, and psychiatry,* vol. 58, no. 3, p. 274, 1995.

[4] I. H. Yang, R. Siddique, S. Hosmane, N. Thakor, and A. Höke, "Compartmentalized microfluidic culture platform to study mechanism of paclitaxel-induced axonal degeneration," *Experimental Neurology,* vol. 218, no. 1, pp. 124-128, 2009/07/01/ 2009, doi: https://doi.org/10.1016/j.expneurol.2009.04.017.

[5] S. Quasthoff and H. P. Hartung, "Chemotherapy-induced peripheral neuropathy," *Journal of neurology,* vol. 249, pp. 9-17, 2002.

[6] M. S. Chong and J. Hester, "Diabetic painful neuropathy: current and future treatment options," *Drugs,* vol. 67, pp. 569-585, 2007.

[7] M. I. Bennett and K. H. Simpson, "Gabapentin in the treatment of neuropathic pain," *Palliative Medicine,* vol. 18, no. 1, pp. 5-11, 2004.

[8] D. J. Goldstein, Y. Lu, M. J. Detke, T. C. Lee, and S. Iyengar, "Duloxetine vs. placebo in patients with painful diabetic neuropathy," *Pain,* vol. 116, no. 1-2, pp. 109-118, 2005.

[9] R. H. Dworkin *et al.*, "Pharmacologic management of neuropathic pain: evidence-based recommendations," *Pain,* vol. 132, no. 3, pp. 237-251, 2007.

[10] B. Xu, G. Descalzi, H.-R. Ye, M. Zhuo, and Y.-W. Wang, "Translational investigation and treatment of neuropathic pain," *Molecular pain,* vol. 8, pp. 1744-8069-8-15, 2012.

[11] Y. Fukuda, Y. Li, and R. A. Segal, "A mechanistic understanding of axon degeneration in chemotherapy-induced peripheral neuropathy," *Frontiers in neuroscience,* vol. 11, p. 481, 2017.

[12] B. A. Weaver, "How Taxol/paclitaxel kills cancer cells," *Molecular biology of the cell,* vol. 25, no. 18, pp. 2677-2681, 2014.

[13] S. Mielke, A. Sparreboom, and K. Mross, "Peripheral neuropathy: a persisting challenge in paclitaxel-based regimes," *European journal of cancer,* vol. 42, no. 1, pp. 24-30, 2006.

[14] A. Cetinkaya-Fisgin *et al.*, "Identification of fluocinolone acetonide to prevent paclitaxel-induced peripheral neuropathy," *Journal of the Peripheral Nervous System,* vol. 21, no. 3, pp. 128-133, 2016.

[15] D. Dornan *et al.*, "Therapeutic potential of an anti-CD79b antibody–drug conjugate, anti–CD79b-vc-MMAE, for the treatment of non-Hodgkin lymphoma," *Blood, The Journal of the American Society of Hematology,* vol. 114, no. 13, pp. 2721-2729, 2009.

[16] S. O. Doronina *et al.*, "Development of potent monoclonal antibody auristatin conjugates for cancer therapy," *Nature biotechnology,* vol. 21, no. 7, pp. 778-784, 2003.

[17] A. Beck, L. Goetsch, C. Dumontet, and N. Corvaïa, "Strategies and challenges for the next generation of antibody–drug conjugates," *Nature reviews Drug discovery,* vol. 16, no. 5, pp. 315-337, 2017.

[18] R. L. Best *et al.*, "Microtubule and tubulin binding and regulation of microtubule dynamics by the antibody drug conjugate (ADC) payload, monomethyl auristatin E (MMAE): Mechanistic insights

into MMAE ADC peripheral neuropathy," *Toxicology and Applied Pharmacology,* vol. 421, p. 115534, 2021.

[19] J. Below, "Vincristine," 2019.

[20] N. Kiguchi, T. Maeda, Y. Kobayashi, F. Saika, and S. Kishioka, "Involvement of inflammatory mediators in neuropathic pain caused by vincristine," *International review of neurobiology,* vol. 85, pp. 179-190, 2009.

[21] M. Tsubaki *et al.*, "Tamoxifen suppresses paclitaxel-, vincristine-, and bortezomib-induced neuropathy via inhibition of the protein kinase C/extracellular signal-regulated kinase pathway," *Tumour Biol,* vol. 40, no. 10, p. 1010428318808670, Oct 2018, doi: 10.1177/1010428318808670.

[22] S. Triarico *et al.*, "Vincristine-induced peripheral neuropathy (VIPN) in pediatric tumors: Mechanisms, risk factors, strategies of prevention and treatment," *International journal of molecular sciences,* vol. 22, no. 8, p. 4112, 2021.

[23] H. Starobova and I. Vetter, "Pathophysiology of chemotherapy-induced peripheral neuropathy," *Frontiers in molecular neuroscience,* vol. 10, p. 174, 2017.

[24] W. H. Organization, "World Health Organization model list of essential medicines: 21st list 2019," World Health Organization, 2019.

[25] S. A. Aldossary, "Review on pharmacology of cisplatin: clinical use, toxicity and mechanism of resistance of cisplatin," *Biomedical and Pharmacology Journal,* vol. 12, no. 1, pp. 7-15, 2019.

[26] C. Meijer, E. G. de Vries, P. Marmiroli, G. Tredici, L. Frattola, and G. Cavaletti, "Cisplatin-induced DNA-platination in experimental dorsal root ganglia neuronopathy," *Neurotoxicology,* vol. 20, no. 6, pp. 883-7, Dec 1999. [Online]. Available: https://www.ncbi.nlm.nih.gov/pubmed/10693969.

[27] A. A. Argyriou, J. Bruna, P. Marmiroli, and G. Cavaletti, "Chemotherapy-induced peripheral neurotoxicity (CIPN): an update," *Critical reviews in oncology/hematology,* vol. 82, no. 1, pp. 51-77, 2012.

[28] E. Merlini, M. P. Coleman, and A. Loreto, "Mitochondrial dysfunction as a trigger of programmed axon death," *Trends in Neurosciences,* vol. 45, no. 1, pp. 53-63, 2022.

[29] A. Trecarichi and S. J. Flatters, "Mitochondrial dysfunction in the pathogenesis of chemotherapy-induced peripheral neuropathy," *International review of neurobiology,* vol. 145, pp. 83-126, 2019.

[30] S. R. Chada and P. J. Hollenbeck, "Mitochondrial movement and positioning in axons: the role of growth factor signaling," *Journal of Experimental Biology,* vol. 206, no. 12, pp. 1985-1992, 2003.

[31] G. M. Smith and G. Gallo, "The role of mitochondria in axon development and regeneration," *Developmental neurobiology,* vol. 78, no. 3, pp. 221-237, 2018.

[32] A. McDonnell, "Chemotherapeutic agents and their uses, dosages, and toxicities," *can be found under https://www. cancernetwork. com/cancermanagement/chemotherapeutic-agents-and-their-uses-dosages-and-toxicities,* 2016.

[33] A. P. Singh and D. K. Shah, "Measurement and mathematical characterization of cell-level pharmacokinetics of antibody-drug conjugates: a case study with trastuzumab-vc-MMAE," *Drug Metabolism and Disposition,* vol. 45, no. 11, pp. 1120-1132, 2017.

[34] J. Neault and H. Tajmir-Riahi, "Interaction of cisplatin with human serum albumin. Drug binding mode and protein secondary structure," *Biochimica et Biophysica Acta (BBA)-Protein Structure and Molecular Enzymology,* vol. 1384, no. 1, pp. 153-159, 1998.

[35] J. A. Silverman and S. R. Deitcher, "Marqibo®(vincristine sulfate liposome injection) improves the pharmacokinetics and pharmacodynamics of vincristine," *Cancer chemotherapy and pharmacology,* vol. 71, no. 3, pp. 555-564, 2013.

[36] M. V. Blagosklonny and T. Fojo, "Molecular effects of paclitaxel: myths and reality (a critical review)," *International journal of cancer,* vol. 83, no. 2, pp. 151-156, 1999.

[37] A. D. Desforges *et al.*, "Treatment and diagnosis of chemotherapy-induced peripheral neuropathy: an update," *Biomedicine & Pharmacotherapy,* vol. 147, p. 112671, 2022.

[38] N. Klafke *et al.*, "Prevention and treatment of chemotherapy-induced peripheral neuropathy (CIPN) with non-pharmacological interventions: Clinical recommendations from a systematic scoping review and an expert consensus process," *Medical Sciences,* vol. 11, no. 1, p. 15, 2023.

[39] D. L. van de Graaf *et al.*, "Experiences of cancer survivors with chemotherapy-induced peripheral neuropathy in the Netherlands: symptoms, daily limitations, involvement of healthcare professionals, and social support," *Journal of Cancer Survivorship,* pp. 1-10, 2023.

[40] S. Butrus, S. Sagireddy, W. Yan, and K. Shekhar, "Defining Selective Neuronal Resilience and Identifying Targets of Neuroprotection and Axon Regeneration Using Single-Cell RNA Sequencing: Computational Approaches," in *Axon Regeneration: Methods and Protocols*: Springer, 2023, pp. 19-41.

[41] A. P. Tiwari, L. J. C. Tristan, B. Albin, and I. H. Yang, "Fluocinolone Acetonide Enhances Anterograde Mitochondria Trafficking and Promotes Neuroprotection against Paclitaxel-Induced Peripheral Neuropathy," *ACS Chemical Neuroscience,* 2023.

[42] S. J. Flatters and G. J. Bennett, "Studies of peripheral sensory nerves in paclitaxel-induced painful peripheral neuropathy: evidence for mitochondrial dysfunction," *Pain,* vol. 122, no. 3, pp. 245-257, 2006.

[43] V. Cepeda, M. A. Fuertes, J. Castilla, C. Alonso, C. Quevedo, and J. M. Pérez, "Biochemical mechanisms of cisplatin cytotoxicity," *Anti-Cancer Agents in Medicinal Chemistry (Formerly Current Medicinal Chemistry-Anti-Cancer Agents),* vol. 7, no. 1, pp. 3-18, 2007.

[44] J. L. Podratz *et al.*, "Cisplatin induced mitochondrial DNA damage in dorsal root ganglion neurons," *Neurobiology of disease,* vol. 41, no. 3, pp. 661-668, 2011.

[45] J. Gräb *et al.*, "Corticosteroids inhibit Mycobacterium tuberculosis-induced necrotic host cell death by abrogating mitochondrial membrane permeability transition," *Nature communications,* vol. 10, no. 1, p. 688, 2019.

[46] R. Prior, L. Van Helleputte, V. Benoy, and L. Van Den Bosch, "Defective axonal transport: a common pathological mechanism in inherited and acquired peripheral neuropathies," *Neurobiology of disease,* vol. 105, pp. 300-320, 2017.

[47] Q. H. Hogan, "Labat lecture: the primary sensory neuron: where it is, what it does, and why it matters," *Regional anesthesia and pain medicine,* vol. 35, no. 3, pp. 306-311-306-311, 2010.

[48] H. Donaghy, "Effects of antibody, drug and linker on the preclinical and clinical toxicities of antibody-drug conjugates," in *MAbs*, 2016, vol. 8, no. 4: Taylor & Francis, pp. 659-671.

[49] E. J. Akin *et al.*, "Paclitaxel increases axonal localization and vesicular trafficking of Nav1. 7," *Brain,* vol. 144, no. 6, pp. 1727-1737, 2021.

[50] G. J. Bennett, T. Doyle, and D. Salvemini, "Mitotoxicity in distal symmetrical sensory peripheral neuropathies," *Nature Reviews Neurology,* vol. 10, no. 6, pp. 326-336, 2014.

[51] D. Pareyson, P. Saveri, A. Sagnelli, and G. Piscosquito, "Mitochondrial dynamics and inherited peripheral nerve diseases," *Neuroscience letters,* vol. 596, pp. 66-77, 2015.

[52] C. Tang, M. J. Livingston, R. Safirstein, and Z. Dong, "Cisplatin nephrotoxicity: new insights and therapeutic implications," *Nature Reviews Nephrology,* vol. 19, no. 1, pp. 53-72, 2023.

[53] A. Coutaux, "Non-pharmacological treatments for pain relief: TENS and acupuncture," *Joint Bone Spine,* vol. 84, no. 6, pp. 657-661, 2017.

[54] M. P. Willand, M.-A. Nguyen, G. H. Borschel, and T. Gordon, "Electrical stimulation to promote peripheral nerve regeneration," *Neurorehabilitation and neural repair,* vol. 30, no. 5, pp. 490-496, 2016.

[55] M.-C. Lu *et al.*, "Effects of electrical stimulation at different frequencies on regeneration of transected peripheral nerve," *Neurorehabilitation and neural repair,* vol. 22, no. 4, pp. 367-373, 2008.

[56] T. Gordon, "Electrical stimulation to enhance axon regeneration after peripheral nerve injuries in animal models and humans," *Neurotherapeutics,* vol. 13, no. 2, pp. 295-310, 2016.

[57] H.-L. Su *et al.*, "Late administration of high-frequency electrical stimulation increases nerve regeneration without aggravating neuropathic pain in a nerve crush injury," *BMC neuroscience,* vol. 19, pp. 1-12, 2018.

[58] K. J. Zuo, T. Gordon, K. M. Chan, and G. H. Borschel, "Electrical stimulation to enhance peripheral nerve regeneration: Update in molecular investigations and clinical translation," *Experimental neurology,* vol. 332, p. 113397, 2020.
[59] K. Elzinga, N. Tyreman, A. Ladak, B. Savaryn, J. Olson, and T. Gordon, "Brief electrical stimulation improves nerve regeneration after delayed repair in Sprague Dawley rats," *Experimental neurology,* vol. 269, pp. 142-153, 2015.
[60] M. J. Devine and J. T. Kittler, "Mitochondria at the neuronal presynapse in health and disease," *Nature Reviews Neuroscience,* vol. 19, no. 2, pp. 63-80, 2018.
[61] D. Trigo, C. Avelar, M. Fernandes, J. Sá, and O. da Cruz e Silva, "Mitochondria, energy, and metabolism in neuronal health and disease," *FEBS letters,* vol. 596, no. 9, pp. 1095-1110, 2022.
[62] R. M. Stassart and K.-A. Nave, "Nerve regeneration: Specific metabolic demands?," *Experimental Neurology,* vol. 269, pp. 90-92, 2015.
[63] M. J. Rossi and G. Pekkurnaz, "Powerhouse of the mind: mitochondrial plasticity at the synapse," *Current opinion in neurobiology,* vol. 57, pp. 149-155, 2019.
[64] S. Maday, A. E. Twelvetrees, A. J. Moughamian, and E. L. Holzbaur, "Axonal transport: cargo-specific mechanisms of motility and regulation," *Neuron,* vol. 84, no. 2, pp. 292-309, 2014.
[65] M. Sajic *et al.*, "Impulse conduction increases mitochondrial transport in adult mammalian peripheral nerves in vivo," *PLoS biology,* vol. 11, no. 12, p. e1001754, 2013.
[66] J. Burgess *et al.*, "Chemotherapy-induced peripheral neuropathy: epidemiology, pathomechanisms and treatment," *Oncology and therapy,* pp. 1-66, 2021.
[67] B. Albin, K. Qubbaj, A. P. Tiwari, P. Adhikari, and I. H. Yang, "Mitochondrial trafficking as a protective mechanism against chemotherapy drug-induced peripheral neuropathy: Identifying the key site of action," *Life Sciences,* p. 122219, 2023.
[68] S. Wolf, D. Barton, L. Kottschade, A. Grothey, and C. Loprinzi, "Chemotherapy-induced peripheral neuropathy: prevention and treatment strategies," *European journal of cancer,* vol. 44, no. 11, pp. 1507-1515, 2008.
[69] S. Horwitz, "Taxol (paclitaxel): mechanisms of action," *Annals of oncology: official journal of the European Society for Medical Oncology,* vol. 5, pp. S3-6, 1994.
[70] E. Gornstein and T. L. Schwarz, "The paradox of paclitaxel neurotoxicity: Mechanisms and unanswered questions," *Neuropharmacology,* vol. 76, pp. 175-183, 2014.
[71] A. Grothey and R. M. Goldberg, "A review of oxaliplatin and its clinical use in colorectal cancer," *Expert opinion on pharmacotherapy,* vol. 5, no. 10, pp. 2159-2170, 2004.
[72] E. Raymond, S. Faivre, S. Chaney, J. Woynarowski, and E. Cvitkovic, "Cellular and molecular pharmacology of oxaliplatin," *Molecular cancer therapeutics,* vol. 1, no. 3, pp. 227-235, 2002.
[73] C. Tofthagen, R. D. McAllister, and S. C. McMillan, "Peripheral neuropathy in patients with colorectal cancer receiving oxaliplatin," *Clinical journal of oncology nursing,* vol. 15, no. 2, 2011.
[74] L. Staurengo-Ferrari, D. Araldi, P. G. Green, and J. D. Levine, "Neuroendocrine mechanisms in oxaliplatin-induced hyperalgesic priming," *Pain,* vol. 164, no. 6, p. 1375, 2023.
[75] K. Sałat, "Chemotherapy-induced peripheral neuropathy—part 2: focus on the prevention of oxaliplatin-induced neurotoxicity," *Pharmacological Reports,* vol. 72, pp. 508-527, 2020.
[76] S. C. Kim *et al.*, "In vivo evaluation of polymeric micellar paclitaxel formulation: toxicity and efficacy," *Journal of controlled release,* vol. 72, no. 1-3, pp. 191-202, 2001.
[77] S. R. Pestieau, J. F. Belliveau, H. Griffin, O. A. Stuart, and P. H. Sugarbaker, "Pharmacokinetics of intraperitoneal oxaliplatin: experimental studies," *Journal of surgical oncology,* vol. 76, no. 2, pp. 106-114, 2001.
[78] L. Pendyala and P. Creaven, "In vitro cytotoxicity, protein binding, red blood cell partitioning, and biotransformation of oxaliplatin," *Cancer research,* vol. 53, no. 24, pp. 5970-5976, 1993.
[79] L. Pendyala, Y. Kidani, R. Perez, J. Wilkes, R. Bernacki, and P. Creaven, "Cytotoxicity, cellular accumulation and DNA binding of oxaliplatin isomers," *Cancer letters,* vol. 97, no. 2, pp. 177-184, 1995.

[80] H. U. Lee *et al.*, "Subcellular electrical stimulation of neurons enhances the myelination of axons by oligodendrocytes," *PloS one,* vol. 12, no. 7, p. e0179642, 2017.
[81] D. Safiulina and A. Kaasik, "Energetic and dynamic: how mitochondria meet neuronal energy demands," *PLoS biology,* vol. 11, no. 12, p. e1001755, 2013.
[82] D. N. Rushton, "Electrical stimulation in the treatment of pain," *Disability and rehabilitation,* vol. 24, no. 8, pp. 407-415, 2002.
[83] J. S. Jara, S. Agger, and E. R. Hollis, "Functional electrical stimulation and the modulation of the axon regeneration program," *Frontiers in Cell and Developmental Biology,* vol. 8, p. 736, 2020.
[84] C.-F. V. Latchoumane *et al.*, "Chronic Electrical Stimulation Promotes the Excitability and Plasticity of ESC-derived Neurons following Glutamate-induced Inhibition In vitro," *Scientific Reports,* vol. 8, no. 1, p. 10957, 2018/07/19 2018, doi: 10.1038/s41598-018-29069-3.
[85] J. Nunnari and A. Suomalainen, "Mitochondria: in sickness and in health," *Cell,* vol. 148, no. 6, pp. 1145-1159, 2012.
[86] A. Grünewald *et al.*, "Mutant Parkin impairs mitochondrial function and morphology in human fibroblasts," *PloS one,* vol. 5, no. 9, p. e12962, 2010.
[87] R. H. Andres *et al.*, "Human neural stem cells enhance structural plasticity and axonal transport in the ischaemic brain," *Brain,* vol. 134, no. 6, pp. 1777-1789, 2011.
[88] P. G. Nagappan, H. Chen, and D.-Y. Wang, "Neuroregeneration and plasticity: a review of the physiological mechanisms for achieving functional recovery postinjury," *Military Medical Research,* vol. 7, no. 1, pp. 1-16, 2020.
[89] O. K. Melemedjian *et al.*, "Local translation and retrograde axonal transport of CREB regulates IL-6-induced nociceptive plasticity," *Molecular pain,* vol. 10, pp. 1744-8069-10-45, 2014.
[90] M.-Y. Lin and Z.-H. Sheng, "Regulation of mitochondrial transport in neurons," *Experimental cell research,* vol. 334, no. 1, pp. 35-44, 2015.
[91] C. Chen *et al.*, "Miro1 provides neuroprotection via the mitochondrial trafficking pathway in a rat model of traumatic brain injury," *Brain Research,* vol. 1773, p. 147685, 2021.
[92] K. H. Lee *et al.*, "High-frequency stimulation of the subthalamic nucleus increases glutamate in the subthalamic nucleus of rats as demonstrated by in vivo enzyme-linked glutamate sensor," *Brain research,* vol. 1162, pp. 121-129, 2007.
[93] A. A. Al-Majed, T. M. Brushart, and T. Gordon, "Electrical stimulation accelerates and increases expression of BDNF and trkB mRNA in regenerating rat femoral motoneurons," *European Journal of Neuroscience,* vol. 12, no. 12, pp. 4381-4390, 2000.
[94] C. E. McGregor and A. W. English, "The role of BDNF in peripheral nerve regeneration: activity-dependent treatments and Val66Met," *Frontiers in cellular neuroscience,* vol. 12, p. 522, 2019.
[95] E. Vögelin, J. Baker, J. Gates, V. Dixit, M. A. Constantinescu, and N. Jones, "Effects of local continuous release of brain derived neurotrophic factor (BDNF) on peripheral nerve regeneration in a rat model," *Experimental neurology,* vol. 199, no. 2, pp. 348-353, 2006.
[96] X. Tao, S. Finkbeiner, D. B. Arnold, A. J. Shaywitz, and M. E. Greenberg, "Ca2+ influx regulates BDNF transcription by a CREB family transcription factor-dependent mechanism," *Neuron,* vol. 20, no. 4, pp. 709-726, 1998.
[97] W. Wenjin *et al.*, "Electrical stimulation promotes BDNF expression in spinal cord neurons through Ca 2+-and Erk-dependent signaling pathways," *Cellular and molecular neurobiology,* vol. 31, pp. 459-467, 2011.
[98] M. Swain, S. K. Soman, K. Tapia, R. Y. Dagda, and R. K. Dagda, "Brain-derived neurotrophic factor protects neurons by stimulating mitochondrial function through protein kinase A," *Journal of Neurochemistry,* 2023.
[99] G. Wei *et al.*, "Platinum accumulation in oxaliplatin-induced peripheral neuropathy," *Journal of the Peripheral Nervous System,* vol. 26, no. 1, pp. 35-42, 2021.
[100] L. Kang, Y. Tian, S. Xu, and H. Chen, "Oxaliplatin-induced peripheral neuropathy: clinical features, mechanisms, prevention and treatment," *Journal of neurology,* vol. 268, pp. 3269-3282, 2021.

[101] N. S. Chandel, "Mitochondria as signaling organelles," *BMC biology,* vol. 12, pp. 1-7, 2014.
[102] G. Doron and M. Brecht, "What single-cell stimulation has told us about neural coding," *Philosophical Transactions of the Royal Society B: Biological Sciences,* vol. 370, no. 1677, p. 20140204, 2015.
[103] D. T. Chang and I. J. Reynolds, "Mitochondrial trafficking and morphology in healthy and injured neurons," *Progress in neurobiology,* vol. 80, no. 5, pp. 241-268, 2006.
[104] B. Su, Y.-S. Ji, X.-l. Sun, X.-H. Liu, and Z.-Y. Chen, "Brain-derived neurotrophic factor (BDNF)-induced mitochondrial motility arrest and presynaptic docking contribute to BDNF-enhanced synaptic transmission*♦," *Journal of Biological Chemistry,* vol. 289, no. 3, pp. 1213-1226, 2014.
[105] R. C. Vergara *et al.*, "The energy homeostasis principle: neuronal energy regulation drives local network dynamics generating behavior," *Frontiers in computational neuroscience,* vol. 13, p. 49, 2019.
[106] D. G. Nicholls and S. L. Budd, "Mitochondria and neuronal survival," *Physiological reviews,* vol. 80, no. 1, pp. 315-360, 2000.
[107] L. Tilokani, S. Nagashima, V. Paupe, and J. Prudent, "Mitochondrial dynamics: overview of molecular mechanisms," *Essays in biochemistry,* vol. 62, no. 3, pp. 341-360, 2018.
[108] R. Wang, H. Hayashi, Z. Zhang, and Y.-B. Duan, "An exploration of dynamics of the moving mechanism of the growth cone," *Molecules,* vol. 8, no. 1, pp. 127-138, 2003.
[109] A. D. Pilling, D. Horiuchi, C. M. Lively, and W. M. Saxton, "Kinesin-1 and Dynein are the primary motors for fast transport of mitochondria in Drosophila motor axons," *Molecular biology of the cell,* vol. 17, no. 4, pp. 2057-2068, 2006.
[110] B. Albin, P. Adhikari, A. P. Tiwari, K. Qubbaj, and I. H. Yang, "Electrical stimulation enhances mitochondrial trafficking as a neuroprotective mechanism against chemotherapy-induced peripheral neuropathy," *Iscience,* vol. 27, no. 3, 2024.
[111] D. J. Heeger and D. Ress, "What does fMRI tell us about neuronal activity?," *Nature reviews neuroscience,* vol. 3, no. 2, pp. 142-151, 2002.
[112] B. Bhatnagar *et al.*, "Chemotherapy dose reduction due to chemotherapy induced peripheral neuropathy in breast cancer patients receiving chemotherapy in the neoadjuvant or adjuvant settings: a single-center experience," *Springerplus,* vol. 3, pp. 1-6, 2014.
[113] B. P. Schneider, D. L. Hershman, and C. Loprinzi, "Symptoms: chemotherapy-induced peripheral neuropathy," *Improving Outcomes for Breast Cancer Survivors: Perspectives on Research Challenges and Opportunities,* pp. 77-87, 2015.
[114] M. Zahiri *et al.*, "Using wearables to screen motor performance deterioration because of cancer and chemotherapy-induced peripheral neuropathy (CIPN) in adults-Toward an early diagnosis of CIPN," *Journal of geriatric oncology,* vol. 10, no. 6, pp. 960-967, 2019.
[115] S. Flatters, P. Dougherty, and L. Colvin, "Clinical and preclinical perspectives on Chemotherapy-Induced Peripheral Neuropathy (CIPN): a narrative review," *BJA: British Journal of Anaesthesia,* vol. 119, no. 4, pp. 737-749, 2017.
[116] R. S. D'Souza, Y. F. Her, M. Y. Jin, M. Morsi, and A. Abd-Elsayed, "Neuromodulation therapy for chemotherapy-induced peripheral neuropathy: a systematic review," *Biomedicines,* vol. 10, no. 8, p. 1909, 2022.
[117] R. A. Stetler, R. K. Leak, Y. Gao, and J. Chen, "The dynamics of the mitochondrial organelle as a potential therapeutic target," *Journal of Cerebral Blood Flow & Metabolism,* vol. 33, no. 1, pp. 22-32, 2013.
[118] W. M. van den Boogaard, D. S. Komninos, and W. P. Vermeij, "Chemotherapy side-effects: not all DNA damage is equal," *Cancers,* vol. 14, no. 3, p. 627, 2022.
[119] H. C. Lehmann, N. P. Staff, and A. Hoke, "Modeling chemotherapy induced peripheral neuropathy (CIPN) in vitro: Prospects and limitations," *Experimental neurology,* vol. 326, p. 113140, 2020.
[120] J. M. Rosenberg, C. Harrell, H. Ristic, R. A. Werner, and A. M. de Rosayro, "The effect of gabapentin on neuropathic pain," *The Clinical journal of pain,* vol. 13, no. 3, pp. 251-255, 1997.

[121] M. P. Lunn, R. A. Hughes, and P. J. Wiffen, "Duloxetine for treating painful neuropathy, chronic pain or fibromyalgia," *Cochrane database of systematic reviews,* no. 1, 2014.
[122] M. Wang, Z. Pei, and A. Molassiotis, "Recent advances in managing chemotherapy-induced peripheral neuropathy: A systematic review," *European Journal of Oncology Nursing,* vol. 58, p. 102134, 2022.
[123] M. T. Aziz, B. L. Good, and D. K. Lowe, "Serotonin-norepinephrine reuptake inhibitors for the management of chemotherapy-induced peripheral neuropathy," *Annals of Pharmacotherapy,* vol. 48, no. 5, pp. 626-632, 2014.
[124] R. Chow *et al.*, "Duloxetine for prevention and treatment of chemotherapy-induced peripheral neuropathy (CIPN): systematic review and meta-analysis," *BMJ Supportive & Palliative Care,* vol. 13, no. 1, pp. 27-34, 2023.
[125] J. F. Wernicke, J. Gahimer, I. Yalcin, M. Wulster-Radcliffe, and L. Viktrup, "Safety and adverse event profile of duloxetine," *Expert opinion on drug safety,* vol. 4, no. 6, pp. 987-993, 2005.
[126] O. Lambert and M. Bourin, "SNRIs: mechanism of action and clinical features," *Expert review of neurotherapeutics,* vol. 2, no. 6, pp. 849-858, 2002.
[127] M. Wang, Y. Yin, H. Yang, Z. Pei, and A. Molassiotis, "Evaluating the safety, feasibility, and efficacy of non-invasive neuromodulation techniques in chemotherapy-induced peripheral neuropathy: A systematic review," *European Journal of Oncology Nursing,* vol. 58, p. 102124, 2022.
[128] Z. Yan *et al.*, "Repetitive transcranial magnetic stimulation for chemotherapy-induced peripheral neuropathy in multiple myeloma: A pilot study," *SAGE Open Medicine,* vol. 11, p. 20503121231209088, 2023.
[129] J. P. Caviston and E. L. Holzbaur, "Microtubule motors at the intersection of trafficking and transport," *Trends in cell biology,* vol. 16, no. 10, pp. 530-537, 2006.
[130] A. K. Singla, A. Garg, and D. Aggarwal, "Paclitaxel and its formulations," *International journal of pharmaceutics,* vol. 235, no. 1-2, pp. 179-192, 2002.
[131] E. L. Gornstein and T. L. Schwarz, "Neurotoxic mechanisms of paclitaxel are local to the distal axon and independent of transport defects," *Experimental neurology,* vol. 288, pp. 153-166, 2017.
[132] A. P. Tiwari, L. J. C. Tristan, B. Albin, and I. H. Yang, "Fluocinolone Acetonide Enhances Anterograde Mitochondria Trafficking and Promotes Neuroprotection against Paclitaxel-Induced Peripheral Neuropathy," *ACS Chemical Neuroscience,* vol. 14, no. 11, pp. 2208-2216, 2023.
[133] S. M. Cohen and S. J. Lippard, "Cisplatin: From DNA damage to cancer chemotherapy," in *Progress in Nucleic Acid Research and Molecular Biology*, vol. 67: Academic Press, 2001, pp. 93-130.
[134] T. Makovec, "Cisplatin and beyond: molecular mechanisms of action and drug resistance development in cancer chemotherapy," *Radiology and oncology,* vol. 53, no. 2, pp. 148-158, 2019.
[135] G. E. Damsma, A. Alt, F. Brueckner, T. Carell, and P. Cramer, "Mechanism of transcriptional stalling at cisplatin-damaged DNA," *Nature structural & molecular biology,* vol. 14, no. 12, pp. 1127-1133, 2007.
[136] L.-Y. Hu, W.-L. Mi, G.-C. Wu, Y.-Q. Wang, and Q.-L. Mao-Ying, "Prevention and treatment for chemotherapy-induced peripheral neuropathy: therapies based on CIPN mechanisms," *Current neuropharmacology,* vol. 17, no. 2, pp. 184-196, 2019.
[137] S. W. Thompson, L. E. Davis, M. Kornfeld, R. D. Hilgers, and J. C. Standefer, "Cisplatin neuropathy. Clinical, electrophysiologic, morphologic, and toxicologic studies," *Cancer,* vol. 54, no. 7, pp. 1269-1275, 1984.
[138] K. J. Cullen, Z. Yang, L. Schumaker, and Z. Guo, "Mitochondria as a critical target of the chemotheraputic agent cisplatin in head and neck cancer," *Journal of bioenergetics and biomembranes,* vol. 39, pp. 43-50, 2007.
[139] R. Marullo *et al.*, "Cisplatin induces a mitochondrial-ROS response that contributes to cytotoxicity depending on mitochondrial redox status and bioenergetic functions," *PloS one,* vol. 8, no. 11, p. e81162, 2013.

[140] H. Ye, M. Cotic, E. E. Kang, M. G. Fehlings, and P. L. Carlen, "Transmembrane potential induced on the internal organelle by a time-varying magnetic field: a model study," *Journal of NeuroEngineering and Rehabilitation,* vol. 7, no. 1, p. 12, 2010/02/20 2010, doi: 10.1186/1743-0003-7-12.

[141] H. Monai, T. Omori, M. Okada, M. Inoue, H. Miyakawa, and T. Aonishi, "An analytic solution of the cable equation predicts frequency preference of a passive shunt-end cylindrical cable in response to extracellular oscillating electric fields," (in eng), *Biophys J,* vol. 98, no. 4, pp. 524-33, Feb 17 2010, doi: 10.1016/j.bpj.2009.10.041.

[142] B. Wang, A. S. Aberra, W. M. Grill, and A. V. Peterchev, "Modified cable equation incorporating transverse polarization of neuronal membranes for accurate coupling of electric fields," (in eng), *J Neural Eng,* vol. 15, no. 2, p. 026003, Apr 2018, doi: 10.1088/1741-2552/aa8b7c.

[143] E. Ege, D. Briggi, P. Vu, J. Cheng, F. Lin, and J. Xu, "Targeting dorsal root ganglia for chemotherapy-induced peripheral neuropathy: from bench to bedside," *Therapeutic Advances in Neurological Disorders,* vol. 17, p. 17562864241252718, 2024.

[144] H. Zhang and P. M. Dougherty, "Enhanced excitability of primary sensory neurons and altered gene expression of neuronal ion channels in dorsal root ganglion in paclitaxel-induced peripheral neuropathy," *Anesthesiology,* vol. 120, no. 6, pp. 1463-1475, 2014.

[145] T.-Y. Yeh, I.-W. Luo, Y.-L. Hsieh, T.-J. Tseng, H. Chiang, and S.-T. Hsieh, "Peripheral neuropathic pain: from experimental models to potential therapeutic targets in dorsal root ganglion neurons," *Cells,* vol. 9, no. 12, p. 2725, 2020.

[146] M. F. Esposito, R. Malayil, M. Hanes, and T. Deer, "Unique characteristics of the dorsal root ganglion as a target for neuromodulation," *Pain Medicine,* vol. 20, no. Supplement_1, pp. S23-S30, 2019.

[147] R. V. Haberberger, C. Barry, N. Dominguez, and D. Matusica, "Human dorsal root ganglia," *Frontiers in cellular neuroscience,* vol. 13, p. 271, 2019.

[148] U. Ernsberger, "Role of neurotrophin signalling in the differentiation of neurons from dorsal root ganglia and sympathetic ganglia," *Cell and tissue research,* vol. 336, no. 3, pp. 349-384, 2009.

[149] L. Liem, E. Van Dongen, F. J. Huygen, P. Staats, and J. Kramer, "The dorsal root ganglion as a therapeutic target for chronic pain," *Regional Anesthesia & Pain Medicine,* vol. 41, no. 4, pp. 511-519, 2016.

[150] R. D. Wilson *et al.*, "Neuromodulation for functional electrical stimulation," *Physical Medicine and Rehabilitation Clinics,* vol. 30, no. 2, pp. 301-318, 2019.

[151] A.-L. Benabid *et al.*, "Therapeutic electrical stimulation of the central nervous system," *Comptes rendus biologies,* vol. 328, no. 2, pp. 177-186, 2005.

[152] H. Ye and S. Kaszuba, "Neuromodulation with electromagnetic stimulation for seizure suppression: from electrode to magnetic coil," *IBRO reports,* vol. 7, pp. 26-33, 2019.

[153] A. M. Lozano *et al.*, "Deep brain stimulation: current challenges and future directions," *Nature Reviews Neurology,* vol. 15, no. 3, pp. 148-160, 2019.

[154] M. Yasir, A. Goyal, and S. Sonthalia, "Corticosteroid adverse effects," 2018.